Charring behavior of cross laminated timber with respect to the fire protection

Comparison of different methods in small, model and large scale with simulations

Mattia Tiso

SP Technical Research Institute of Sweden

SP Wood Technology

SP Report 2014:27

Charring behavior of cross laminated timber with respect to the fire protection

Comparison of different method in small, model and large scale with simulations

Mattia Tiso

SP Technical Research Institute of Sweden

SP Technical Research Institute of Sweden
Box 857, 501 15 Borås, Sweden (headquarters)

SP Report 2014:27
ISBN 978-91-88001-12-2
ISSN 0284-5172

Abstract

Timber buildings made with Cross-laminated Timber (CLT) panels are becoming wide spread in Europe. The fire resistance of CLT panels depends upon several parameters, including the number of layers and their thickness. At the present, EN 1995-1-2:2004 does not provide specific information on the fire design of CLT panels. Several fire resistance tests of CLT panels were performed in different scales by furnace testing using the standard fire curve according to ISO 834-1:1999, however the large number of possible combination of CLT products makes testing too complicated and expensive as a tool for the verification of the fire resistance of several combinations. In this report are presented nine small-scale tests carried-out at SP Wood Technology (Technical Research Institute of Sweden). The tests consisted in specimens of CLT and massive timber exposed at a two steps of constant heat flux in a cone calorimeter (50 and 75 kW/m2). Some specimens were exposed with two different types of fire protection (gypsum plasterboard type F and plywood) and some were tested unprotected. Later, thermal simulations with the same set-up of tests were implemented on the finite element software package in Safir 2007, with the time-temperature curve given by ISO 834 as input; also the analytical calculation of the charring depth following the Eurocode 5 part 1-2 was done. The target of this thesis is to compare performed CLT furnace tests with the small-scale cone calorimeter tests carried out, the numerical results of the thermal model and the analytical results obtained.

Key words: Cross-laminated timber, CLT, Fire resistance, Cone calorimeter, Fire protection, SP Wood Technology

Abstract

Edifici realizzati con elementi portanti in legno lamellare a strati incrociati (CLT) sono sempre più diffusioni in Europa. La resistenza al fuoco dei pannelli CLT dipende da vari parametri, tra cui il numero e lo spessore degli strati. Al momento, la norma europea EN 1995-1-2:2004 non fornisce informazioni specifiche sulla progettazione antincendio dei pannelli CLT. Alcune prove di resistenza al fuoco di questi pannelli sono state eseguite in diverse scale con test in fornace, utilizzando come esposizione la curva d'incendio standard secondo ISO 834-1:1999, tuttavia il gran numero di possibili combinazioni dei CLT presenti in commercio rende il test troppo complicato e costoso come strumento per la verifica della resistenza al fuoco di tutte le diverse combinazioni. In questa relazione sono presentate nove prove su piccola scala, eseguite presso SP-Wood Technology (Technical Research Institute of Sweden) a Stoccolma. Le prove comprendono provini di CLT e legno massiccio esposti, in un cono calorimetrico, a due livelli di flusso di calore costante (50 e 75 kW/m2). Alcuni provini sono stati esposti con due diversi tipi di protezione antincendio (cartongesso tipo F e compensato) alcuni sono stati testati non protetti al fuoco. In seguito sono state implementate simulazioni termiche, per mezzo del software che implementa elementi finiti Safir 2007, con lo stesso settaggio dei test e con l'esposizione al fuoco secondo la curva tempo-temperatura fornita dalla norma ISO 834. E' stato eseguito anche un calcolo analitico della profondità di carbonizzazione secondo le disposizioni fornite dall'Eurocodice 5 parte 1-2. L'obiettivo di questa tesi è di confrontare eseguite le prove al fuoco del CLT eseguite su fornace con i test su piccola scala effettuati con il cono calorimetrico, i risultati numerici del modello termico e i risultati analitici ottenuti.

Acknowledgements

A grateful acknowledgement goes to the SP Wood Technology of Stockholm, which hosted me for my internship. In particularly I would like to thank Joachim Schmid as one the greatest points of reference of this thesis, and also I would like to thank the other researchers of SP Wood Technology that followed and gave me precious suggestions for this work, as Birgit Östman, Alar Just and Lazaros Tsantaridis.

I would like to express my deepest gratitude to Professor Isaia Clemente for his availability to supervise my master thesis. I would like to extend my gratitude also to Massimo Fragiacomo that managed the contacts for realize this work, and Agnese Menis who gave me the precious data for extend the investigations.

I am grateful with my family that have ever believed in me and supported my studies not without any sacrifices. I want to thank my girlfriend Chiara, because she encouraged me to doing the internship abroad and her presence for me is a reason to look ahead.

I should nevertheless like to express my thanks to all my friends; their company relieved me to the load of the exams in these years of study.

Contents

List of tables

List of figures

Index of abbreviations

CLT	Cross-laminated timber
csw	Compression side warm
EC5	EN 1995-1-2:2004 Eurocode 5 part 1-2 [2]
EMC	Equilibrium moisture content
FSITB	Fire safety in timber buildings [8]
GP	Gypsum plasterboard
iwe	Infinitive wide element
MUF	Melamine urea formaldehyde
niwe	Non-infinitive wide element
PU	Polyurethane
PW	Plywood
RH	Relative humidity
T	Timber
TC	Thermocouple
tsw	Tension side warm
W	Wood

1 Introduction

Timber buildings made with Cross-laminated Timber (CLT) panels are becoming wide spread in Europe. The advantages of this massive construction system are the good structural performance, the better thermal and acoustic insulation properties, the high degree of prefabrication and the rapidity of erection.

The fire resistance of CLT panels depends upon several parameters, including the number of layers and their thickness, the adhesives using during production, and the use as floor or wall component. At the present, EN 1995-1-2:2004 [2] does not provide specific information on the fire design of CLT panels [10].

The fire resistance tests of CLT panels were performed in different scales by furnace testing using the standard fire curve according to ISO 834-1:1999 [4] which corresponds to EN 1363-1:1999 [5], however the large number of possible combination of CLT products makes testing too complicated and expensive as a tool for the verification of the fire resistance of several combinations, therefore some numerical models are already available in literature and also EC5 provide specific indications on advanced calculation method for the massive timber but no specific information on CLT. Some numerical simulations on CLT panels were recently carried out to investigate their fire behavior.

The focus of this thesis is to compare performed CLT furnace tests with a small-scale cone calorimeter test carried out by the author at SP Wood Technology in Stockholm and numerical results of a thermal model implemented in Safir 2007 [27] a finite element software package for the analysis of structures under ambient and elevated temperature conditions.

1.1 Purpose and aim

1.1.1 Purpose of the thesis

The purpose of this thesis is compare the start of charring and the charring rate of small scale CLT specimens exposed at heat flux by a cone calorimeter with the start of charring and the charring rate obtained by several performed furnace tests and a thermal model.

1.1.2 Aim of the thesis

The aim is to verify that the results from the cone calorimeter tests, the furnace tests and the thermal model agree and understand if it is possible to achieve significant parameters regarding the fire safety design of timber elements only with small-scale cone calorimeter tests.

1.2 Disposition

First of all the thesis will give a state of art and a literature review of the CLT behavior exposed to fire, furthermore the report will describe the performed furnace tests that are considered to compare the results.

The thesis will describe the tests being conducted to both types of materials (CLT and Solid Timber) i.e. how they were planned, tested and equipped and the following simulations with the characterization of the material properties by the time. For obtaining also a reference with the current regulations, a design of the charring behavior according with the Eurocode 5 part 1-2 [2] will be done.

Afterwards test results will be analyzed and compared with each other and the simulations for give reliable answer to the purpose of the conducted tests.

2 Literature review

2.1 Behavior of timber members exposed to fire

The wood combustion is surely a negative aspect of this material for two reasons: the charring of the wood reduce the resistant section and consequently the load bearing capacity; later the physical phenomena, if it remain in its exothermic phase, it allows the propagation of the fire due to the additional combustible that it finds in the structure.

It is difficult to deem that the behavior of the timber exposed to fire is firmly better than other materials. As to the timber decay, it proceeds slightly from the outside towards inside the cross section, and the area not reached by the flames presents unchanged mechanical properties; for all that the load bearing capacity is easily predictable. The charred layer shown retreat phenomena that easily allows the combustible gas transfer towards the underlying timber surface; this layer usually does not burn because there is not sufficient oxygen for the oxidation of the charred material. The surface temperature of the charred layer is close to the fire temperature, but decrease quickly through the charred layer. The transition among the charred layer and the not charred material is rather clear and correspond with the reaching of a temperature close to 300ºC. Under the charred layer there is a warmed up layer with a thickness around 35 mm, in the warmer zone (T ≥ 200ºC) there are pyrolysis phenomena; in the underlying colder zone (T ≥ 100ºC) there is the evaporation of the moisture, whereas the center remains nearly at the initial temperature for a rather long time.

Regarding the temperatures of the wood below the charred layer, the Eurocode 5 [2] gives the following relation for the evaluation of the temperature T(ºC):

$$T = T_i + \left(T_p - T_i\right) \cdot (1 - x/a)^2 \qquad (1)$$

where

T_i is the initial temperature of the wood (ºC),

T_p is the carbonization temperature (300ºC),

x is the distance from the internal surface of charred layer (mm),

a is the thickness of the layer involved from the heat (mm).

2.2 Thermal degradation of the wood

The problem of the fire resistance of timber elements was analyzed from the behavior that the material shows when it is exposed to fire. For understand the problem three fundamental phenomena have to be evaluated:

- workings of combustion
- workings of heat transfer
- evolutions of the wood mechanical properties respect the temperature

The workings of combustion can be distinguished with or without the presence of the air: the pyrolysis starts in absence of the air, with energy absorption and gives back coal and a portion of gas.

With the presence of the air there is a flaming combustion of the material with significant energy production (on average 4400 kcal/kg) that self-sustaining the process to the depletion of the combustible; there will be the solid residue composed by ash.

The workings of combustion proceeds from the exposed surface towards inside of mass with a certain rate; this rate depends on the wooden species at equal boundary conditions. Other factors that can influence the charring rate are the contained moisture and the treatments subjected at the material.

The depth of the charred material is proportional at the time of fire exposure.

As has been said the process could take place with or without the presence of the air; now the two cases are going to be analyzed. With the presence of a sufficient amount of oxygen will assist to the process of flaming combustion that coincides with at the temperature interval among 200ºC and 300ºC. It is essential know the charring rate because it allow to know the depth of charred material and the material properties below that layer. Experimental facts have proved that this zone could be considered as the zone with the unchanged mechanical properties of the wood, except for a reduced part which is subjected at temperature increase above the 100ºC. This behavior is validated from intrinsic material properties, reduced thermal conductivity, elevated specific heat and the lower coefficient of thermal expansion.

A not negligible factor is hygroscopic aptitude of the material: it contains water in a percentage which depends on the thermo-hygrometric external conditions. Another not negligible factor is the material zone with the temperatures included among 100ºC and 260ºC presents thickness of few millimeters, so not very significant from an engineering point of view.

When the temperature increase the first effect is the loss of water, this effect can be considered complete just above the 100ºC; the temperature will be constant up to the complete evaporation of the water. This first phase is irreversible.

When the temperature increase, the irreversible reactions that lead at decay start to be not negligible; the point of no return it is conventionally define at 170ºC, there will be a release of vapor, carbon dioxide and other gas. If the temperature continues to increase, continues the distillation of condensable products and the emission of gases; the limit of this phase can be considered among 240ºC and 280ºC. Around the 280ºC the process become exothermic, the increase of temperature produce an increase of gaseous emissions and combustible products and proceed up to 350-400ºC, in this point the material starts to decrease due to pyrolysis and the phenomena are lessen. Around the 500ºC the pyrolysis can be considered finished.

With the presence of oxygen at the beginning the processes are exothermic due to the combustion of gaseous volatile substances (around 140-260ºC). Among 200ºC and 280ºC there is an intense developed of carbon dioxide and gas for the combustion of organic substances, for example the lignin, whose decomposition increase around 300ºC. Among 300ºC and 400ºC the rapid combustion is shown with flames and development of embers. Without activation flame, the combustion finds it hard to start, meanwhile if it starts, it activates the combustion of surrounding gases. Over the 500ºC the coal become incandescent and then it generates embers (more or less bright) but it releases heat in the final phase, there is a decreasing of the gaseous emissions, the ember is consumed without flame.

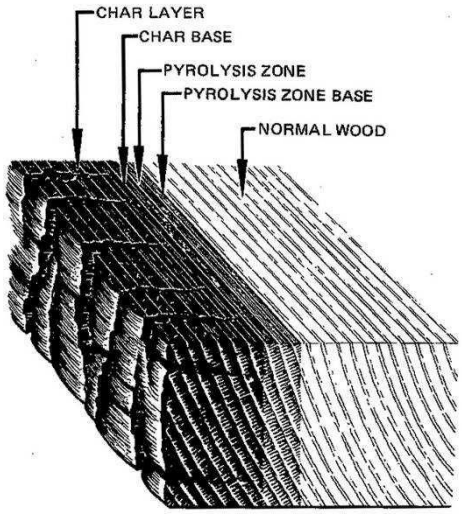

Figure 2-1 Different phases of degradation of wood [28]

The wood is bad heat conductor, and this is the reason why most of the propagation occurs by diffusion of hot gases within the mass, which rises the temperature up to trigger the thermal demolition with the onset of carbonization. Instead in the charring zone these gases reduce the rise of the ember temperature.

These facts shown how could be complicate describe the behavior of a timber element exposed to fire; a representative model has to take account a large series of hardly to predictable variables. For these reasons were studied and proposed a series of simplified aspect for take account those various aspects, sometimes in fictitious way, trying to reproduce in the real way this phenomena [9].

2.3 Design model in accordance with EC 5 part 1-2

The Eurocode 5 part 1-2 proposes three different methods of analysis for evaluate the mechanical resistance (criterion R) for wooden structures:

- reduced cross-section method
- reduced properties method
- general methods of calculating (charring models depending on the temperature curve and the content of moisture in the section)

The verification of mechanical resistance is assumed to be satisfied when the load-bearing function is maintained during the required time of fire exposure; this time depends on load of combustible material present in the compartment.

In this regard should be specified that for verification of mechanical resistance, the design values of strength and stiffness properties shall be determined from:

$$f_{d,fi} = k_{mod,fi} \cdot \frac{f_{20}}{\gamma_{M,fi}} \tag{2}$$

$$S_{d,fi} = k_{mod,fi} \cdot \frac{S_{20}}{\gamma_{M,fi}} \tag{3}$$

where

$f_{d,fi}$ is the design strength fire,

$S_{d,fi}$ is the design stiffness property in fire,
f_{20} is the 20 % fractile of a strength property at normal temperature,
S_{20} is the 20 % fractile of a stiffness property at normal temperature,
$k_{mod,fi}$ is the modification factor for fire,
$\gamma_{M,fi}$ is the partial safety factor for timber in fire.

2.3.1 Reduced cross-section method

This method is the simplest and with a safest approach; an effective cross-section should be calculated by reducing the initial cross-section by the charring depth resulting during the fire exposed. The effective charring depth is determined by the distance from the side exposed to fire:

$$d_{ef} = d_{char,n} + k_0 \cdot d_0 \quad (4)$$

$$d_{char,n} = \beta_n \cdot t \quad (5)$$

where

d_{ef} is the effective charring depth,
$d_{char,n}$ is the notional charring depth,
d_0 is 7 mm,
k_0 as shown in the following table,
β_n is the notional design charring rate, the magnitude of which includes for the effect of corner roundings and fissures (mm/min),
t is the time of fire exposure in minutes (min).

Table 2-1 Determination of k_0 for unprotected surfaces with t in minutes

k_0	
$t < 20\ min$	$1/t$
$t > 20\ min$	1

The notional design charring rate provided by the code does not refer at a one-dimensional charring, but consider the charring in more sides taking account of the corner rounding and fissure. The one dimensional charring should be calculated as:

$$d_{char,0} = \beta_0 \cdot t \quad (6)$$

where

$d_{char,0}$ is the one-dimensional charring depth,
β_n is the one-dimensional charring rate (mm/min),
t is the time of fire exposure in minutes (min).

However, in that case, if there is charring in more sides have to be consider the corner roundings and which present a radius equal to the charring depth $d_{char,0}$. This is the reason why the code provides a charring rate β_n greater than β_0, with this the rounding corners shall be negligible.

For the cross-lam, despite the element geometry suggests an one-dimensional propagation

of the heat flux, to consider the imperfections should take the β_n charring rate value instead of β_0.

The code reports different values of charring rates depending on the material; for the cross-lam should be consider the "softwood and beech" category with density over to 290 kg/m^3, it means β_n of 0,7 mm/min.

2.3.2 Reduced properties method

The following rules apply to rectangular cross-sections of softwood exposed to fire on three or four sides and round cross-sections exposed along their whole perimeter. The residual section should be determinate through:

$$d_{char,n} = \beta_n \cdot t \tag{7}$$

while the factor $k_{mod,fi}$, for the first 20 min. is 1, over shall be taken respect the action that has to be considered:

$$k_{mod,fi} = 1 - \frac{1}{200} \cdot \frac{P}{A_r} \tag{8}$$

for bending strength

$$k_{mod,fi} = 1 - \frac{1}{125} \cdot \frac{P}{A_r} \tag{9}$$

for compressive strength

$$k_{mod,fi} = 1 - \frac{1}{330} \cdot \frac{P}{A_r} \tag{10}$$

for tensile strength and modulus of elasticity

where

P is the perimeter of the fire exposed residual cross-section (m),

A_r is the area of the residual cross-section (m^2),

It means that this method makes a verification on the cross section without the charred layer and considers the material properties reduced with the coefficients that depends on geometry factors and not on the temperature.

It is also important highlight that on CLT is not possible to use this method since a perimeter of a fire exposed residual cross section (P) cannot be calculated on elements exposed to fire only on one side.

2.3.3 Advanced calculation method

Advanced calculation method should be used for determination of charring depth, development and distribution of the temperature, evaluation of structural behavior or one of its parts. Each thermal simulation shall be based on the theory of heat transfer and takes account the variation of thermal properties with respect to the temperature and the moisture.

If the calculation method do not consider phenomena as the raise of the heat due to the

vaporization of the moisture, the cracking in the wood, the mass transfer, etc, the coefficients used should be evaluated and modified for obtain a reliable result.

The EC 5 provides the tables with the trend of thermal conductivity, specific heat and density ratio with respect to temperature. Such laws of variation of thermal properties in the wood involve by implication above quoted phenomena. However this simplification is valid only in reference to the standard ISO 834 fire curve.

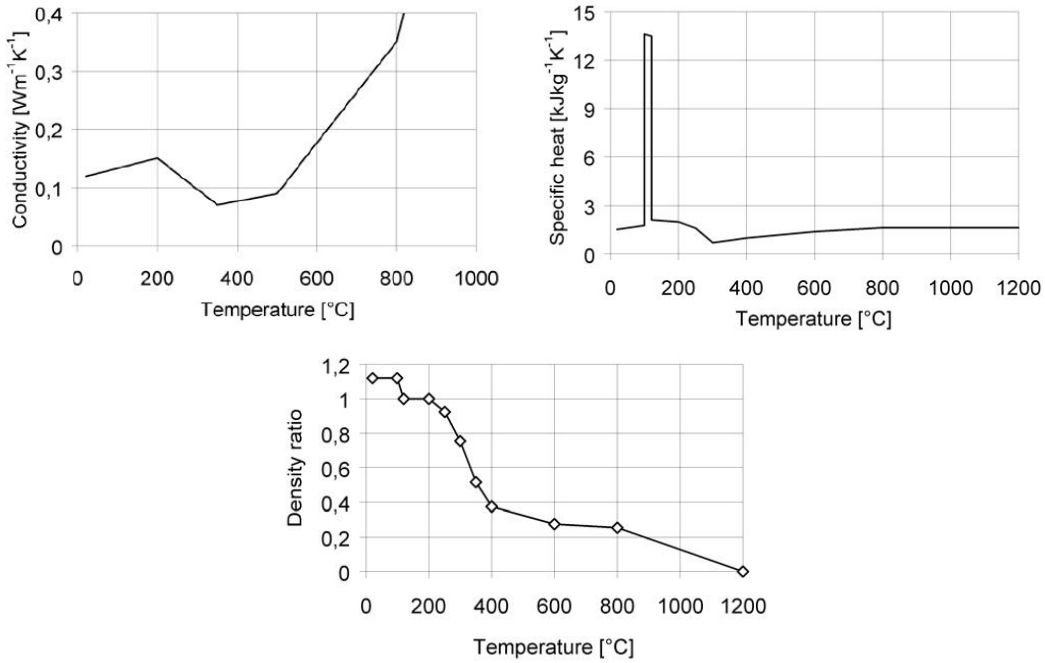

Figure 2-2 Conductivity, specific heat and density ratio with respect to the temperature provide by EC5

Ones obtained the trend of the temperature inside the section, the Eurocode provides the value of reduction factors of strength and modulus of elasticity which depends on the temperature and the load applied. In this way is possible to know the load bearing capacity of the section by the generic time.

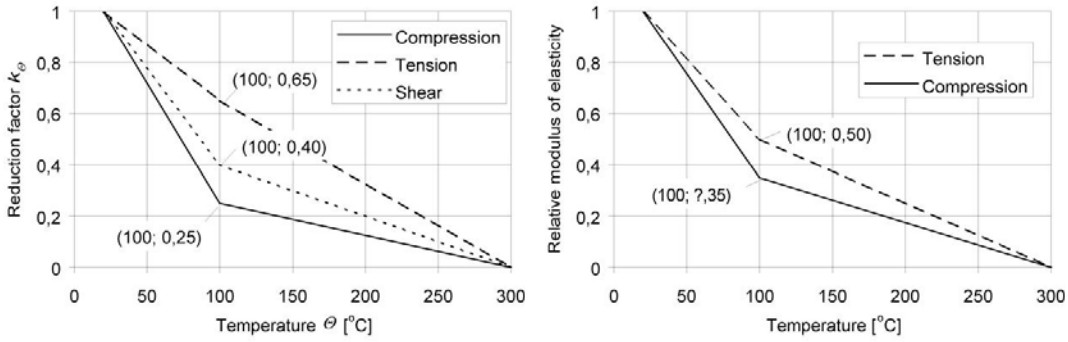

Figure 2-3 Reduction factor of strength and modulus of elasticity with respect to the temperature provide by EC5

2.4 Problem of heat conduction

The heat conduction should be defined as a process where the heat moves from a part of body with greater temperature to another with a lower temperature without matter transfer.

In the one-dimensional heat conduction through a layer, the heat Q that passes in a section during a unit of time should be obtained by:

$$\frac{dQ}{dt} = -\lambda \cdot S \cdot \frac{d\vartheta}{dx} \tag{11}$$

where

- λ is a constant of proportionality called thermal conductivity (W/m K),
- $d\theta$ is the infinitesimal temperature,
- S is the surface of the element.

Some considerations suggest that:

- the heat transferred of a body increases with the raise of its temperature.
- two bodies with the some with the same material and the same temperature. transfer different quantities of heat if their masses are different, in particular the bigger mass transfers more heat.
- the quantity of heat transfers from a body depend on the properties of the body itself.

These concepts could be summarized with:

$$Q = m \cdot c \cdot \vartheta \tag{12}$$

where

- m is the mass of the body,
- θ is the temperature of the body,
- c is a constant of proportionality called specific heat.

The specific heat is the quantity of heat necessary for increase the temperature of 1 kelvin degree of 1 kg of material.

Dividing (11) for the volume of the body is obtained:

$$U = \rho \cdot c \cdot \cot\vartheta \tag{13}$$

Where

- U is the density of thermal energy possessed by the body at the temperature θ,
- c is the density of the material (kg/m^3).

Taking the equation of heat balance that explains that the heat product into a region in a time interval in part is accumulated inside the region and in part comes out through the contour of the region itself, and substituting with equations (10) and (12) it could be written:

$$\rho c \frac{\partial\vartheta}{\partial t} = div(\lambda \cdot grad\vartheta) + w \tag{14}$$

where

w is the quantity of heat generated in the unit of volume.

If it is considered only one-dimensional propagation, the equation (14) could be simplified in:

$$\frac{\partial \vartheta}{\partial t} = \frac{\partial^2 \vartheta}{\partial x^2} \frac{\lambda}{\rho c} \tag{15}$$

where

w is the quantity of heat generated in the unit of volume.

In the end is necessary write the initial conditions of the temperature $\vartheta(x, y, z, t_0) = \vartheta_0 = (x, y, z)$, and boundary conditions that describe the heat transfer on the contour; for those is needed introduce other two modality of heat transfer: convection and radiation.

$$q = q_{conv} + q_{rad} \tag{16}$$

$$q_{conv} = \alpha_c \left(\vartheta_{surf} + \vartheta_{ext}\right) \tag{17}$$

$$q_{rad} = \epsilon \cdot \sigma \cdot \left(\vartheta_{surf}^4 + \vartheta_{ext}^4 \right) \tag{18}$$

where

ϑ_{surf} is the temperature of the body surface,

ϑ_{ext} is the temperature of the external environment,

α_c is the coefficient of convection heat transfer, suggested value 25 W/m^2 K [1],

σ is the Boltzmann constant,

ϵ is the surface emissivity, suggested value 0,80 [1].

2.5 Surface protection

It is a common practice protects the surface exposed to fire with a fittingly resistant material for give at the timber elements a greater fire resistance; usually are applied gypsum plasterboard panels. The Eurocode 5 [2] provides the information also for the design of protected wood elements:

- the start of charring is retarded at t_{ch};
- the charring could start before the falling of the surface protection, but with a lower rate until the failure of the protection t_f;
- after the falling of the protection (at t_f) the charring rate increases with respect to the values shown in the table 3.1 of EC5 [2] until the time t_a described below;
- the charring depth is equal to the lower value between 25 mm or the depth of same element unprotected, the charring rate returns at a value expressed in the table 3.1 of EC5 [2].

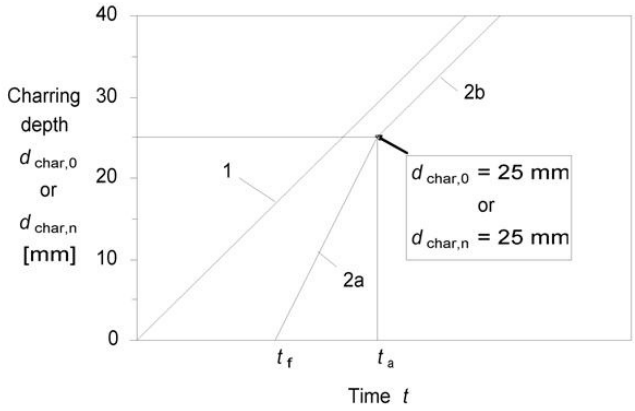

Figure 2-4 Variation of charring depth with time when $t_{ch}=t_f$ and charring depth at time t_a is at least 25 mm

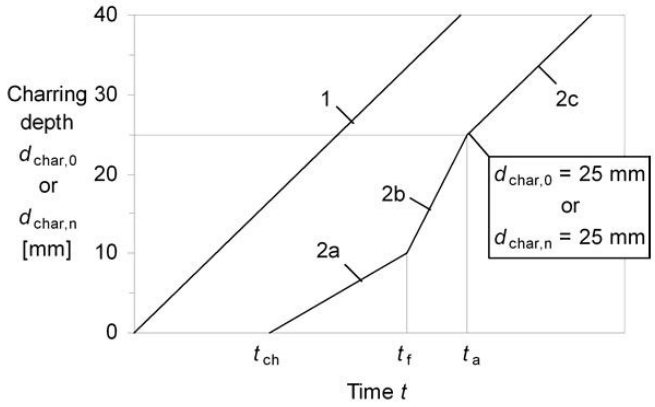

Figure 2-5 Variation of charring depth with time when $t_{ch}<t_f$

Regarding the values of t_{ch}, t_f and the their charring rate in the intervals, could be related at experimental tests or abide by the following dispositions.

For $t_{ch} < t < t_f$ (when the gypsum plasterboard is not still collapsed but the charring of wood is started) the reference charring rate should be multiplied for a factor k_2. When the timber is protected by a single layer of gypsum plasterboard type F, k_2 should be considered as:

$$k_2 = 1 - 0{,}018 \cdot h_p \tag{19}$$

where

h_p is the thickness of gypsum plasterboard in millimeters.

If the protection is composed of more layers, this value should be taken as the thickness of the more internal layer.

For $t_f < t < t_a$ (when the gypsum plasterboard is fallen but the charring rate is not at full capacity) the reference charring rate should be multiplied for a factor $k_3=2$. Over t_a could be considered the charring rate that referring to a non-protected element (β_n).

The time limit t_a could be taken for $t_{ch} = t_f$ as:

$$t_a = \min \begin{cases} 2 \cdot t_f \\ \dfrac{25}{k_3 \cdot \beta_n} + t_f \end{cases} \tag{20}$$

Or for $t_{ch} < t_f$

$$t_a = \frac{25 - (t_f - t_{ch}) k_2 \cdot \beta_n}{k_3 \cdot \beta_n} + t_f \tag{21}$$

For the protection in gypsum plasterboard type A, F or H according to EN 520:2004 [6] the time when the charring starts t_{ch} will be taken, in internal positions or on the contour next to a sealed off union (or at least with a gap lesser or equal to 2 mm) as:

$$t_{ch} = 2{,}8\, h_p - 14 \tag{22}$$

An important study of the behavior of fire protections with respect to their properties was performed by Tsantaridis, Östman and König (1999) and has conducted at these results:

- using the gypsum plasterboard panels, independently of the type, the time when the charring starts in the timber members is delayed and the charring rate is decreased,
- the best factor for predict the onset of charring in the wood is the thickness of gypsum plasterboard,
- the start time of carbonization may also be determined based on the weight per square meter of gypsum plasterboard, but it is not valid for the high density plasterboards,
- the charring rate of wood protected by gypsum plasterboard is predicted best by using the area weight of the boards, anyway for the gypsum plasterboard commonly used as wall and ceiling claddings the prediction is fairly good using also the board thickness.

This study included a good number of tests using various commercial gypsum plasterboards from five different countries. From the test results it is also possible point out that the scatter of t_{ch} for gypsum plasterboard protected specimens is limited [11].

2.6 Delamination effect of CLT

Delamination only occurs in multi-layered timber and earlier tests have proved it to cause a faster charring rate. A homogenous beam will have a slower charring-rate due to the insulating layer formed by charring. When CLT burns the insulating charred layer will fall off after each layer is completely charred. This will expose the following layer to an increased direct temperature exposure causing a faster charring rate.

As resulted in the work of Frangi, Fontana, Knoblock, and Bochicchio (2008) the fire behavior of cross-laminated solid timber panels depends on the behavior of the single layers. If the charred layers fall off, an increased charring rate needs to be taken into account. They observed the same effect for initially protected timber members after the fire protection has fallen off; therefore they have concluded that the fire behavior of cross-laminated solid timber panels can be strongly influenced by the thickness and the number of layers [12].

2.7 Effect of the adhesives

In the market are present chiefly two kinds of adhesives: melamine urea formaldehyde (MUF) that is cheap and has lower time of hardening, and one component polyurethane (PU) that is without formaldehyde. Firsts studies carried out by Empa (Swiss Federal Laboratories for Materials Testing and Research) at Duebendorf, reported that the specimens bonded by PU adhesives have presented the falling of charred layers, while in the specimens made by MUF this phenomena is not verified [14]. However latest investigations were performed at CNR-IVALSA in San Michele all'Adige, Italy. CLT panels unprotected with the layers glued by a polyurethane adhesive from Canadian SPF wood were tested on large-scale fire tests under constant loading. The tests showed that the effects of failing off of charred layers in these panels are not significant [15].

2.8 Actions and thermal properties of the wood exposed to the natural fire

In order to implement a thermal analysis for timber members using conventional simplified heat transfer models, thermal conductivity values of timber are normally calibrated to test results such that implicitly take into account influences such as mass transport that are not included in the model, König (2006) has obtained that, such analysis may use the properties of materials that EC5 part 1-2 gives, but such simplifications are valid only in the reference to a standard fire curve provides by ISO 834. The effective thermal conductivity of charred layer strongly depends on the charring rate, so it changes during a natural fire scenario. Furthermore the coal oxidation during the decay phase of natural fire has an important influence in the development of temperature in the timber members, since the temperature of charred layer is greater of temperature of gases contained in the furnace. Good results may be obtained evaluating the temperatures of gas in furnace more elevates in a fictitious way and changing the values of conductivity in the wood and in the charred depth [17].

2.9 Charring of wood investigated in small-scale tests

The charring of wood stud protected by gypsum plasterboard and unprotected has been studied by Tsantaridis and Östman (1998) in the cone calorimeter at constant heat flux (50 kW/m^2) and compared to data from full-scale furnace tests. The results obtained from this work are:

- it is possible measure the temperature profiles and charring of wood studs with or without protective boards in the cone calorimeter,
- charring depth obtained in the cone calorimeter at 50 kW/m^2 agrees well with those obtained in furnace tests during 30-40 min.

However the authors wrote that the results of charring depth can be improved by using empirical ratio to convert the data [16].

3 Overview of performed work

In this section some fire tests will be shortly described. These tests, that regard timber and CLT, were chosen in different scales and method with the aim to achieve different information to compare with the CLT small-scale test that will be analyzed. Particular attention will be given at the CLT large-scale fire tests performed with the same product that it will be tested in the cone calorimeter, in order to compare the two different methods.

3.1 CLT model-scale fire tests in horizontal furnace performed at SP Wood Technology

The tests were performed at the fire lab of SP Technical Research Institute of Swedish – Wood Technology in Stockholm, it consisted on CLT-beams loaded and exposed to fire in a horizontal furnace. More information about these can be found on the bachelor thesis of Per Willinder (2010) [20]. In the thesis there are reported tests of two types of CLT products but in this report will be considered only the MF-type.

3.1.1 Method, description of test set-up and equipment

The specimens tested were CLT-beam measuring 95 mm x 150 mm (height x width) with a span of 3300 mm, provided by the Swedish company Martinsons. The different laminations were bonded together using MUF adhesive.

Prior the fire tests, reference bending tests were conducted based on the standardized method of EN 789:2004 [7] for determine the CLTs bending strength and stiffness at normal temperature. To expose the beams to ISO standard fire [4] a model furnace at SP Wood Technology was used. All CLTs were subjected to different, but constant, amount of load during the test in order to apply bending-forces in compression or tension mode; the range of load was in general between 20%-40% of CLT-beams bearing capacity. The fire exposed of the beam was 1000 mm; before testing the beams were conditioned in climate room at 20ºC and RH 60%.

Figure 3-1 A CLT-beam mounted in to the horizontal furnace during test at SP Wood Technology, Stockholm

All CLTs were equipped with wooden boards and gypsum plasterboard on its side to prevent charring and heating from the side and minimize the effect of fire spreading around the beam keeping the heat exposure one-dimensional. Half of the tests were made with additional protection of gypsum plasterboard type F on the fire-exposed side of the CLTs; see the

Table 3-1 for more details. To be able to follow and analyze the heat subjected to CLTs during the tests the CLTs were equipped with thermocouples on its bottom side, positioned in between the beam and the gypsum plasterboard; additional thermocouples were equipped also inside the beams from the lateral side. For the exact positions of the thermocouples see *Table 4-1*.

Figure 3-2 Detail of the side protection and beam from the bottom view of specimen MF03

During the tests observations were done. The pressure inside the furnace was recorded, temperature measured, the applied load was controlled and deflection recorded.

3.1.2 Results

A compilation of the tests conducted can see below.

Table 3-1 Compilation of MF series furnace test

Beam number	Type of load	GP protection	Amount of total bearing capacity	Time of failure (min)
MF05	tsw	no	37%	49
MF02	tsw	no	48%	14
MF07	tsw	no	37%	54
MF06	tsw	yes	35%	94
MF10	tsw	yes	26%	106
MF03	tsw	yes	26%	91
MF04	tsw	yes	50%	26
MF08	tsw	yes	50%	30
MF11	csw	no	31%	39
MF14	csw	no	38%	37

The temperature data recorded during the tests were elaborated in order to gain for each specimen the charring depths, from the temperature value available were pinpointed the times when the thermocouples have reached the 300°C. i.e. the moment when the wooden material starts to char; as suggested in the Eurocode 5 part 1-2 [2]. Since the temperature recordings are available in time steps of 5 s, linear interpolation was used to define the time when the char-line reaches the thermocouple position.

Following will be shown in two different graphs these times versus the corresponding thermocouple; the results plotted were separated for the in “fire protected tests” and “fire unprotected tests”.

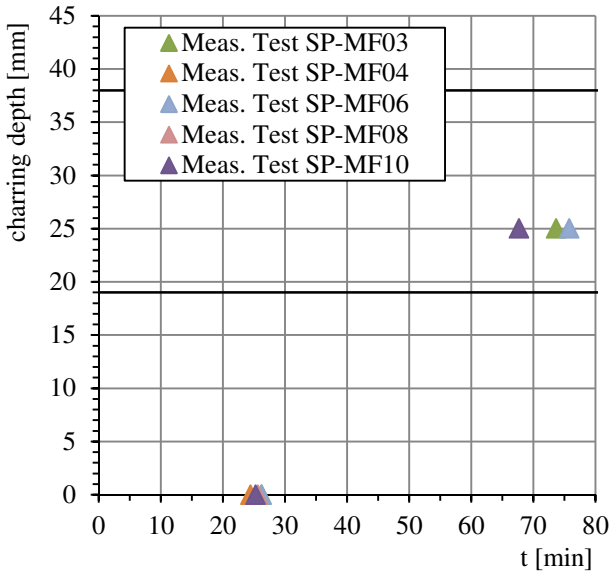

Figure 3-3 Analysis of charring for the fire protected tests performed at SP Wood Technology

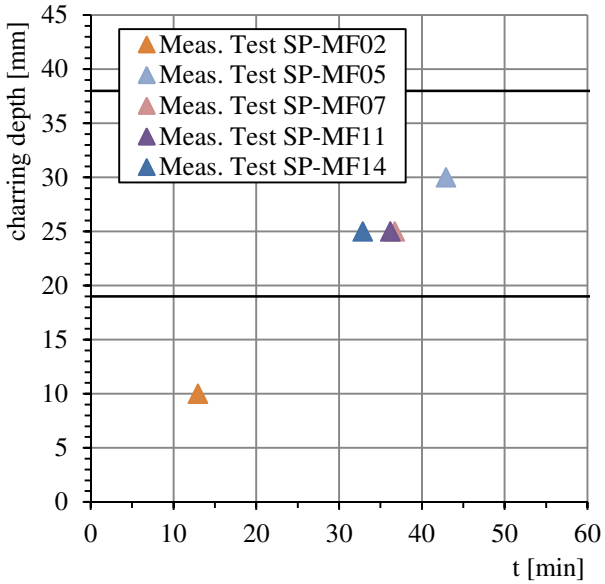

Figure 3-4 Analysis of charring for the fire unprotected tests performed at SP Wood Technology

3.2 CLT large-scale fire tests in vertical furnace performed at CNR-IVALSA

The tests were performed at the laboratory of reaction and fire resistance of Trees and Timber Institute CNR–IVALSA in San Michele all´Adige, Italy. It consisted on CLT-stripes loaded and exposed to fire in a vertical furnace. An extensive discussion of these tests can be found on the master thesis of Matia Goina (2010) [21]. In the thesis there are reported tests of two types of CLT products but in this report will be considered only the MF-type.

3.2.1 Method, description of test set-up and equipment

The specimens used had a height of 95 mm, width 600 mm and length of 3300 mm; with the layer bonded using MUF adhesive. Also these specimens were provided by the Swedish company Martinsons. Before the fire test, specimens of the same type were tested at compression parallel and perpendicular to wood fiber and buckling load of the panel, all of them with test methods according to EN 789 [7]. The specimens were exposed to a standard fire according to ISO 834 [4] in a vertical furnace at CNR-IVALSA which has a square opening of 3x3 m; the load levels chosen for these tests were at 11% and 21% of the breaking load of panel tested at room temperature. The tests were performed following EN 1363-1 [5] which required the control of the furnace temperature by means of plate thermometer. One of three specimens was protected with a panel of gypsum plasterboard on fire-exposed side. To facilitate an one-dimensional heat propagation were placed protections composed by a wood board and a layer of gypsum plasterboard on the longer sides of the specimens; the thicknesses of the board wood and gypsum plasterboard were respectively 21 mm and 15 mm. To gain the internal temperature of CLTs were placed thermocouples in three different depths and were embedded from the lateral side; more information about that can find in the *Table 4-1*.

3.2.2 Results

All the three tests were stopped before the breaking of the panel due to a leakage of flames from the side unexposed to fire. A compilation of the tests conducted can see below.

Table 3-2 Compilation of LFV series furnace test

Test number	GP protection	Amount of total bearing capacity	Duration of the test (min)
LFV002	no	11%	103
LFV003	no	21%	68
LFV004	yes	11%	124

Also for these tests from the temperature data recorded were pinpointed the times when the thermocouples have reached the 300°C in order to gain for each specimen the charring depths. See below the results of the charring depth divided in two graphs, respectively for the “fire protected tests” and the “fire unprotected tests”.

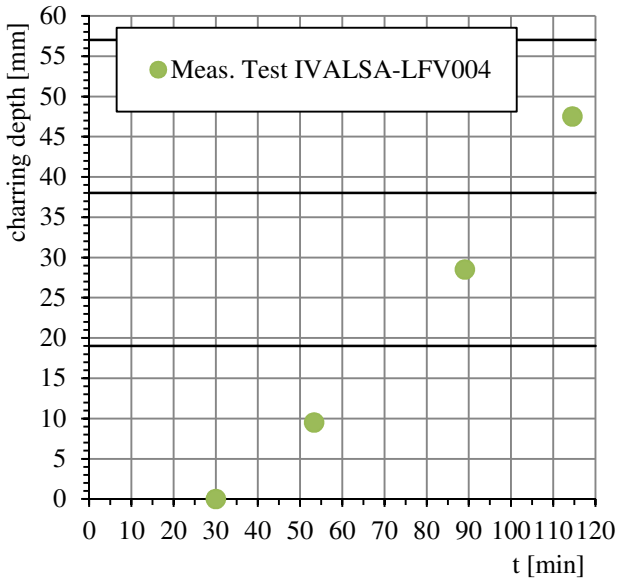

Figure 3-5 Analysis of charring for the fire protected tests performed at CNR-IVALSA

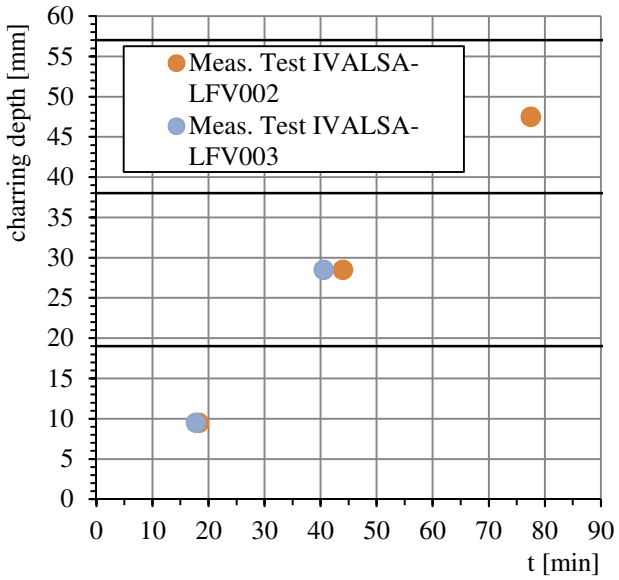

Figure 3-6 Analysis of charring for the fire unprotected tests performed at CNR-IVALSA

4 Experiments

4.1 Description of test set-up and equipment

4.1.1 CLT specimens

The cross laminated timber specimens used were provided by the Swedish company Martinsons. The specimens were composed by 5 layers (depth h_i=19 mm) for a total thickness h=95 mm. Were used 1 set of 5 specimens, the dimensions are 95x100x45 mm. The different layers were bonded together using MUF adhesive. The measure of the CLT specimens showed deviance from their expected dimensions of about +/- 1 mm in each direction. All the specimens were conditioned in a controlled climate chamber at 20ºC and 60% RH, corresponding EMC 11,8% [19], before testing and the range of conditioned density was between 444 and 476 kg/m^3 and the mean density measured was 454 kg/m^3. Following these samples will be called type MF.

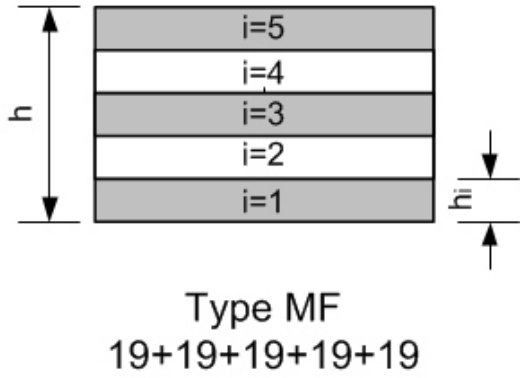

Figure 4-1 Layout of CLT specimens used in the tests

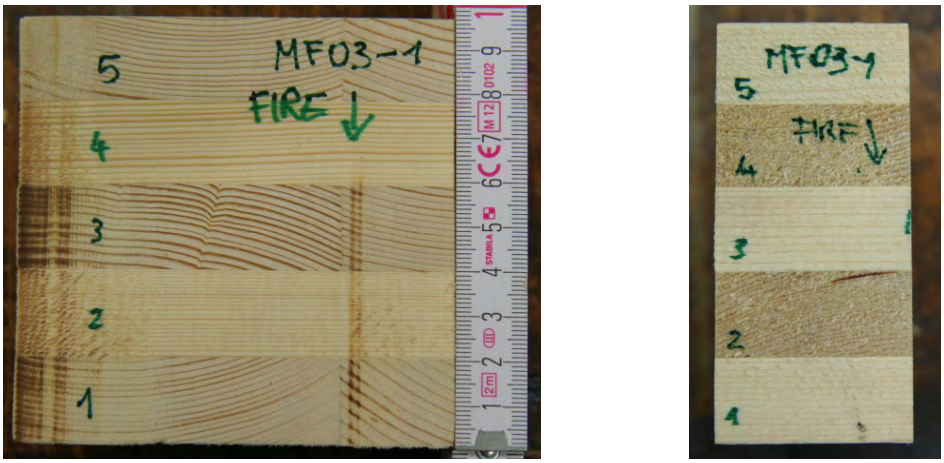

Figure 4-2 CLT specimens used in the tests

4.1.2 Massive Timber specimens

The massive timber specimens were chosen of spruce responded at C30 class in according to EN 338:2009 [3] and fairly free from knots. Were used 1 set of 6 specimens, the dimensions are 135x100x45 mm. The specimens were selected form a timber studs with a width of 45 mm and a height of 135 mm. The range of conditioned density was between 413 and 422 kg/m^3 and the mean density measured was 418 kg/m^3. Following these samples will be called type T.

Figure 4-3 Massive Timber specimens used in the tests

4.1.3 Gypsum plasterboard as fire protection

Samples of Gypsum plasterboard type F according to EN 520:2004 [6] were chosen as fire protection. The average thickness was of 14,6 mm by a calculated area weight between 13,9 and 14,2 kg/m^2.

Figure 4-4 Samples of gypsum plasterboard used in the tests

4.1.4 Plywood panel as fire protection

The plywood samples used were chosen by birch wood and provided by the Finnish company Metsä Wood. The samples were composed by 7 layers for a total nominal thickness h=9 mm. The different layers were bonded together using with a weather and boil-resistant phenolic resin adhesive. A calculated mean density was 661 kg/m^3.

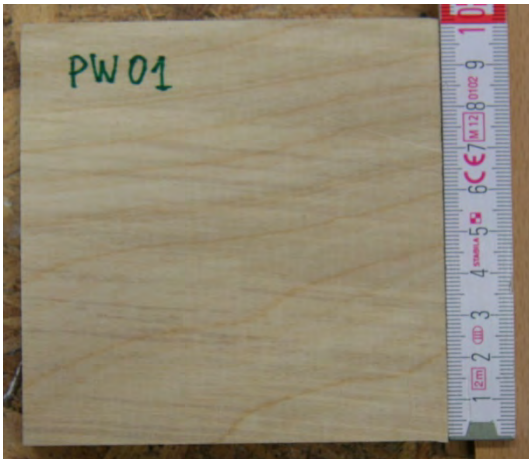

Figure 4-5: Sample of plywood used in the test as fire protection

4.1.5 Insulation

The insulation material used was stone wool produced by the company Paroc, Finland. The product presented a nominal thickness of 45 mm and a CE certificated conductivity of 0,037 W/(m K). An average density of 32 kg/m^3 was measured.

4.1.6 Thermocouples

Thermocouples type K with a diameter of 0,25 mm were used. The wire (batch nº D7768-A) was produced by Pentronic AB, Sweden, it was calibrated by the producer and it showed at 300ºC a correction of +0,5ºC and a tolerance ±0,2 ºC.

4.1.7 Preparation of the specimens

The test specimens consisted of wooden sample (MF and T type) and stone wool insulation on both sides to simulate an one-dimensional heat propagation. In most cases a fire protection was attached to exposed side, see *Figure 4-9.* Thermocouples of chromel-alumel were located in holes of 1 mm diameter and 25 mm length. These holes were drilled perpendicular to the wide side of the wooden studs; further considerations about the positioning of the thermocouples can be found in the following sections. The thermocouples were kept in full contact with the surrounding wood by fixing the wires with metal staple

Figure 4-6 Diameter and length of the drill

4.1.8 Test procedure

The tests were performed at SP Technical Research Institute of Swedish – Wood Technology in Stockholm.
The same procedure was used for all the tests performed:

1. measuring of dimensions and weight for the CLT specimens, massive timber specimens, fire protection and lateral thermal insulation;
2. drilling the holes for placement of the thermocouples;
3. placing of thermocouples type K;
4. covering of the wooden sample with fire protection (when required) and lateral insulation and placing in the specimen holder;
5. connection the thermocouples to the device for saving data;
6. switching on of the cone calorimeter and setting the heat flux at 50 kW/m^2;
7. waiting for the stabilization of the value of heat flux;
8. positioning of the specimen holder (contained the specimen) in the cone calorimeter;
9. switching of the heat flux value at 75 kW/m^2 after 23 minutes by the positioning;
10. removing the specimen holder from the cone calorimeter;
11. extinguishment of the specimen;
12. evaluation of residual cross section.

4.1.9 Description and calibration of the test machine

To expose the specimens to the heat flux a cone calorimeter at SP Wood Technology was used. This device is a small-scale instrument to measure rate of heat release, ignition time and smoke production of building products. This unit was constructed at SP Wood Technology, with main parts from State University of Gent, and completed in 1987. A square specimen of 100 mm x 100 mm is exposed to radiant heat flux of an electric heater. The heater has the shape of truncate cone (hence the name of the instrument) and is capable of providing heat fluxes to the specimen in the range of 0-100 kW/m^2. The upper and lower diameters of the cone heater are 80 and 177 mm, respectively. The heater is normally in the horizontal orientation with specimen 25 mm underneath the base plate. The power supplied is controlled by an electronic temperature controller using a chromel-alumel thermocouple of type K. Calibration of heat flux as function of heater temperature is performed with a total heat flux meter of the Schmidt-Boelter type. Such a meter consists of a circular target receiving radiation. The target is flat, water-cooled and coated with a durable matt black finish. Two thermocouple junctions are located at different depths belows the exposed surface. Under steady conditions, thermocouple output is proportional to the incident flux. Due to various factors such as ageing of the heater coil, the relationship between heat flux and heater temperature changes with time. The heat flux calibration has therefore to repeated frequently [18].

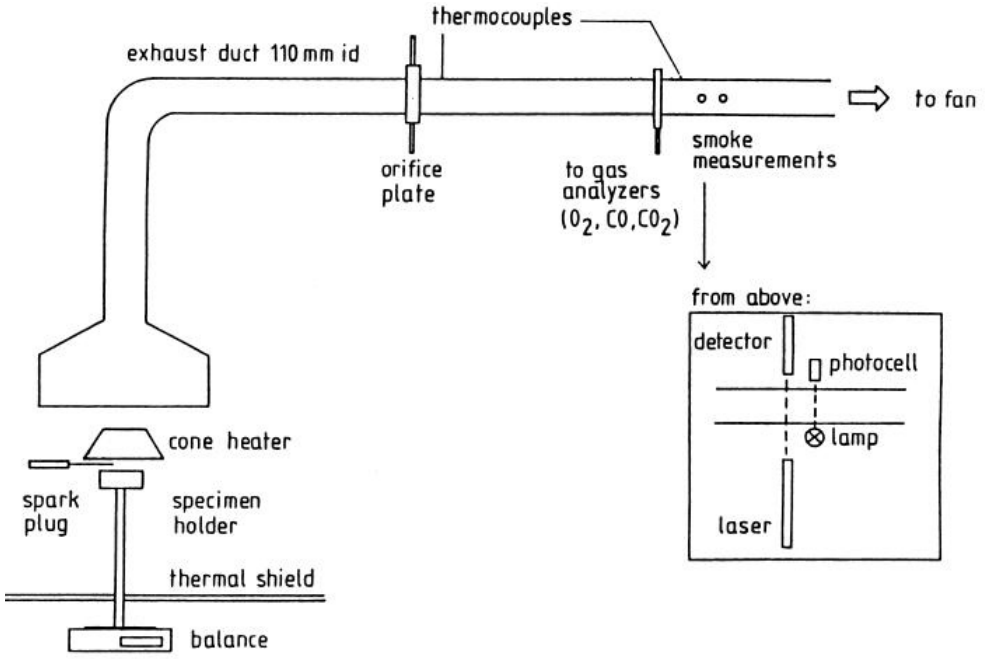

Figure 4-7 Schematic set-up of the Cone Calorimeter used at SP Trätek/Wood Technology

The calibration consist in the measuring of an electrical potential from the heat flux meter and its correlation with an heat flux; two heat flux values were measured by an analogical voltmeter with the precision of 0,1 mV. Since the corresponding values of electrical potential needed a precision of 0,01 mV the heat flux could have a certain error which it is sought to minimize appreciating as far as the eye can see the value of the electric potential required.

In this study the heat flux values were measured at the start of the tests; the electronic temperature control system was adjusted so that the conical heater produces the required heat flux as measure by heat flux meter.

As Tsantaridis obtained in his work, a heat flux of 50 kW/m^2 corresponds roughly to the ISO 834 standard time-temperature curve during the first 30-40 min [16] then corresponds to a higher heat flux. During the calibration once the 50 kW/m^2 heat flux was stabilized, it was moved to a value of 75 kW/m^2 in three, more o less equal, steps and were measured the heat flux values every 30 s until the flux was stabilized. The data obtained from these measuring were compared with the "SP furnace" time-heat flux curve [16] that is the heat flux values measured during an ISO 834 standard fire test in a furnace without any specimen inside. All that in order to find the moment of changing of heat flux value that allow a better fitting with "SP furnace" time-heat flux curve, as shown in *Figure 4-8*.

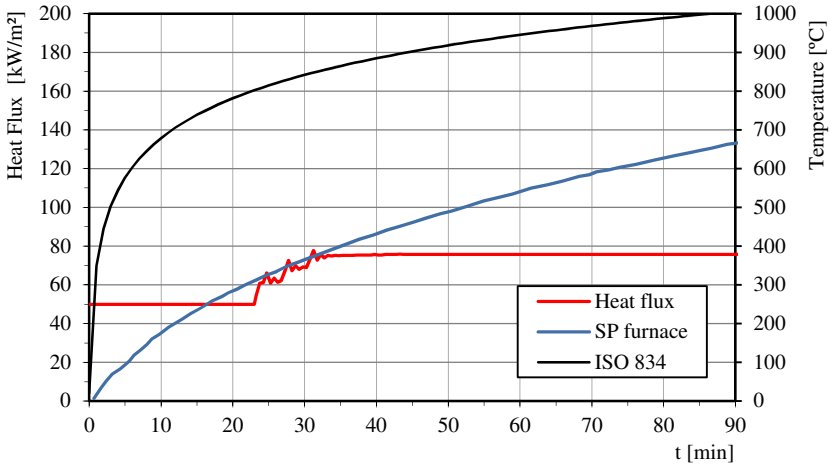

Figure 4-8 "SP furnace" time-heat flux curve and heat flux measured during the calibration of the cone calorimeter

4.1.10 Positions of thermocouples

To compare the results of the cone calorimeter test in the specimens made in CLT and massive timber with other test in full, medium and small scale test performed with furnace and cone calorimeter, then the thermocouple´s positions of those tests have to be considered. See in the *Table 4-1* the products and its thermocouples positions for considered tests.

Table 4-1 Products, methods and location of the thermocouples in the performed tests

Tests:							
Goina [21]		Wilinder MF [16]		Schmid [22]		König S4-S5 [23]	
Product:							
CLT h = 95 mm (19x5)		CLT h = 95 mm (19x5)		Massive Timber h = 135 mm		Massive Timber h = 95 mm	
Supplier:							
Martinsons		Martinsons		Unknown		Unknown	
Method:							
Furnace Large scale test		Furnace Full scale test		Cone calorimeter Small scale test		Furnace Large scale test	
Protection to fire:							
NOT ALL		NOT ALL		YES		NO	
Position of TC (from the fire exposed side of wooden member): [mm]							
TC1	0	TC 1	0	TC 1	0	TC 1	12
TC 2	9,5	TC 2	10	TC 2	6	TC 2	36
TC 3	28,5	TC 3	25	TC 3	12	TC 3	60,5
TC 4	47,5			TC 4	18	TC 4	84
				TC 5	30		
				TC 6	42		
				TC 7	54		
				TC 8	68		

The tests performed by Goina [21] considered the thermocouples position at mid-height of first three layers from the fire exposed side. Wilinder [20] and Schmid [22] considered the first thermocouple in the interface between the protection and the timber element. Also Wilinder [20] has positioned the thermocouples in the first and second layer of CLT but not at mid-height. Schimd [22] has positioned the first three thermocouples every 6 mm and the other four every 12 mm. The tests performed by Köning [23] were chosen as a comparison to the size of the sample coincides with that of type specimens MF.

Since it could be important to know the temperature in the interface between the protection (if available) and in the first two CLT layers from the exposed fire side; but could be also interesting to know the temperature in the bonded layers of first two elements. The thermocouple positions in the layers would be in middle, however could be difficult collimate half millimeter. See in the *Table 4-2* the thermocouples position choices.

Table 4-2 Products, methods and location of the thermocouples in the tests to carry out

Specimens:			
MF		T	
Product:			
CLT h = 95 mm (19x5)		Massive Timber h = 135 mm	
Supplier:			
Martinsons		Unknown	
Method:			
Cone calorimeter Small scale		Cone calorimeter Small scale	
Position of TC to give (from the fire exposed side of wooden member):			
TC 1	0 mm	TC 1	0 mm
TC 2	6 mm	TC 2	6 mm
TC 3	10 mm	TC 3	10 mm
TC 4	19 mm	TC 4	19 mm
TC 5	29 mm	TC 5	29 mm
TC 6	69 mm	TC 6	69 mm

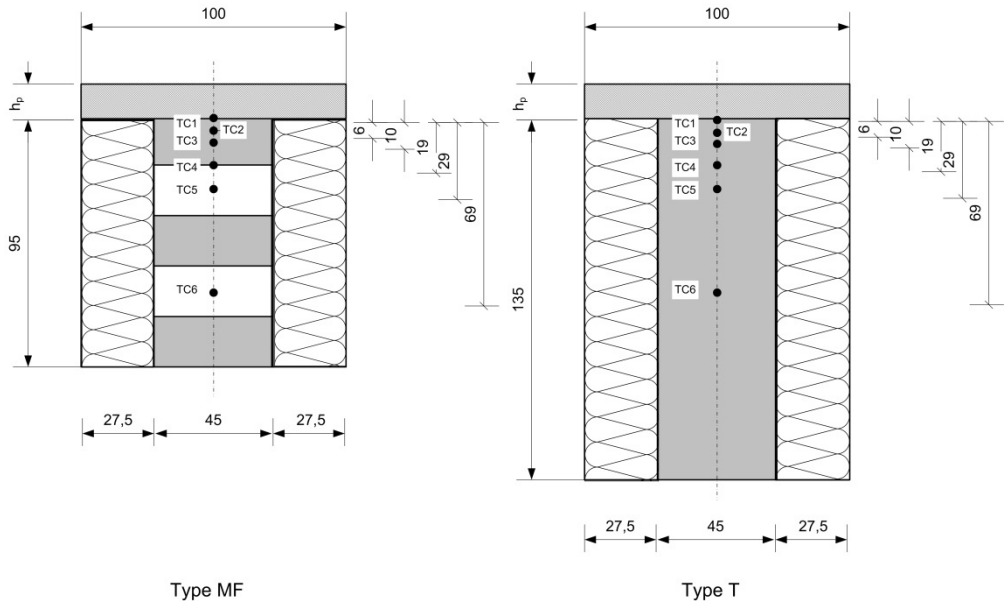

Figure 4-9 Cross section of test samples with the fire protection on the top and the thermocouples, dimensions in mm

4.1.11 Problems in the placement of the thermocouples

To avoid not all of the thermocouples were inserted in the exact middle axis of the specimen overlap. To estimate the maximum distance of the thermocouples from the middle axis of specimen a simulation was performed of half CLT specimen exposed to a fire ISO standard. *Figure 4-10* shows that the isotherm at 300ºC (see the red region) for the first 10 mm from the middle axis is rather horizontal; it means that it is acceptable that the thermocouples deviate up to 10 mm from the middle axis without significant temperature difference from the temperature at the middle axis.

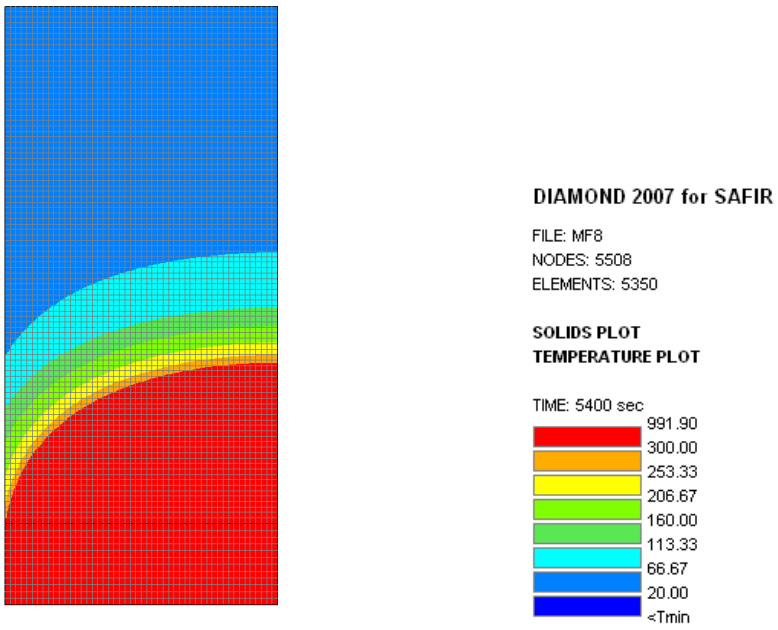

Figure 4-10 SAFIR 2007 simulation of half MF-type specimen view from the wider cross section. The timber mesh measure 1mm x 1mm; the GP mesh measure 1,25mm x 1 mm

Another problem was found in the placement of thermocouples number 4 in the CLT specimens. The problem involved the drilling of the hole in the bond line between two wood layers: the drill bit could not keep the right position in bond line, but could shift in the upper layer or in the lower layer. Avoid this problem the drill hole was to located at the position in the bond line where there are only earlywood for both the CLT layers bonded.

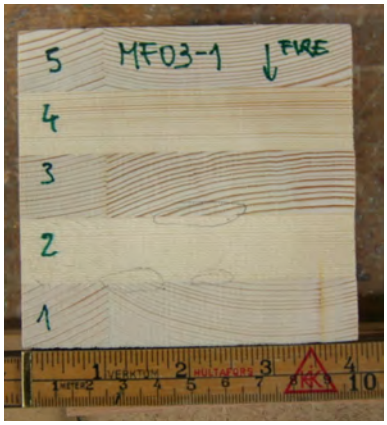

Figure 4-11 Individuation of drill hole point for the specimen MF03-1

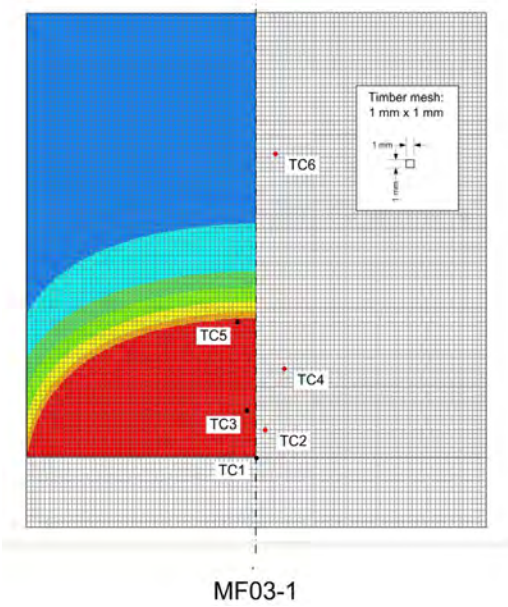

Figure 4-12 Design of thermocouples positions for the specimen MF03-1

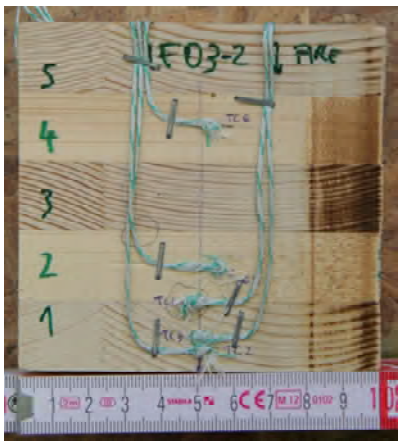

Figure 4-13 Thermocouples placed in a CLT sample

4.1.12 Observation during the tests

During tests observations were done. The temperature was recorded, times of start smoking and glowing paper were written for the tests protected by gypsum plasterboard, times of start smoking and ignition time were written for the unprotected specimens tested.

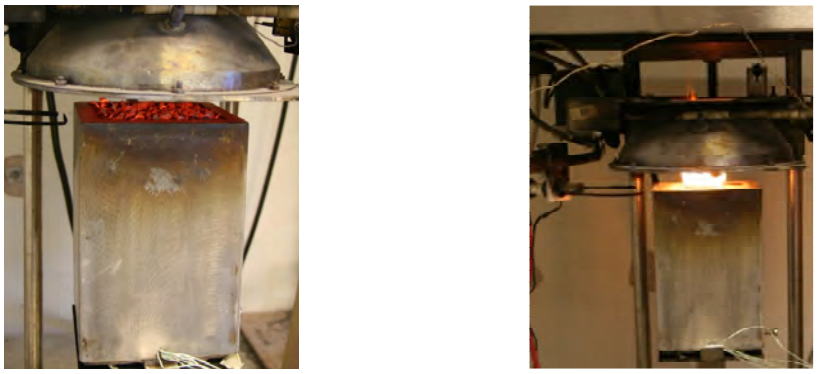

Figure 4-14 Start of glowing paper in the gypsum plasterboard for a fire protected test and ignition in a wooden specimen for an unprotected test

4.1.13 Investigation for the delamination effect

At the time does not exist a standard for verify the delamination in the CLT, an heat durability test exist for the plywood, as described in CSA Standard O151 [24] and NIST PS 1-07 [25] is a standard test that involves exposing to a Bunsen burner flame for 10 minutes a plywood specimen bonded with the adhesive. Not being able to find similarities between this test and the test designed for this study a different investigation was conducted for the delamination. After the extinguishing the test specimen was allowed to cool, then was tried to break with the hands the specimen on the first not-charred bond line and was verified if the test had success or not. One test was stopped when the thermocouple placed in the first bond line from the fire-exposed side (TC 4) reached the 300ºC.

4.2 Test 01

4.2.1 Overview of the test

Table 4-3 Summary of Test 01

Specimen	Fire protection	Duration
T04	GP01	60 min

Figure 4-15 Set-up of Test 01

4.2.2 Observation during the test

Table 4-4 Observations of Test 01

Time from the start of test	Observations
01:02	lot of smoke
01:32	glowing paper
-	temperatures read with significant deviations from the temperatures expected for TC02, TC03, TC04 and TC05
60:12	end time
-	delamination-control: it was not possible to break the specimen

4.2.3 Data recorded by the thermocouples during the test

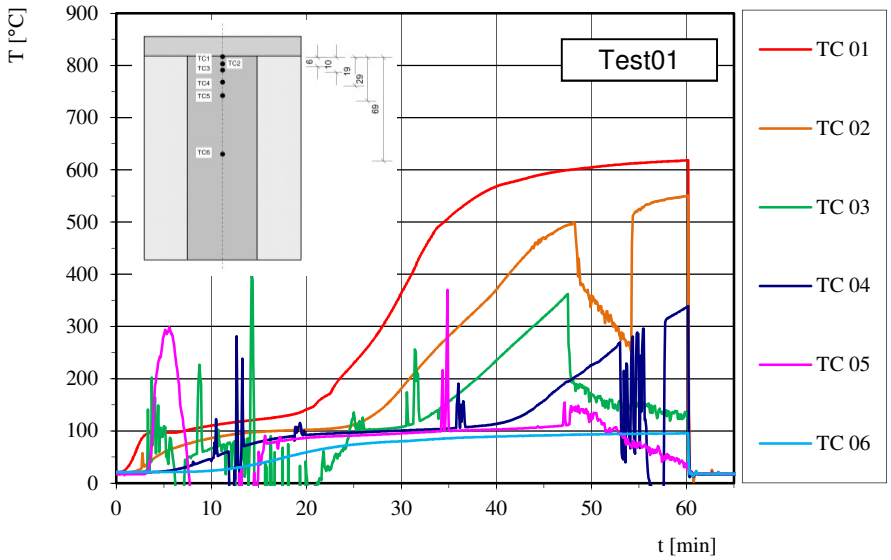

Figure 4-16 Data recorded by the thermocouples during the Test 01

4.3 Test 02

4.3.1 Overview of the test

Table 4-5 Summary of Test 02

Specimen	Fire protection	Duration
T05	GP02	60 min

Figure 4-17 Set-up of Test 02

4.3.2 Observation during the test

Table 4-6 Observations of Test 02

Time from the start of test	Observations
00:45	lot of smoke
02:23	glowing paper
33:50	heat flux of 75 kW/m^2 is stable
-	no problem found during testing
60:17	end time
-	delamination-control: it was not possible to break the specimen

4.3.3 Data recorded by the thermocouples during the test

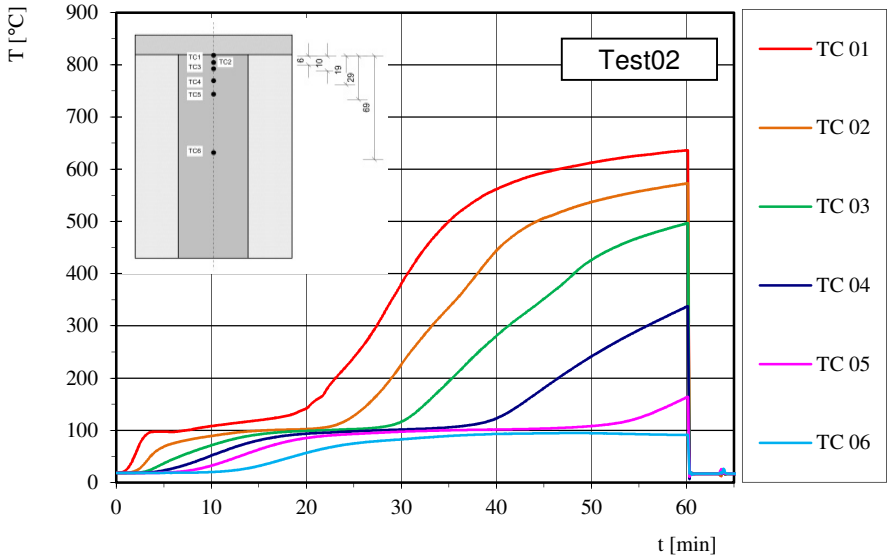

Figure 4-18 Data recorded by the thermocouples during the Test 02

4.4 Test 03

4.4.1 Overview of the test

Table 4-7 Summary of Test 03

Specimen	Fire protection	Duration
MF04-2	GP05	60 min

4.4.2 Observation during the test

Table 4-8 Observations of Test 03

Time from the start of test	Observations
00:29	first smoke
00:51	lot of smoke
01:21	first glow in the paper
01:41	glowing in all the paper
-	TC01 does not register increasing of temperature
06:35	TC01 back to work
28:05	temperatures read with significant deviations from the temperatures expected for TC02
34:13	heat flux of 75 kW/m^2 is stable
60:19	end time
-	delamination-control: it was not possible to break the specimen

4.4.3 Data recorded by the thermocouples during the test

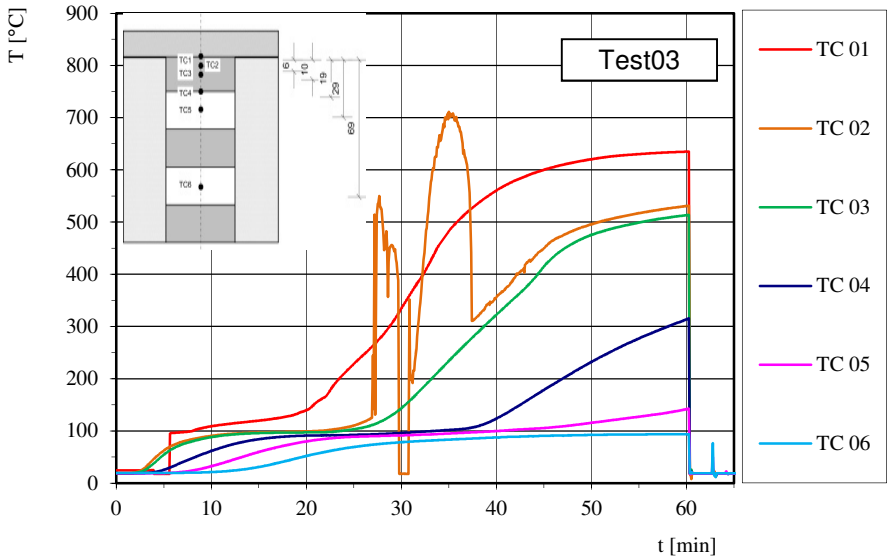

Figure 4-19 Data recorded by the thermocouples during the Test 03

4.5 Test 04

4.5.1 Overview of the test

Table 4-9 Summary of Test 04

Specimen	Fire protection	Duration
T01	GP11	90 min

4.5.2 Observation during the test

Table 4-10 Observations of Test 04

Time from the start of test	Observations
00:47	lot of smoke
02:27	glowing paper
-	no problem found during testing
90:07	end time
-	delamination-control: it was not possible to break the specimen

4.5.3 Data recorded by the thermocouples during the test

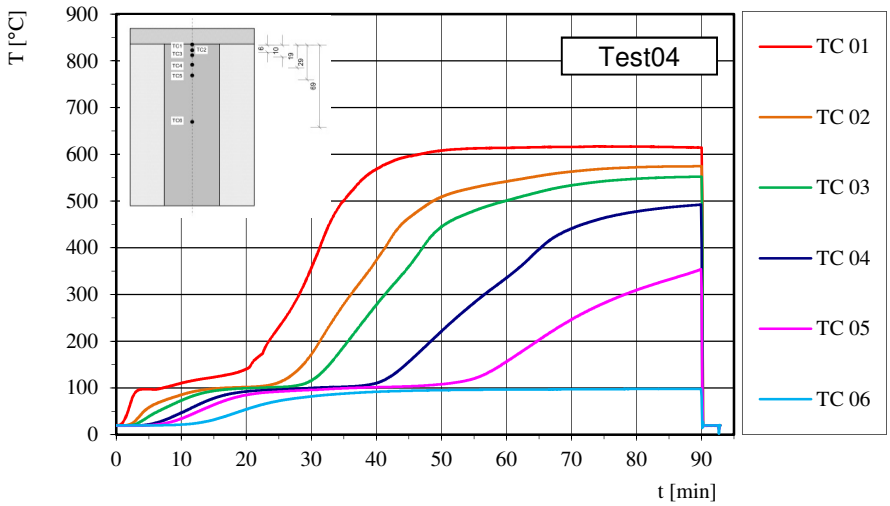

Figure 4-20 Data recorded by the thermocouples during the Test 04

4.6 Test 05

4.6.1 Overview of the test

Table 4-11 Summary of Test 05

Specimen	Fire protection	Duration
MF03-1	unprotected	60 min

4.6.2 Observation during the test

Table 4-12 Observations of Test 05

Time from the start of test	Observations
00:21	lot of smoke
00:31	ignition
-	temperatures read with significant deviations from the temperatures expected for TC01
14:14	TC01 back to work
32:43	heat flux of 75 kW/m^2 is stable
60:51	end time
-	delamination-control: it was not possible to break the specimen

4.6.3 Data recorded by the thermocouples during the test

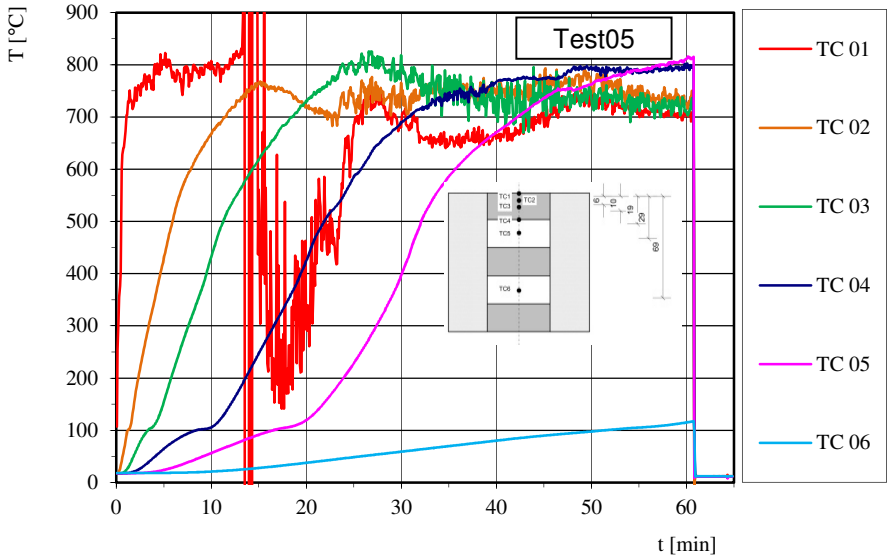

Figure 4-21 Data recorded by the thermocouples during the Test 05

4.7 Test 06

4.7.1 Overview of the test

Table 4-13 Summary of Test 06

Specimen	Fire protection	Duration
MF03-2	GP03	61,2 min

This test was stopped when the TC04 reached a temperature of 300ºC.

4.7.2 Observation during the test

Table 4-14 Observations of Test 06

Time from the start of test	Observations
00:47	first smoke
01:02	lot of smoke
01:47	glowing paper
29:17	heat flux of 75 kW/m^2 is stable
41:42	temperatures read with significant deviations from the temperatures expected for TC02
61:14	end time
-	delamination-control: it was not possible to break the specimen

4.7.3 Data recorded by the thermocouples during the test

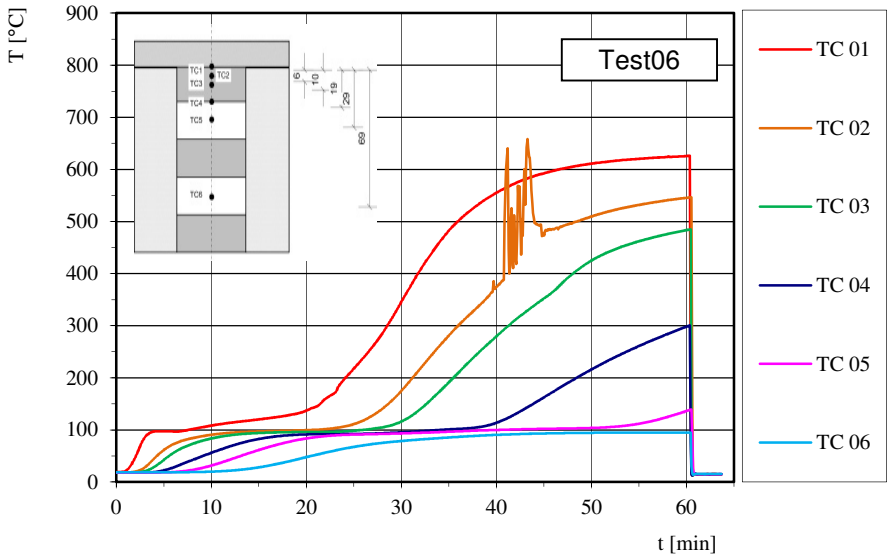

Figure 4-22 Data recorded by the thermocouples during the Test 06

4.8 Test 07

4.8.1 Overview of the test

Table 4-15 Summary of Test 07

Specimen	Fire protection	Duration
T03	unprotected	60 min

Figure 4-23 Specimen T03 in the specimen holder before testing

4.8.2 Observation during the test

Table 4-16 Observations of Test 07

Time from the start of test	Observations
00:14	lot of smoke
00:19	ignition
31:27	heat flux of 75 kW/m^2 is stable
-	no problem found during testing
61:17	end time
-	delamination-control: it was not possible to break the specimen

4.8.3 Data recorded by the thermocouples during the test

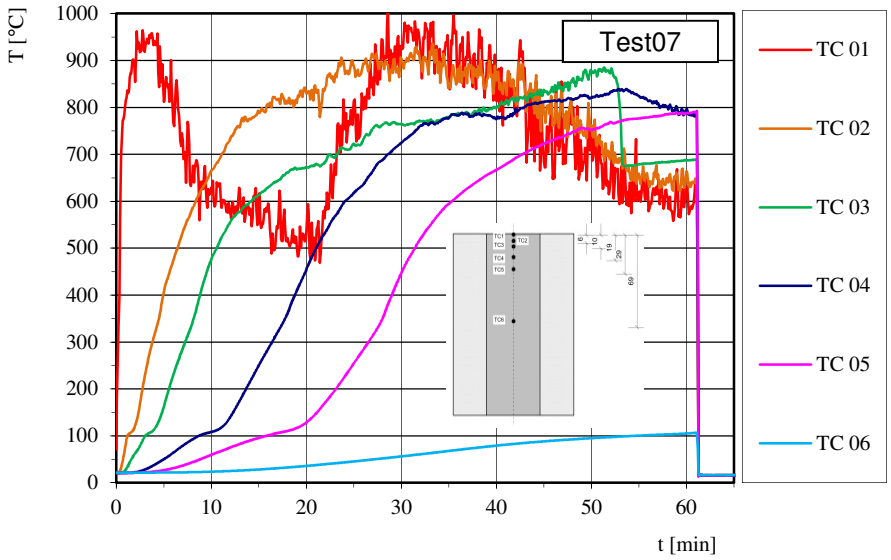

Figure 4-24 Data recorded by the thermocouples during the Test 07

4.9 Test 08

4.9.1 Overview of the test

Table 4-17 Summary of Test 08

Specimen	Fire protection	Duration
T02	PW01	60 min

Figure 4-25 Set-up of Test 08

4.9.2 Observation during the test

Table 4-18 Observations of Test 08

Time from the start of test	Observations
00:14	lot of smoke
00:19	ignition
35:14	heat flux of 75 kW/m^2 is stable
-	no problem found during testing
60:08	end time
-	delamination-control: it was not possible to break the specimen

4.9.3 Data recorded by the thermocouples during the test

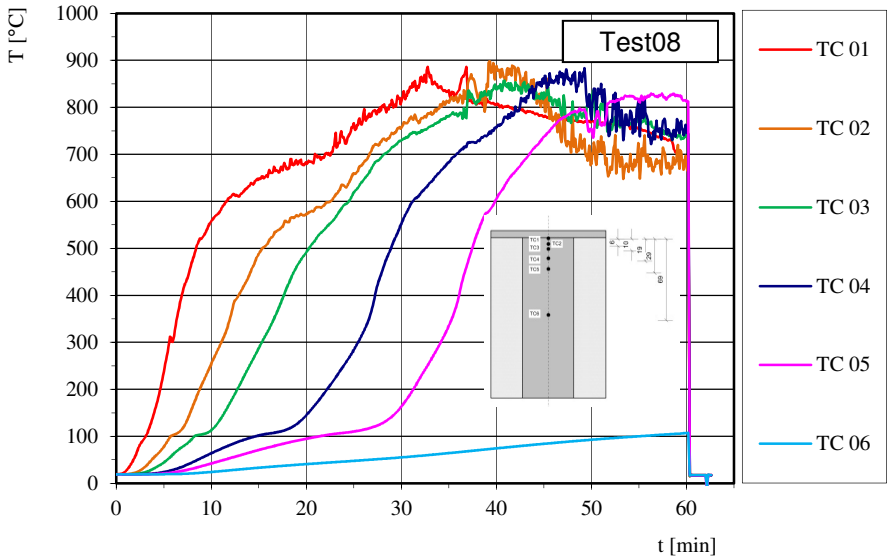

Figure 4-26 Data recorded by the thermocouples during the Test 08

4.10 Test 09

4.10.1 Overview of the test

Table 4-19 Summary of Test 09

Specimen	Fire protection	Duration
MF04-1	PW02	60 min

4.10.2 Observation during the test

Table 4-20 Observations of Test 09

Time from the start of test	Observations
00:24	lot of smoke
00:35	ignition
37:17	heat flux of 75 kW/m^2 is stable
-	no problem found during testing
60:42	end time
-	delamination-control: it was not possible to break the specimen

4.10.3 Data recorded by the thermocouples during the test

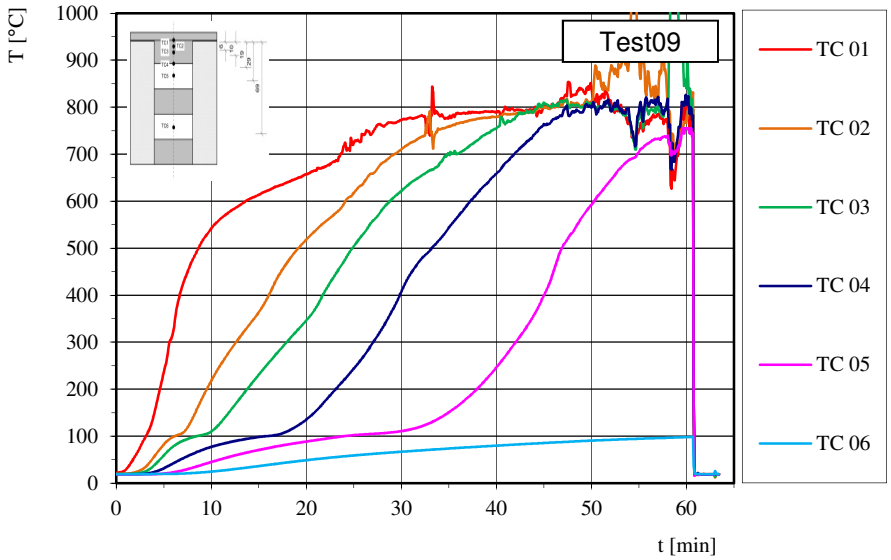

Figure 4-27 Data recorded by the thermocouples during the Test 09

4.11 Description of analysis of specimens post test

4.11.1 Documentation of specimen post-cone calorimeter

The specimens were documented after the cone calorimeter test by photography. All the photographs have a point of reference as a folding ruler. Since the charring depth is crucial data for the project the specimens were cut into two pieces along 100 mm long area which have been exposed to fire.

Figure 4-28Specimen MF04-2 after the extinguishing and after the cutting in two pieces

4.11.2 Recording of the residual cross section and analysis

To compare the result of the tests and simulations residual cross sections were recorded. This is important for describe the rate of charring and the charring depth. Analysis was done by inverting the colors of the photograph to get a good clean image. All the edges of the specimen were important for achieve other design values that will be described in this report.

To be able to determine moment of inertia ($I_{z,res}$) and the remaining area after the tests the software AutoCAD was used. Using the folding ruler as a reference the photographs were scaled. Using the command “polyline” the regions not charred of inverted photographs of the residual cross sections was marked. It is important remind, only the actual load bearing part of the cross section is of interest and therefore the shape did not include any remaining charring. When using an inverted photograph, these sections are represented by having white color for the charred region and the load bearing part is close to blue by using the command “massprop”, data concerning the area, moment of inertia, extreme points of the not charred section could be extracted automatically. This data will be analyzed in the “Results” section.

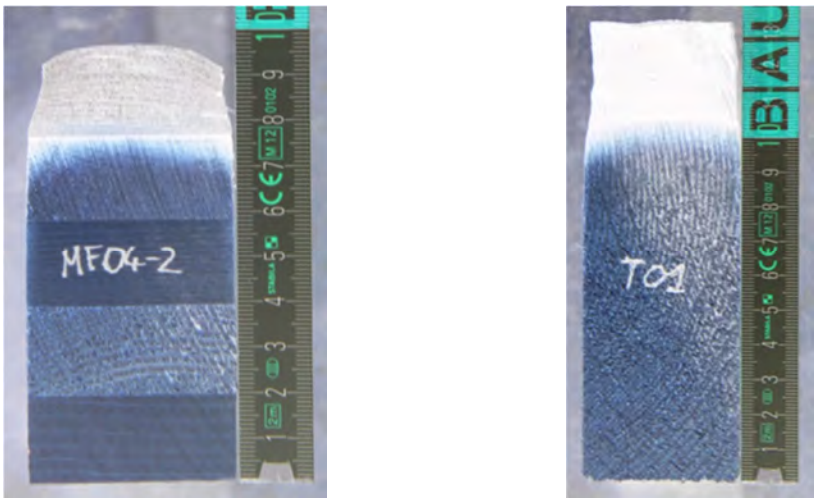

Figure 4-29 Examples of inverted images used for determination of residual cross sections

5 Results

In this section will be described how the data obtained by the cone calorimeter tests were managed and after that the results will be shown for each test carried out.

5.1 Compilation of test

A compilation of all test conducted on the cone calorimeter can see below stating the kind of specimen, the kind of fire protection used and duration time.

Table 5-1 Compilation of cone-calorimeter tests

Test	Specimen	Fire protection	Duration [min]
01	T04	GP01	60
02	T05	GP02	60
03	MF04-2	GP05	60
04	T01	GP11	90
05	MF03-1	unprotected	60
06	MF03-2	GP03	61,2
07	T03	unprotected	60
08	T02	PW01	60
09	MF04-1	PW02	60

5.2 Selection of temperature values recorded

Since for some tests the temperature values recorded have proved that differ from those expected the data have been selected. The selection was made by identifying the data quite clearly differed from the expected results and these data were discarded.

One reason why some data differed from the expected data could be caused by a not perfect preparation of the thermocouples and them connections, especially when the unexpected data can be found from the beginning of the test. Another cause may be due to the fact that the wire for the thermocouples was guaranteed for temperatures up to 500ºC; this aspect can be seen in some data series when they begin to diverge from the expected data at the high temperatures.

The tests subject to correction of the temperature values are Test 01, Test 03, Test 05 and Test 06.

5.2.1 Selected temperature values for the Test 01

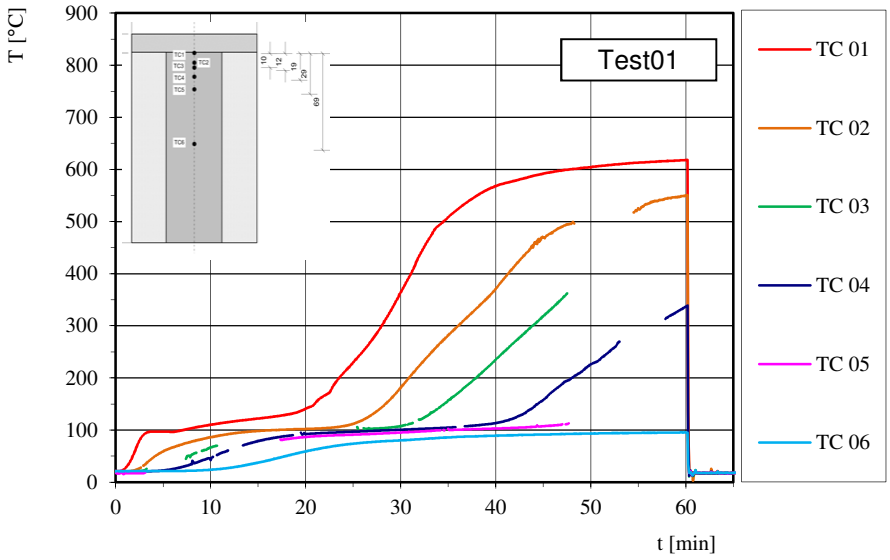

Figure 5-1 Selected temperature values for the Test 01

5.2.2 Selected temperature values for the Test 03

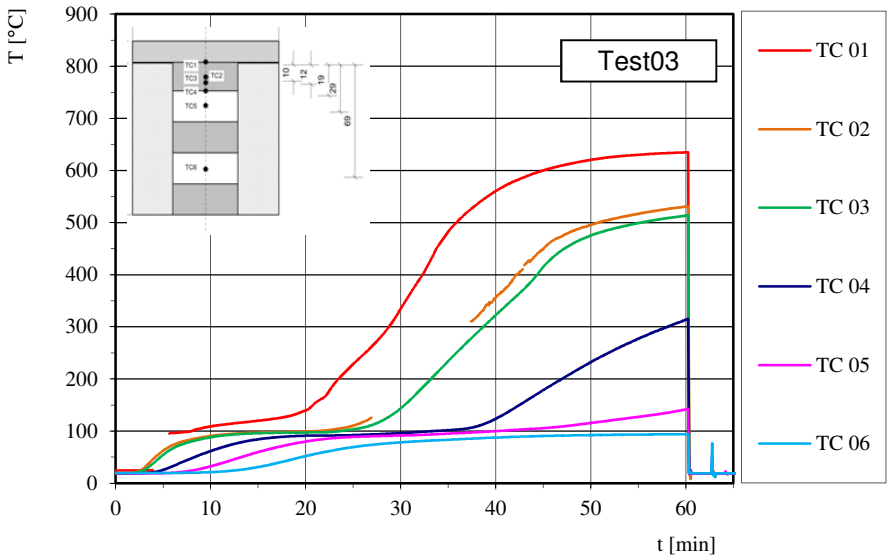

Figure 5-2 Selected temperature values for the Test 03

5.2.3 Selected temperature values for the Test 05

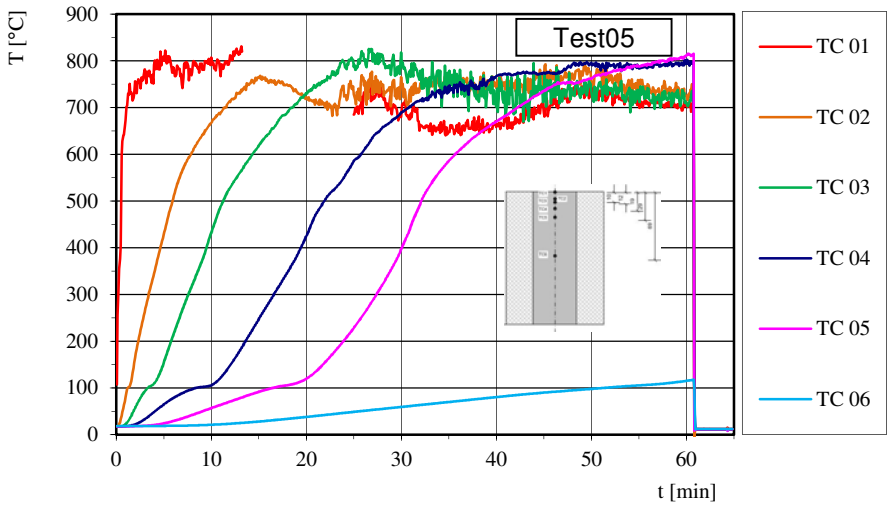

Figure 5-3Selected temperature values for the Test 05

5.2.4 Selected temperature values for the Test 06

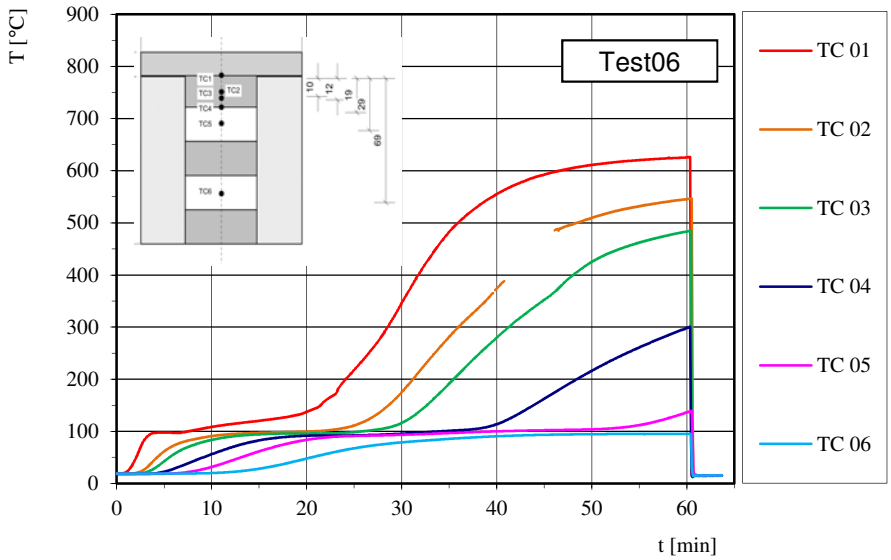

Figure 5-4 Selected temperature values for the Test 06

5.3 Charring depth

5.3.1 Analysis of charring with temperature recorded

As provided to Eurocode 5 part 1-2, the position of the char-should be taken as the position of the 300-degree isotherm [2]. Later at the correction of the temperature values, for each test were pinpointed the times when the thermocouples have reached the 300°C; i.e. the moment when the wooden material starts to char. Since the temperature recordings are available in time steps of 5 s, linear interpolation was used to define the time when the char-line reaches the thermocouple position.

Afterwards will be shown in a graph these times versus the corresponding thermocouple

depth and a linear regression line tries to follow the trend of the charring in that test. It is important highlight that the x-intercept of the trend line was forced through the t_{ch} value.

5.3.2 Residual cross-section

As mentioned in the *Chapter 4.11.2* with the documentation of the specimens post-cone calorimeter the depths of the residual cross-section were recorded for each specimen. These values were obtained by command "massprop" in particularly through the "y" coordinates extreme of the polyline that characterizes the specimen cross-section.

The values of the residual cross-section depth at the end of the tests are shown in the following graphs with the analysis of the charring with temperature recorded.

5.3.3 Analysis of charring for the Test 01

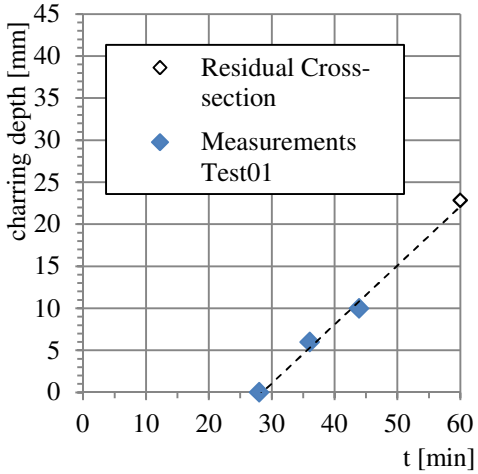

Figure 5-5 Analysis of charring for the Test 01

5.3.4 Analysis of charring for the Test 02

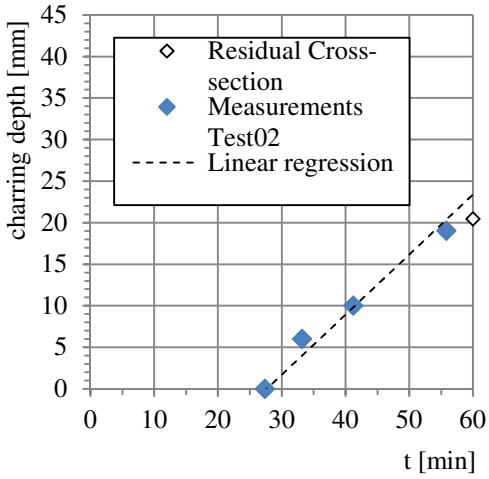

Figure 5-6 Analysis of charring for the Test 02

5.3.5 Analysis of charring for the Test 03

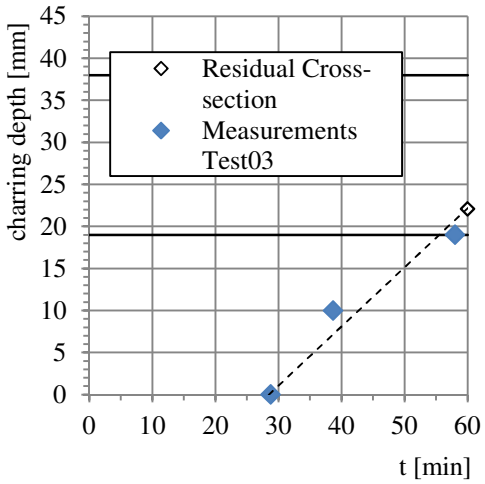

Figure 5-7 Analysis of charring for the Test 03

5.3.6 Analysis of charring for the Test 04

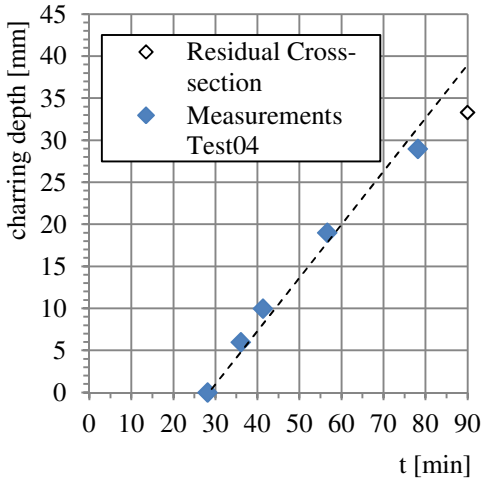

Figure 5-8 Analysis of charring for the Test 04

5.3.7 Analysis of charring for the Test 05

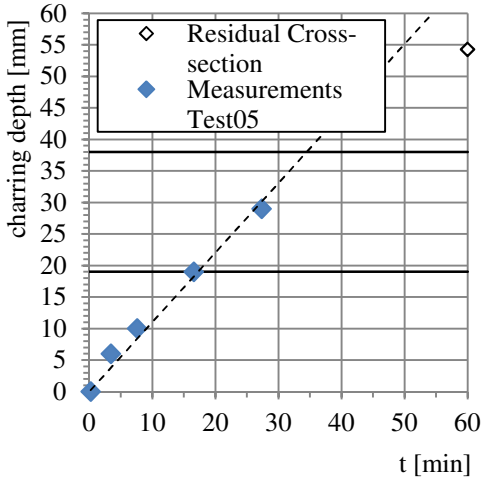

Figure 5-9 Analysis of charring for the Test 05

5.3.8 Analysis of charring for the Test 06

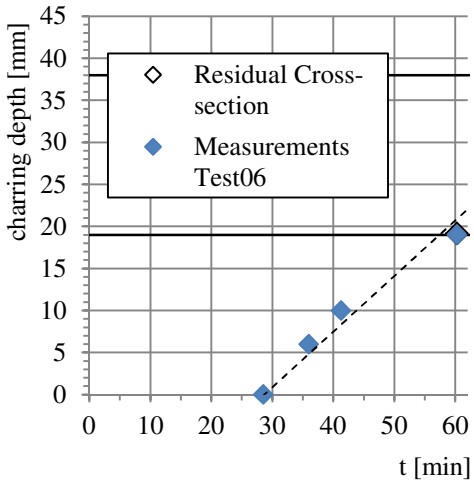

Figure 5-10 Analysis of charring for the Test 06

5.3.9 Analysis of charring for the Test 07

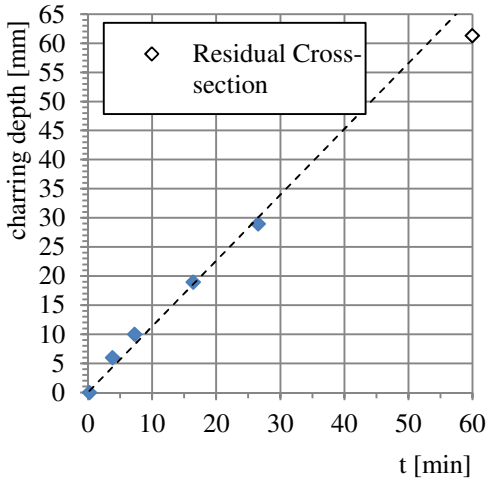

Figure 5-11 Analysis of charring for the Test 07

5.3.10 Analysis of charring for the Test 08

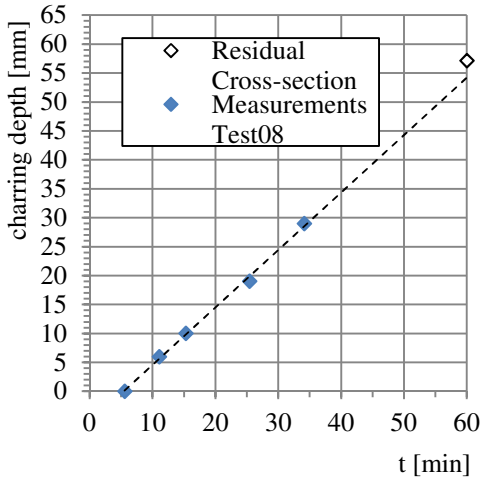

Figure 5-12 Analysis of charring for the Test 08

5.3.11 Analysis of charring for the Test 09

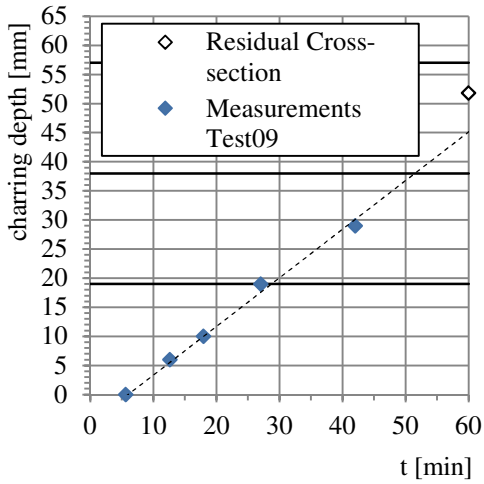

Figure 5-13 Analysis of charring for the Test 09

5.4 Analogy with a non-infinitive wide element

The Annex C of Eurocode 5 part 1-2 provides the rules for the design of load-bearing floor joists and wall studs in assemblies whose cavities are completely filled with insulation; these elements could be considered "non-infinitive wide elements". The main difference between an infinitive wide element and a non-infinitive wide element is in the propagation of the char front in the fire-exposed elements. The propagation of the char-line is affected by the heat coming from the insulating elements placed in the sides perpendicular to the fire-exposed side of the element and a one-dimensional propagation of the heat should not be considered. The tests described in the *Chapter 4 "Experiments*" show a set-up in analogy with the configuration dealt in the Annex C. For this reason will be analyzed some factor that influence the behavior of the charring in non-infinitive wide elements exposed to fire.

5.4.1 The k_s cross-section factor

The Annex C of EC5 part 1-2 gives a cross-section factor called ks for convert the one-dimensional charring rate β0 in the effective charring rate along the center line of the element βm. In the EC5 the ks factor depends on the width of the timber member; see in Table 5 2 the value for ks given by EC5.

Table 5-2 Values of k_s factor given by EC5 [2]

b [mm]	**k_s**
38	1,4
45	1,3
60	1,1

Following the terms of EC5 part 1-2 the cross-section factor ks considering an increased charring in non-infinitive wide elements is given to:

$$k_s = \frac{\beta_m}{\beta_o} \tag{23}$$

where

β_0 is the one-dimensional charring rate according to EC5 (mm/min),

β_m is the charring along the center line during the tests (mm/min).

In the tests β_m was calculated between the TC03 and the TC01, i.e. in the first 10 mm. For each test the k_s factors were determined, the results of the determination are shown in the *Table 5-3*.

Table 5-3 Determination of the cross-section factors k_s

	Test 01	Test 02	Test 03	Test 04	Test 05	Test 06	Test 07	Test 08	Test 09
t_{ch}	28,0	27,4	28,8	28,1	0,2	28,5	0,2	5,6	5,6
$t_{300,TC03}$	43,9	41,3	38,7	41,3	7,6	41,3	7,3	15,3	17,9
$t_{300,TC03}$-t_{ch}	15,9	13,9	9,9	13,2	7,4	12,7	7,1	9,8	12,3
β_m	0,63	0,72	1,01	0,76	1,36	0,79	1,42	1,03	0,81
β_0	0,65	0,65	0,65	0,65	0,65	0,65	0,65	0,65	0,65
k_s	**0,97**	**1,11**	1,55	**1,17**	**2,09**	**1,21**	**2,18**	**1,58**	**1,25**

It is easier to see the results of k_s arranged in a graph where in the x-axis there is the number of test and in the y-axis the corresponding value of k_s. As references was marked the k_s value given by EC5 part 1-2, the mean value for the tests protected by gypsum plasterboard, plywood and the unprotected tests. See also *Table 5-4* where are shown the mean values of k_s calculated for the different types of fire protection.

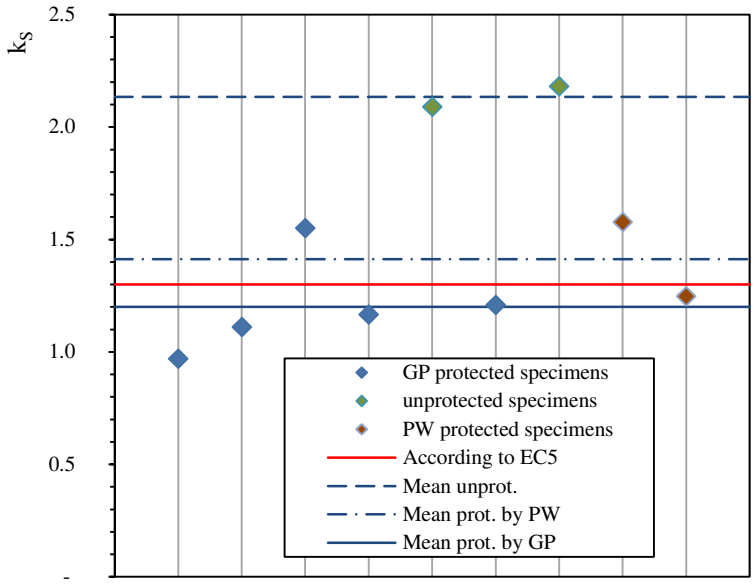

Figure 5-14 The k_s values obtained arranged by the test number

Table 5-4 Mean values of k_s calculated for the different types of fire protection

Protection type	***k*s**
unprotected	2,13
protected with GP	1,20
protected with PW	1,41

5.4.2 The k_n cross-section factor

The factor that takes account the corner roundings and the shape of the charred cross-section in the Annex C of EC5 part 1-2 is called notional cross-section factor kn. This factor is the conversion factor between the real geometry of the residual cross-section flange and an equivalent rectangular cross-section with the original width of the flange and the same modulus of inertia.

Using the inverted image of the residual cross-section by AutoCAD modulus of inertia Iz,res, residual depth, and centroid were determined (see also Chapter 4.11.2). From the residual depth was calculated the charring depth at the end of the test dchar,m. The charring depth of the equivalent rectangular cross-section was obtained from the inverted formula for the modulus of inertia in the centroid for a rectangle

$$d_{char,n} = h - \left(\frac{12 \cdot I_{z,res}}{b}\right)^{1/3} \tag{24}$$

where

h is the height of the specimen before testing,

b is the base of the specimen before testing,

$I_{z,res}$ is the modulus of inertia of the residual cross-section.

Following the terminology of Eurocode 5 part 1-2 the notional cross-section factor k_n was determined using the relationship given to:

$$k_n = \frac{d_{char,n}}{d_{char,m}} \tag{25}$$

where

$d_{char,n}$ is the charring depth of the equivalent rectangular cross section,

$d_{char,m}$ is the charring depth at the end of the test.

The value of k_n given by the Annex C of EC5 part 1-2 is $k_n=1,5$. In the *Table 5-5* are reported the values obtained for the tests, arranged by the kind of wooden specimen.

Table 5-5 Determination of k_n for different residual cross-sections

Specimen	Test	$d_{char,m}$ [mm]	$d_{char,n}$ [mm]	k_n
MF03-1	Test 05	54,3	55,9	1,03
MF03-2	Test 06	19,2	20,9	1,09
MF04-1	Test 09	51,8	51,9	1,00
MF04-2	Test 03	22,1	24,0	1,09
T01	Test 04	33,3	35,3	1,06
T02	Test 08	57,2	61,6	1,08
T03	Test 07	61,3	63,8	1,04
T04	Test 01	22,8	25,7	1,13
T05	Test 02	20,4	24,2	1,18

Also the results of k_n were arranged in a graph where in the x-axis there is the number of test and in the y-axis the corresponding value as was done for the k_s factor; was marked the k_n value given by EC5 part 1-2, the mean value for the tests protected by gypsum plasterboard, plywood and the unprotected tests. In the *Table 5-6* are shown the mean values of k_n calculated for the different types of fire protection.

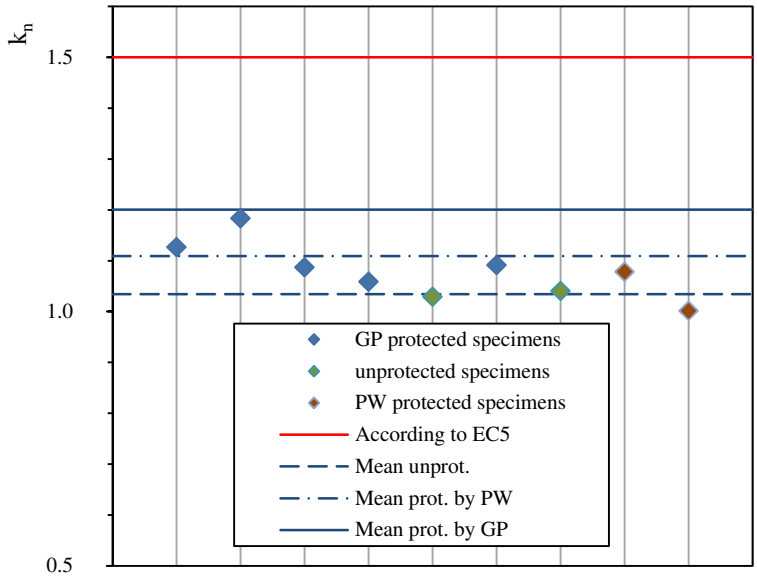

Figure 5-15 The k_n values obtained arranged by the test number

Table 5-6 Mean values of k_n calculated for the different types of fire protection

Protection type	$\boldsymbol{k_n}$
unprotected	1,03
protected with GP	1,11
protected with PW	1,04

6 Simulations

In a simulation the initial problem is understand the mode by which heat is propagated inside the material and the speed by which temperature increases. For determination of the temperature distribution of tested elements an advanced calculation using finite-element model it has been performed. Several models with the same dimensions of the specimens tested were implemented, the aim was to simulate the fire behavior of wooden specimens under fire conditions and validate the numerical modeling with the experimental results obtained from tests described previously.

6.1 Software and discretization

The thermal analyses were executed using the calculation code Safir 2007 [27]. The choice of the model and its simplifications is very important for the validity of the output results. It is necessary checked how much the mesh has to be dense; a dense grid gives accurate results, but the calculation time is considerable. However the specimens were very small so these dimensions need an adequate density mesh. For save simulation time nothing prevents from implement only a cross-section of the specimen and takes advantage of its symmetry.

The models chosen for the analysis were in a 2D elements. Were implemented a half cross-section (exploiting the symmetry) of the 45 mm-long side of the wooden specimens (see in the *Figure 6-1*).

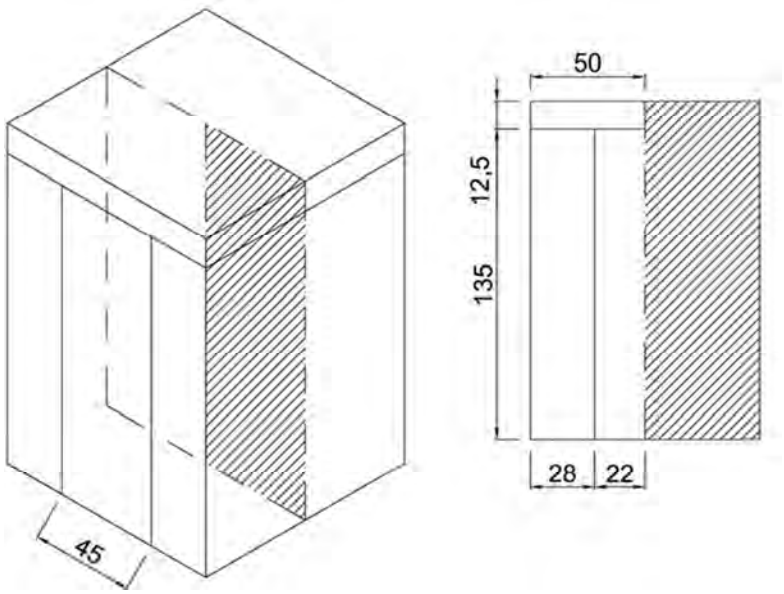

Figure 6-1 Geometry of a T-type specimens in with fire protection and insulation (a) and two-dimensional finite element model (b)with dimensions in mm

The mesh chosen for the wooden specimens and the insulation was composed by a grid of square elements with the side 1 mm-long. The same grid was used for the fire protection composed by plywood. The fire protection composed by gypsum plasterboard was modeled with a grid of rectangular elements with the horizontal side of 1 mm and the vertical side 1,25 mm long; this choice was done for reduce the number of elements, in fact for this material is not necessary know the temperature values inside, but only how the heat flux goes through.

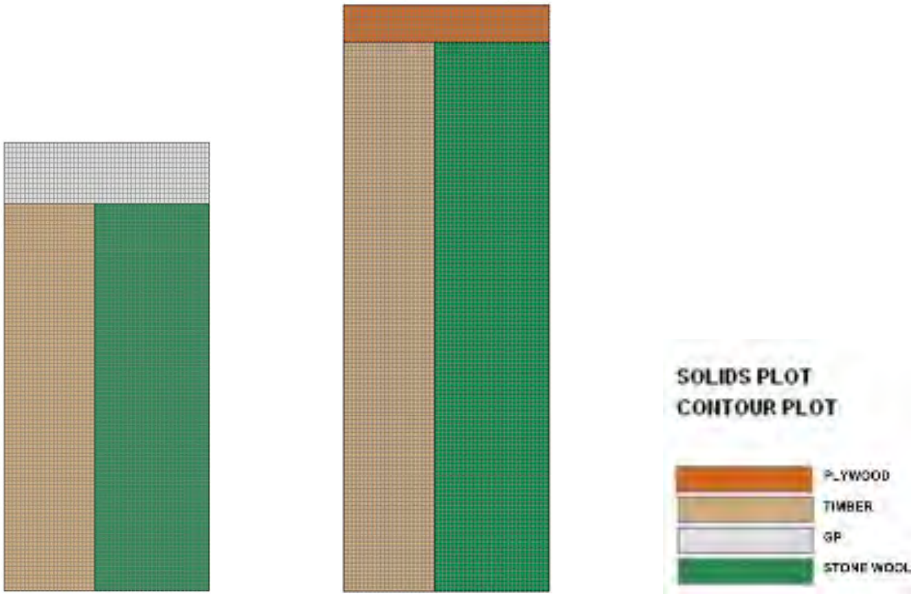

Figure 6-2 Discretisation for the thermal analysis; set-up Test 03 (a) and set-up Test 08 (b)

The Safir 2007 data output from analyses are temperature values with a time step of 30 s for the four nodes of each element; for obtained the charring depth in the time was developed a program written as a Visual Basic macro embedded in Microsoft Excel. The program takes account the temperature output from the heat transfer calculation, pinpoints when the node reaches a temperature of 300°C and considering the position of the node gives back the charring depth versus the time.

6.2 Thermal properties

A short chapter will describe the thermal properties as thermal conductivity, specific heat capacity and the loss in density that were assumed for each material presents in the simulations. Regarding the mode of heat transfer at the frontier that it is independent from the material, is takes into account the transfer by convection and by radiation. The convection coefficients on hot and cold surfaces and the relative emissivity were obtained from the EN 1991-1-2:2002 [1] and reported in *Table 6-1*.

Table 6-1 Coefficients for the heat transfer by convection and by radiation at the frontier

Convection coefficient on hot surfaces:	α_c	=	25,0	W/m^2 K
Convection coefficient on cold surfaces:	α_c	=	9,0	W/m^2 K
Relative emissivity:	ε_m	=	0,8	

6.2.1 Massive timber and CLT

The EC5 part 1-2 [2] gives in the Annex B the thermal properties of wood that implicitly consider phenomena such as evaporation, charring of wood and different conductivity at different temperatures. The properties considered were the thermal conductivity, specific heat capacity and the ratio of density to dry density (*cf. Chapter2.3.3Advanced calculation method*). The unique difference between the massive timber and CLT used in the tests, i.e. specimens MF type and T type, is in the loss in density because the two kinds of specimens presented different mean densities at 20°C; see also *Chapters and.*

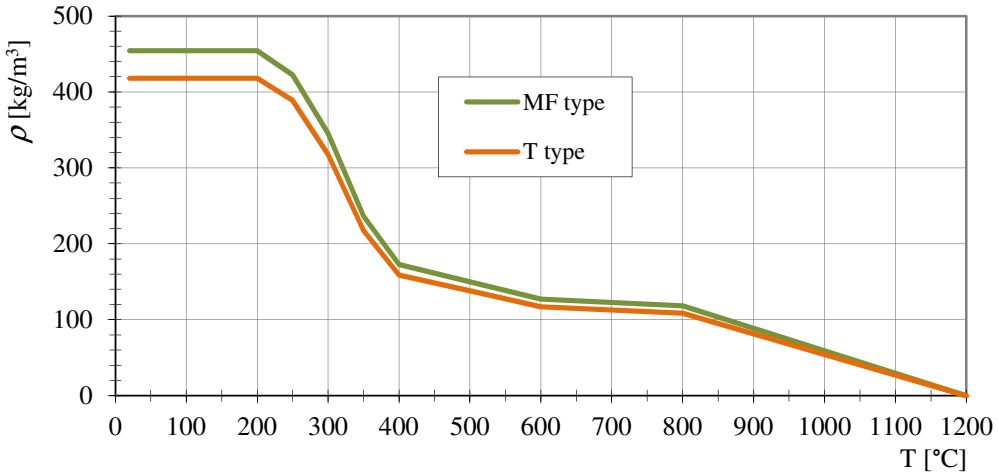

Figure 6-3 Functions for the loss in density vs. temperature used in the thermal analysis for the MF type and T type specimens

6.2.2 Gypsum plasterboard

The thermal properties for an advanced calculation of gypsum plasterboard exposed to fire cannot find in the Eurocodes, but the variation of conductivity, specific heat capacity and the ratio of density by the temperature are given by the European Handbook for the Fire Safety in Timber Building [8]. However for these simulations were chosen other two proposals for gypsum plasterboard thermal properties in order to achieve different behavior of the charring in the wood and compare different solutions of simulations. The first proposal regards the properties that König (2006) used in his report written for investigate the behavior of I-joist in floor assemblies exposed to fire [26]; the second proposal is based on the first, but with a different function for the conductivity; this proposal will be called “König modified”. In the following figures will be shown the trends of the three functions that describe the thermal properties of gypsum plasterboard.

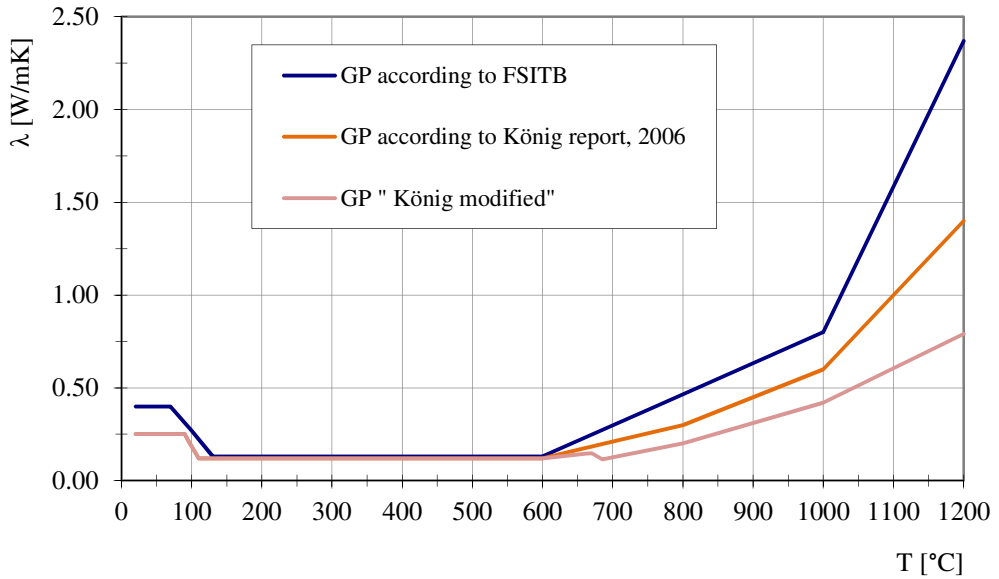

Figure 6-4 Functions of the thermal conductivities of gypsum plasterboard used in the simulations

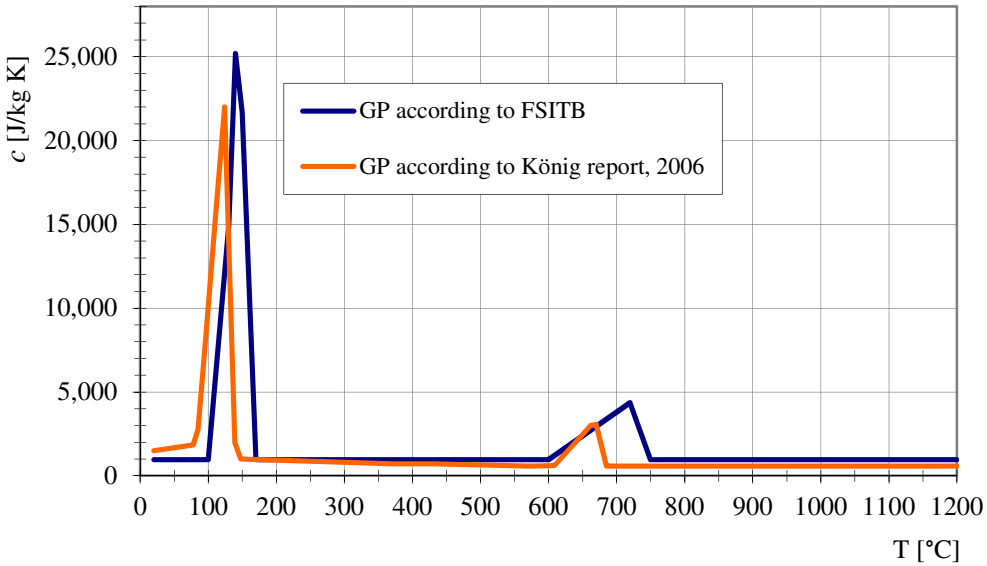

Figure 6-5 Functions of the specific heat capacities of gypsum plasterboard used in the simulations

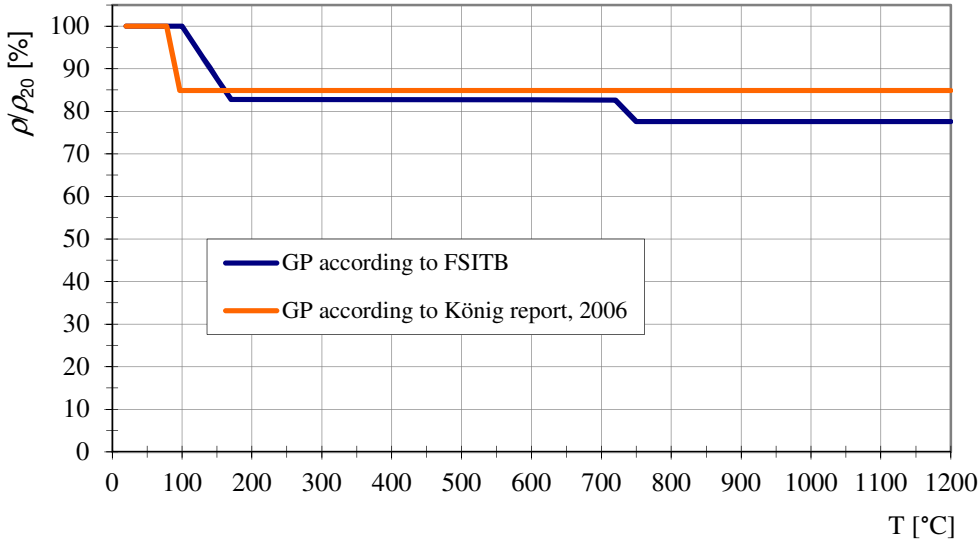

Figure 6-6 Functions of the density ratios of gypsum plasterboard used in the simulations

6.2.3 Plywood

Despite the plywood is composed by wooden layers, the European Handbook for the Fire Safety in Timber Building suggests a different function for the thermal conductivity due to premature fall-off of charcoal. The specific heat capacity and the ratio of density, instead, are taken from the functions that the EC5 part 1-2 gives for the wood.

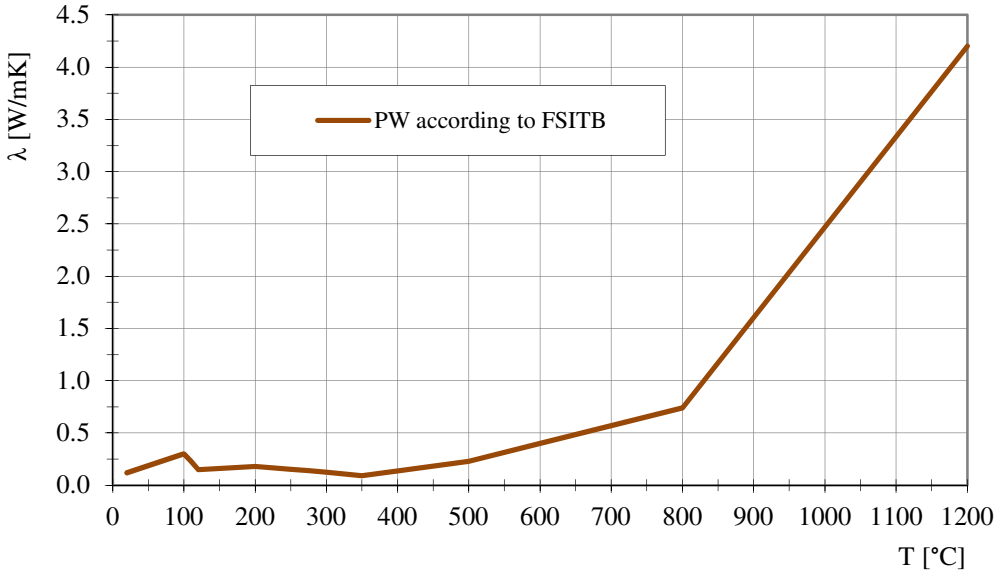

Figure 6-7 Plywood thermal conductivity according to FSITB

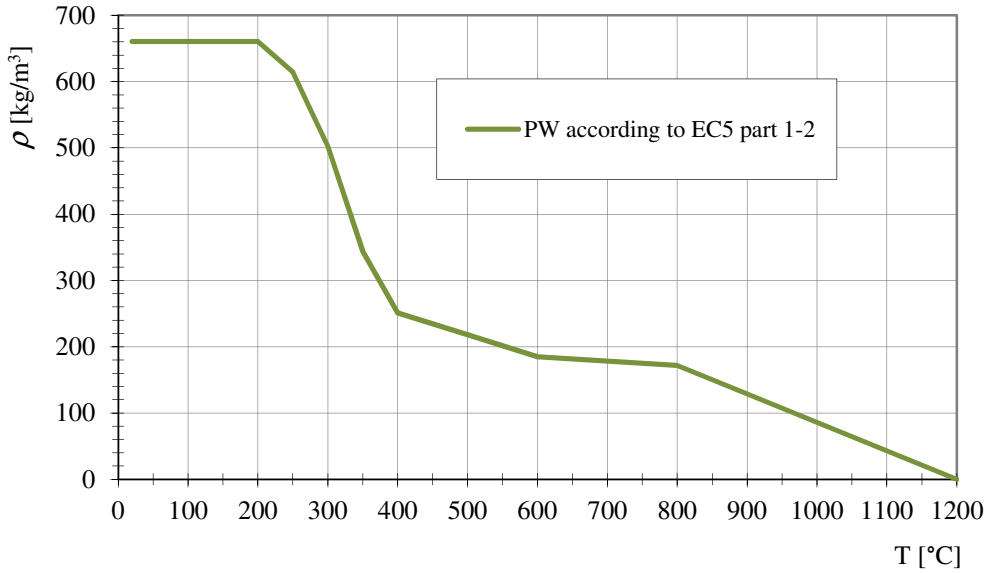

Figure 6-8 Loss in density vs. temperature for the plywood according to EC5 part 1-2

6.2.4 Insulation

As describe in the *Chapter 4.1.5*the material chosen for the insulation was the stone wool. Also for this material the thermal properties for an advanced calculation are given by the European Handbook for the Fire Safety in Timber Building; the figures below show the trend of the variation of conductivity, specific heat capacity and the ratio of density with respect to the temperature. Regarding the density of the stone wool was used a value of 32 kg/m^3 as the average density obtained from the measuring of insulation element used on the tests (*cf. Chapter4.1.5*).

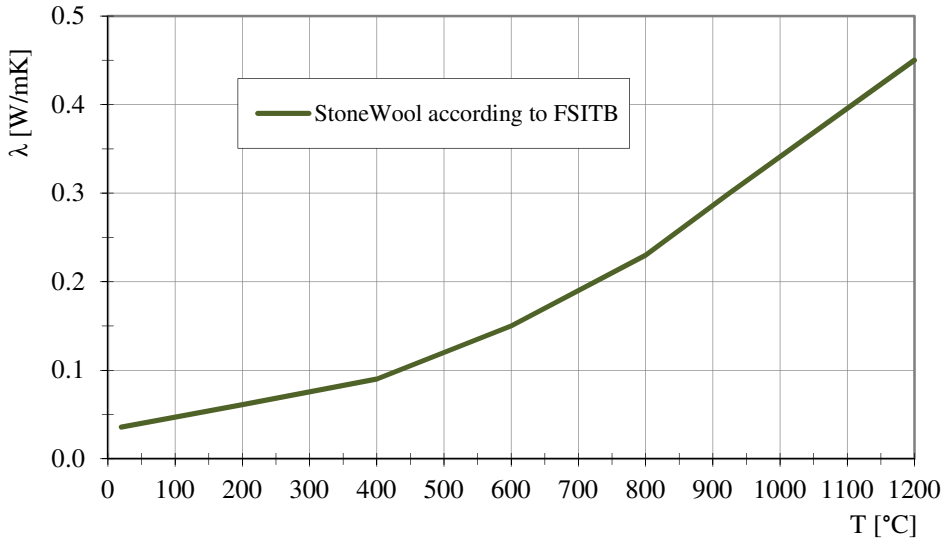

Figure 6-9 Stone wool thermal conductivity according to FSITB

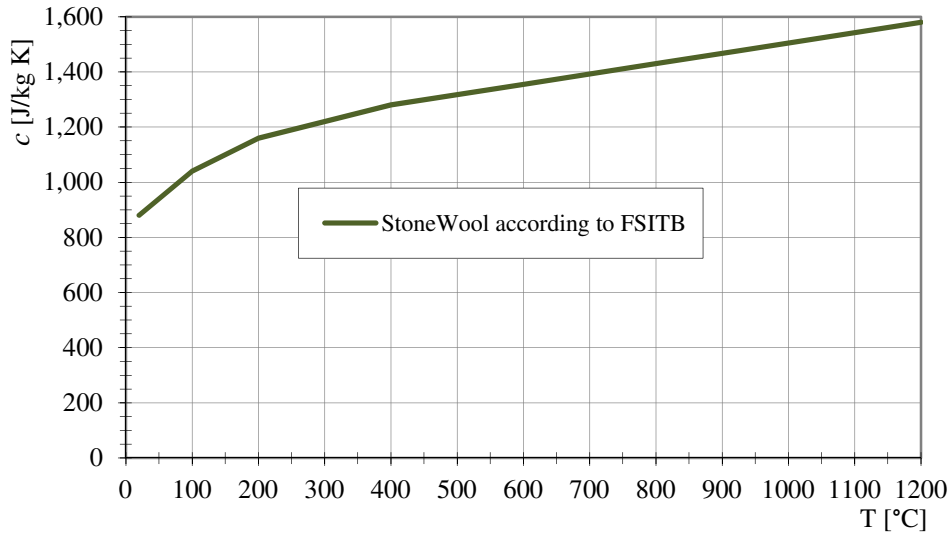

Figure 6-10 Stone wool specific heat capacity according to FSITB

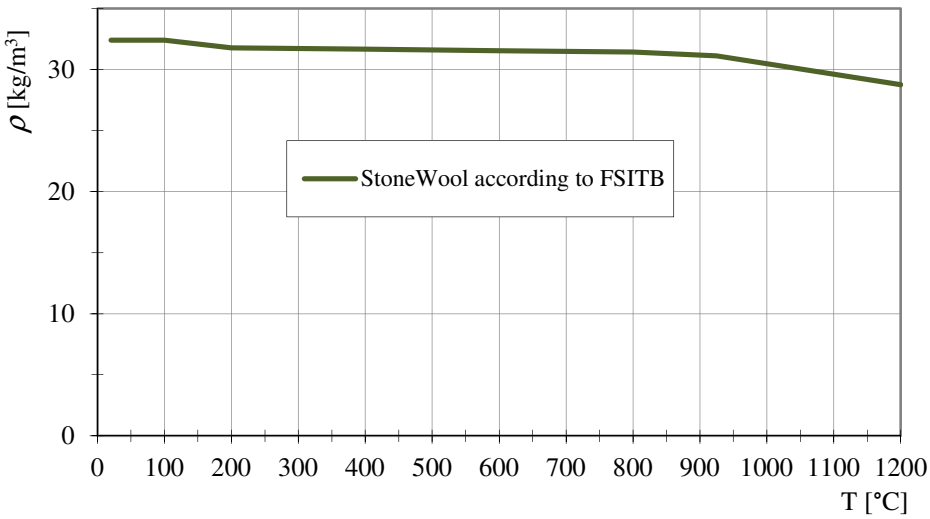

Figure 6-11 Loss in density vs. temperature for the stone wool according to FSITB

6.3 Frontiers

The last important parameter to defining for the simulations is the frontiers of the model. Safir 2007 accepts as frontiers functions of temperature in the time. As explained in the *Chapter 1.1* the aim of this report is compare the cone calorimeter test with a furnace test, as well as a fire according to the ISO 834 standard temperature-time curve [4]. Therefore in the 2D models the fire exposure was modeling with ISO 834 fire curve. The function that describes the temperature ϑ trend is:

$$\vartheta = 20 + 345 \cdot \log_{10}(8 \cdot t + 1) \tag{26}$$

where

t is the time in minutes.

For the model sides not exposed to fire were assigned a constant temperature of 20°C for all the exposure-time as suggested in the Eurocode 1 part 1-2 [1].

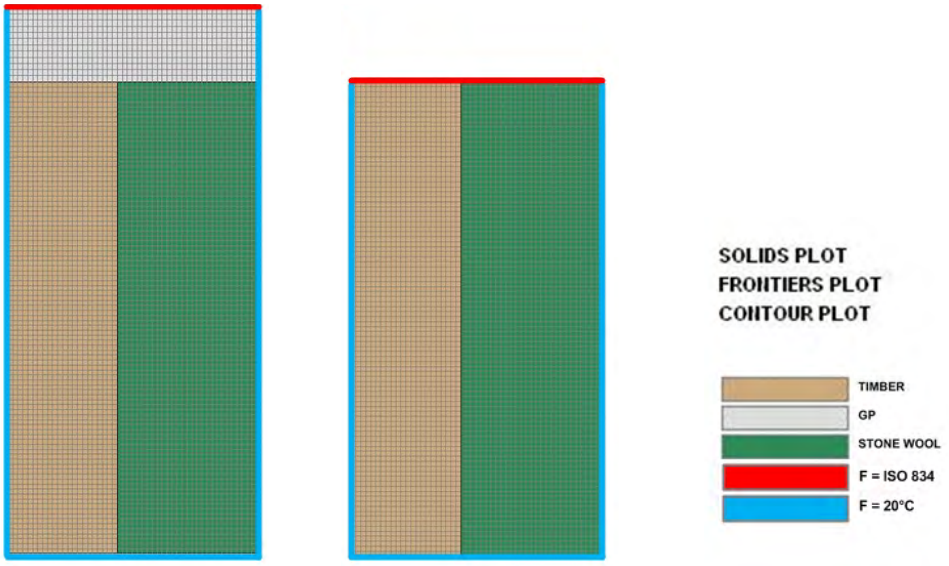

Figure 6-12 Frontiers for the thermal analysis; set-up Test 03 (a) and set-up Test 05 (b)

6.4 Numerical analysis Test 01

6.4.1 Charring analysis for Test 01

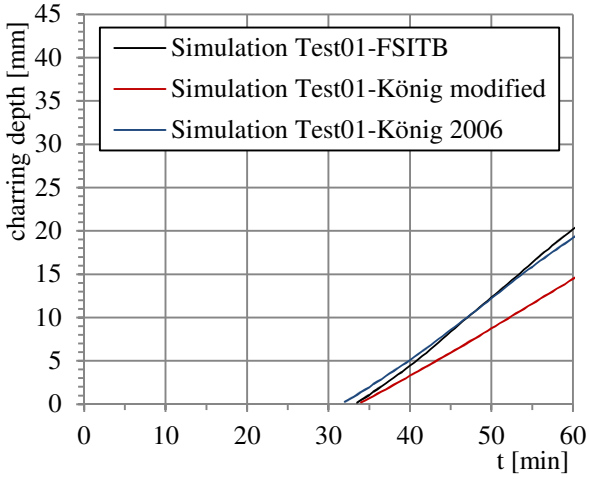

Figure 6-13 Analysis of charring for the Test 01 simulations

6.4.2 Temperature distribution for Test 01

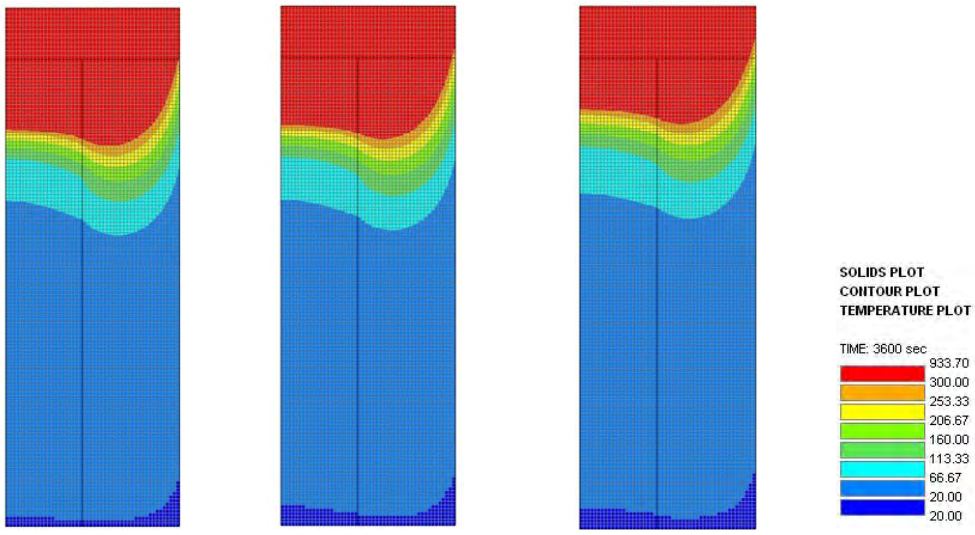

Figure 6-14 Temperature distributions at 60 min for Test 01 with GP according to FSITB (a), König 2006 (b) and König modified (c)

6.5 Numerical analysis Test 02

6.5.1 Charring analysis for Test 02

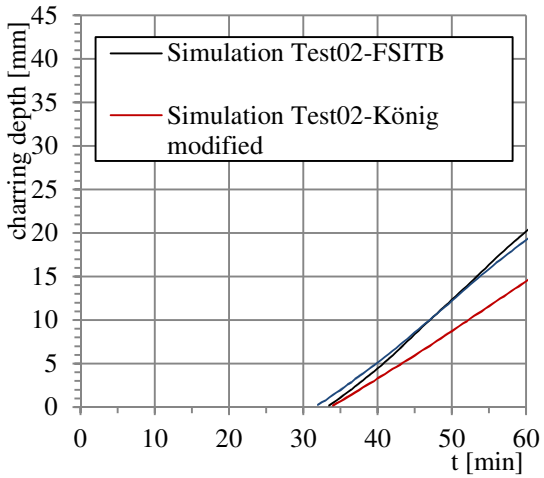

Figure 6-15 Analysis of charring for the Test 02 simulations

6.6 Numerical analysis Test 03

6.6.1 Charring analysis for Test 03

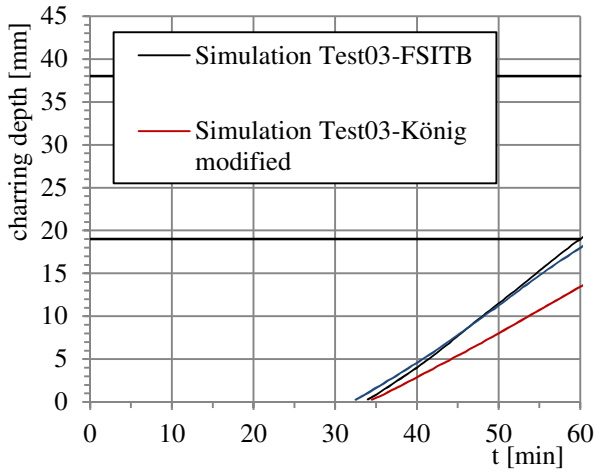

Figure 6-16 Analysis of charring for the Test 03 simulations

6.6.2 Temperature distribution for Test 03

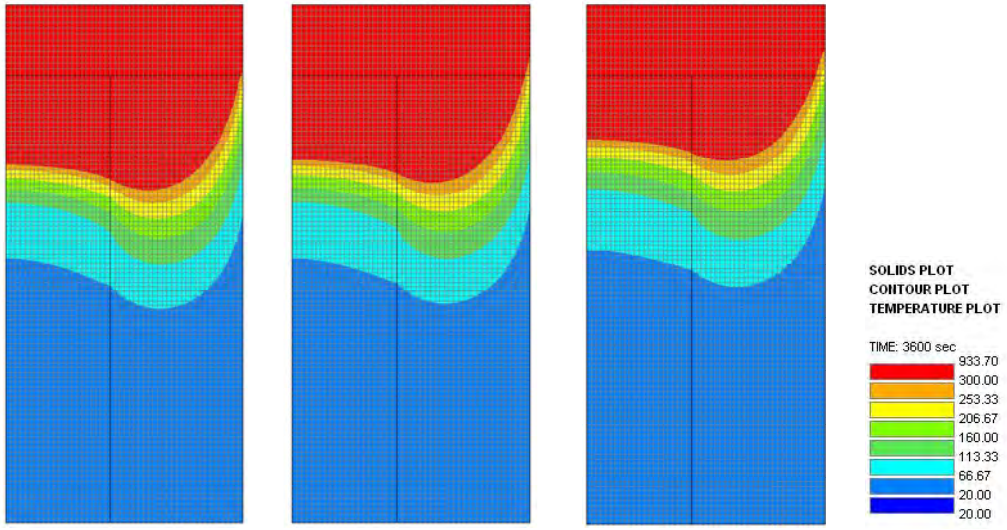

Figure 6-17 Temperature distributions at 60 min for Test 03 with GP according to FSITB (a), König 2006 (b) and König modified (c)

6.7 Numerical analysis Test 04

6.7.1 Charring analysis for Test 04

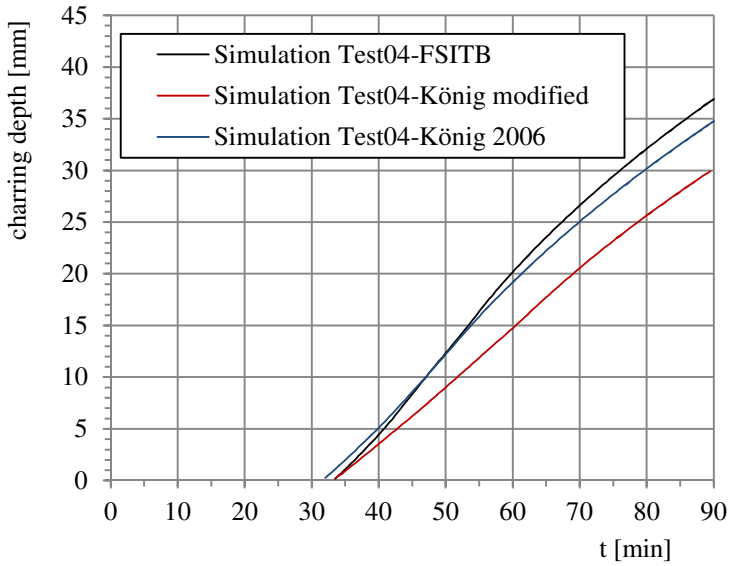

Figure 6-18 Analysis of charring for the Test 04 simulations

6.7.2 Temperature distribution for Test 04

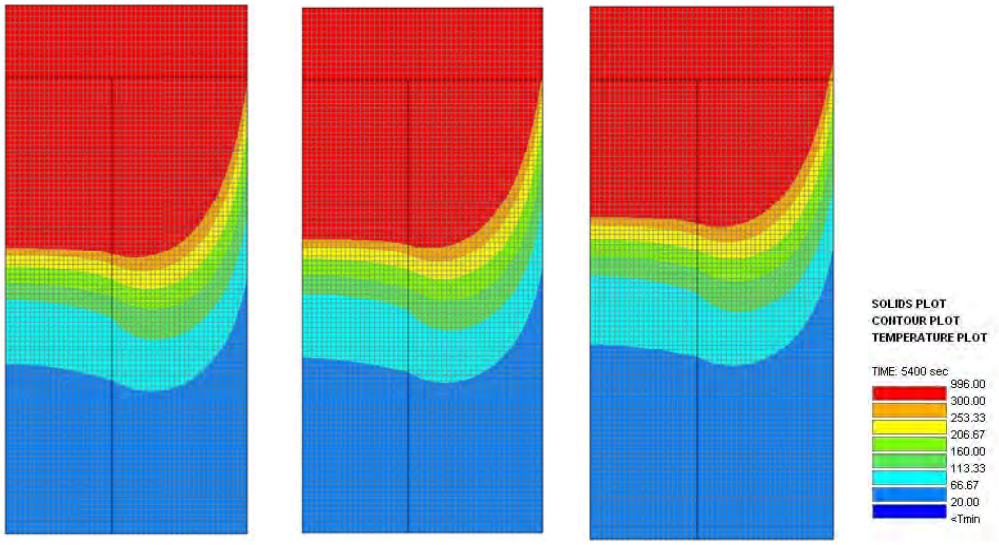

Figure 6-19 Temperature distributions at 90 min for Test 04 with GP according to FSITB (a), König 2006 (b) and König modified (c)

6.8 Numerical analysis Test 05

6.8.1 Charring analysis for Test 05

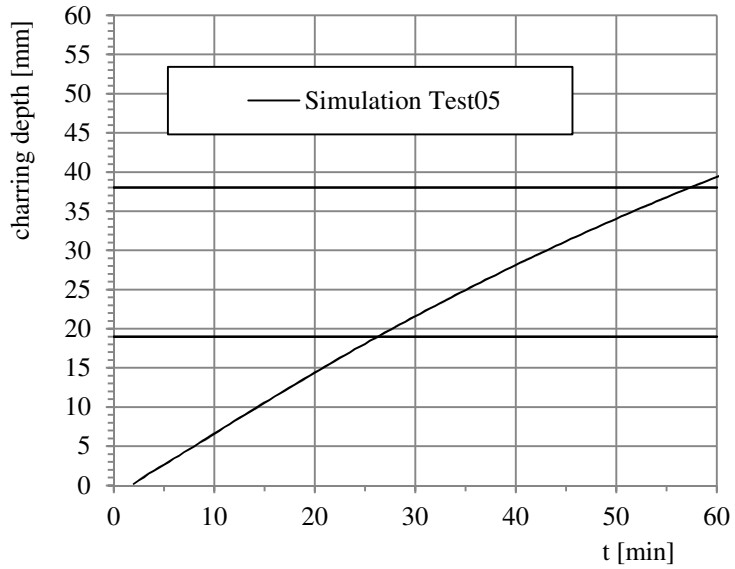

Figure 6-20 Analysis of charring for the Test 05 simulation

6.8.2 Temperature distribution for Test 05

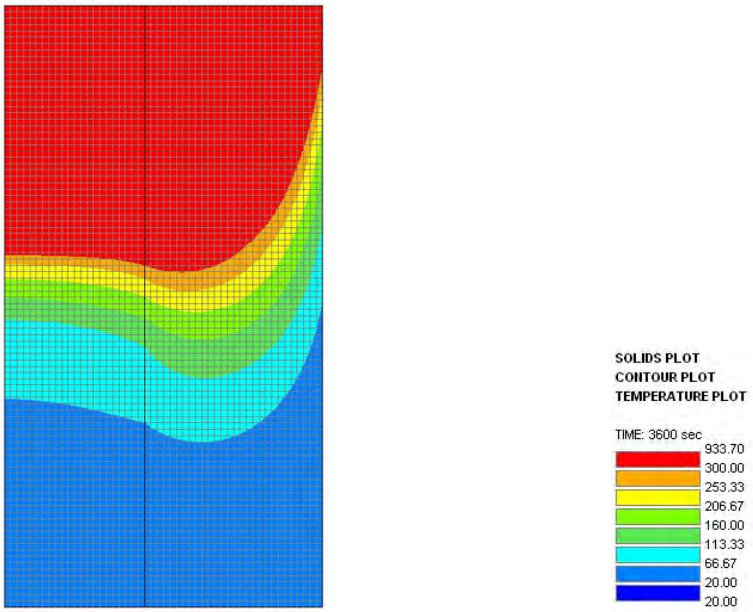

Figure 6-21 Temperature distribution at 60 min for Test 05

6.9 Numerical analysis Test 06

6.9.1 Charring analysis for Test 06

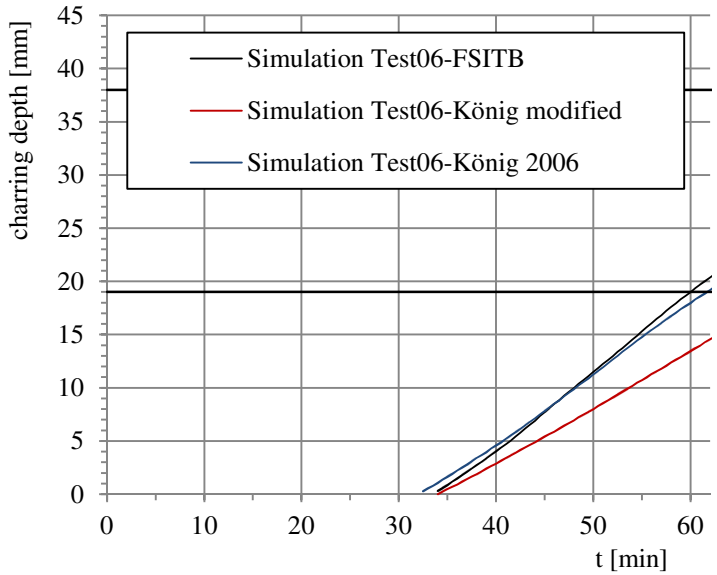

Figure 6-22 Analysis of charring for the Test 06 simulations

6.10 Numerical analysis Test 07

6.10.1 Charring analysis for Test 07

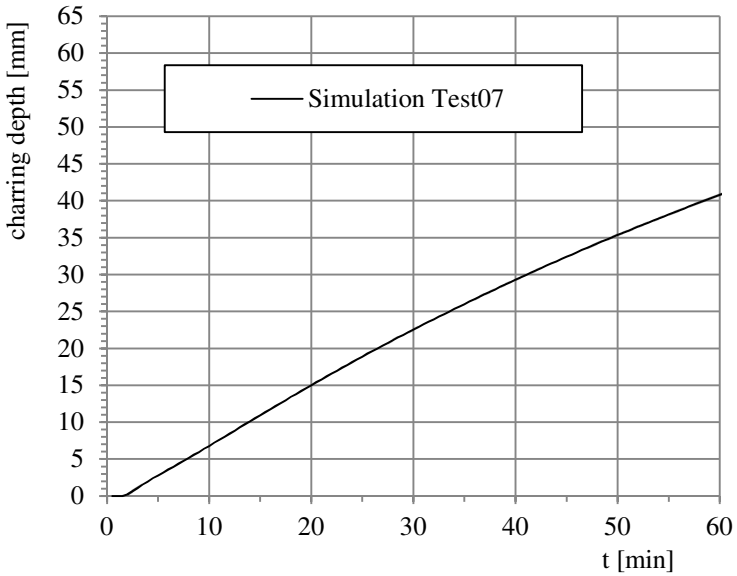

Figure 6-23 Analysis of charring for the Test 07 simulation

6.10.2 Temperature distribution for Test 07

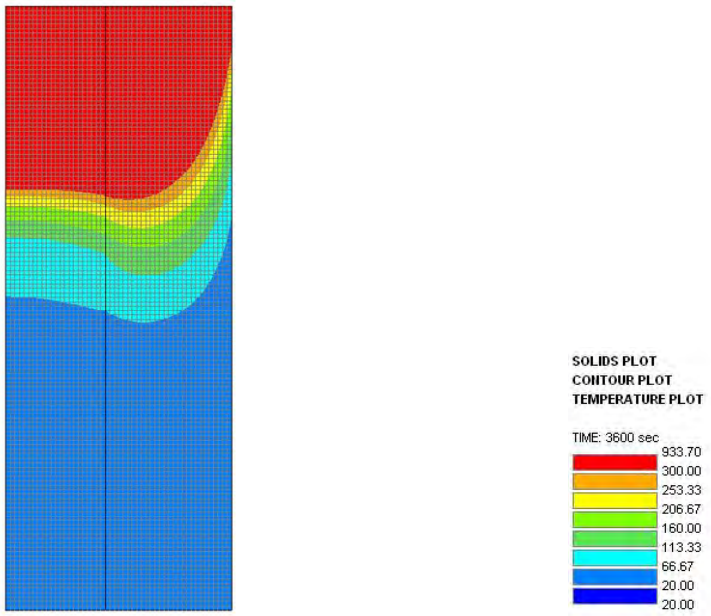

Figure 6-24 Temperature distribution at 60 min for Test 07

6.11 Numerical analysis Test 08

6.11.1 Charring analysis for Test 08

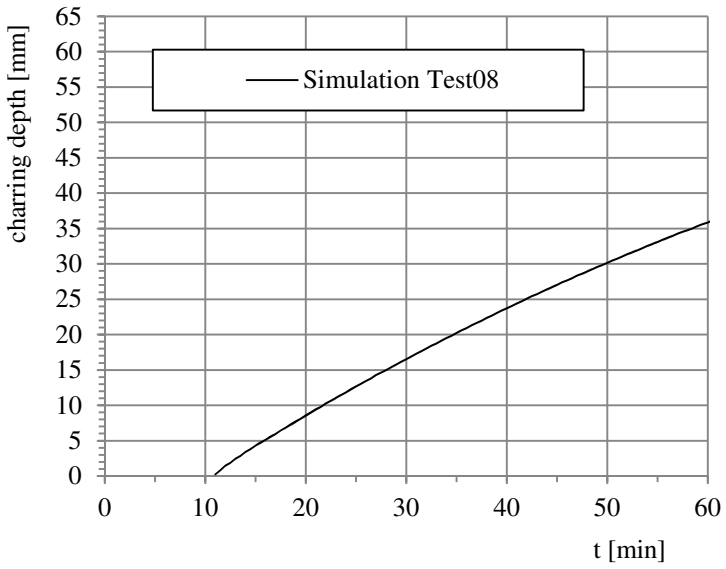

Figure 6-25 Analysis of charring for the Test 08 simulation

6.11.2 Temperature distribution for Test 08

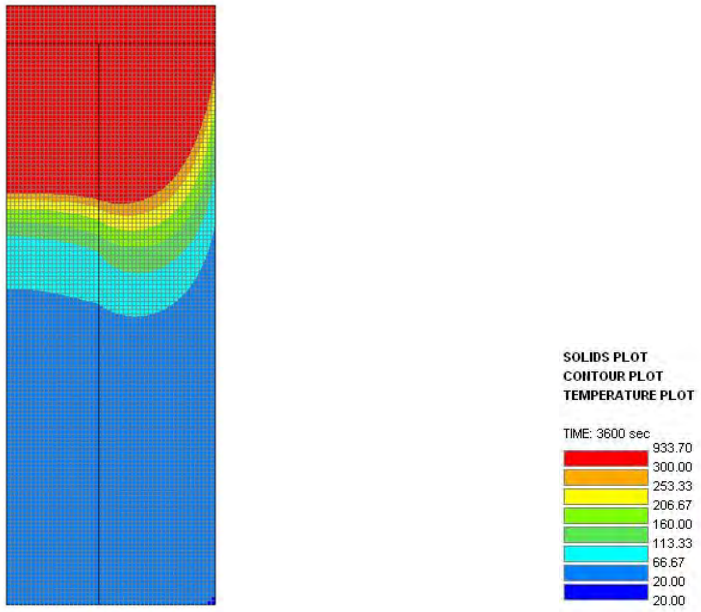

Figure 6-26 Temperature distribution at 60 min for Test 08

6.12 Numerical analysis Test 09

6.12.1 Charring analysis for Test 09

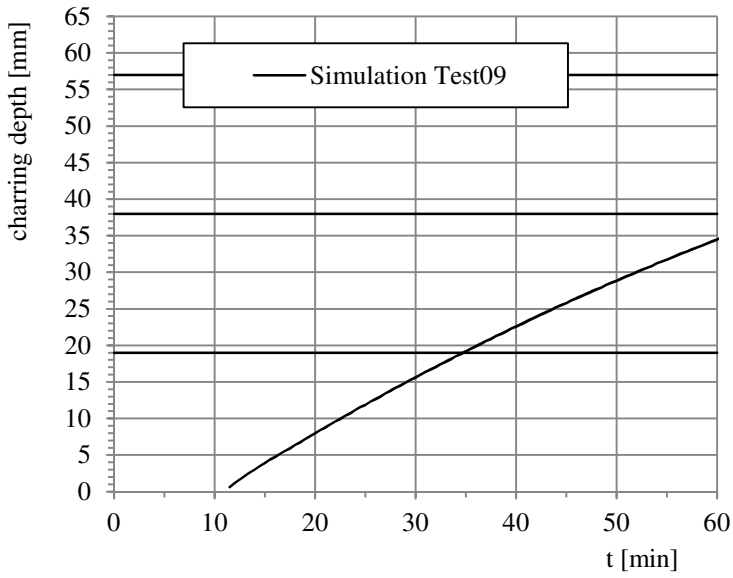

Figure 6-27 Analysis of charring for the Test 09 simulation

6.12.2 Temperature distribution for Test 09

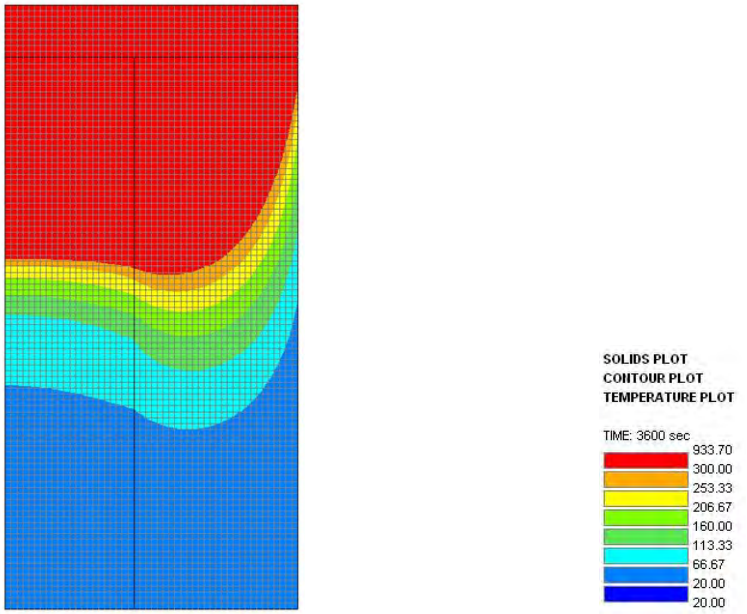

Figure 6-28 Temperature distribution at 60 min for Test 09

7 Charring depth according to EC5 part 1-2

In the comparisons between the test and simulation results could be useful have a reference to regulations; following will be describe as the charring depth in accordance to EC5 part 1-2 [2] was obtained. Will be considered the section as an infinitive wide element and a non-infinitive wide element. Since some tests have the same set-up the charring depth can be the same; elements with the same results will be gathered together.

7.1 Charring depth considering an infinitive wide element

7.1.1 Notional design charring depth

As can be found on the EC5 part 1-2 for the elements without a fire protection the charring rate could be considered one-dimensional and the charring depth should be calculated as (6), however the one-dimensional design charring rate has to be applied for cross-section with an original minimum width b_{min}, where:

$$b_{min} = \begin{cases} 2\,d_{char,0} + 80 & for\ \ d_{char,0} \geq 13\,mm \\ 8{,}15\,d_{char,0} & for\ \ d_{char,0} < 13\,mm \end{cases} \tag{26}$$

where

$d_{char,0}$ is given by (6).

Since all the specimens present a nominal cross-section width of 45 mm and b_{min} for a time exposure of 60 min and charring rate of 0,65 mm/min (softwood and beech) is approximately 158 mm, no specimen has the the width greater $b_{min.}$ Therefore for all the specimens the notional design charring depth according to (5) was followed; the values of β_n given by EC5 part 1-2 are summarized in the *Table 7-1*:

Table 7-1 Design charring rates β_n of softwood and beech

	β_n [mm/min]
a) Softwood and beech	
Glued laminated timber with a characteristic density of ≥ 290 kg/m^3	0,7
Solid timber with a characteristic density of ≥ 290 kg/m^3	0,8

For the specimens MF-type was chosen the value of β_n given for the glued laminated timber and for the T-type the value for the solid timber.

7.1.2 Charring behind the fire protection

In the *Chapter 2.5* are summarized the rules given by EC5 part 1-2 for dealing with timber elements protected by gypsum plasterboard. For the specimens used in the tests and protected by gypsum plasterboard the start of charring was calculated with the formula (22). The failure of the protection was not considered due to the set-up of the test: as explained in *Chapter 4* the gypsum plasterboard is placed over the specimen and it stays in place for all the time of testing. The charring rate β_n for the first 25 mm was correct with the factor k_2 given by (19); after the reaching of that charring depth, the charring rate increases to a value of β_n.
For the specimens protected by plywood was different. The start of charring behind the protection was calculated as:

$$t_{ch} = \frac{h_p}{\beta_0} \tag{27}$$

where

h_p is the nominal thickness of the plywood (mm);

β_0 is the one-dimensional charring rate for the plywood (mm/min).

The one-dimensional charring rate for the plywood in the EC5 part 1-2 is 1,0 mm/min but it is valid for a panel with the thickness of 20 mm and density of 450 kg/m^3; for different thicknesses and densities the charring rate should be corrected as:

$$\beta_{0,\rho,t} = \beta_0 \cdot k_\rho \cdot k_h \tag{28}$$

with

$$k_\rho = \sqrt{\frac{450}{\rho_k}} \tag{29}$$

$$k_h = \sqrt{\frac{20}{h_p}} \tag{30}$$

where

ρ_k is the characteristic density of the plywood (kg/m^3);

h_p is the nominal thickness of the plywood (mm);

For this set-up the charring rate of the wooden elements should not be corrected with any factor.

7.2 Charring depth considering a non-infinitive wide element

The analogy between the specimens and a non-infinitive wide element explained in the *Chapter 5.4* it is used also for another version of the analitical calculation of the charring depth using the rules given by the annex C of EC5 part 1-2.

7.2.1 Charring behind the fire protection

For the specimens protected with gypsum plasterboard the time of start charring behind the fire protection was calculated in the same way of the infinitive wide element with the formula (22). For the elements protected by wood-based panels (in this case plywood) the annex C gives a different formula deference the infinitive wide elements:

$$t_{ch} = \frac{h_p}{\beta_{0,\rho,t}} - 4 \tag{31}$$

where

h_p is the nominal thickness of the plywood (mm);

$\beta_{0,\rho,t}$ is the charring rate corrected for the plywood (mm/min).

The value of charring rate corrected $\beta_{0,\rho,t}$ is calculated as (28).The correction for the charring rate of the wooden specimens is explained in the following chapter.

7.2.2 Charring rate

The annex C of EC5 part 1-2 distinguishes the charring rate for protected element between before and after the time of failure of the protection. For the elements protected by gypsum plasterboard it is easy consider the formula for the charring before the failure for all the fire exposure time (in this tests the protection does not fail):

$$\beta_n = k_2 \cdot k_s \cdot k_n \cdot \beta_0 \tag{32}$$

where

- k_2 is the insulation factor;
- k_n is a factor to convert the irregular residual cross section into a notional rectangular cross-section;
- k_s is the cross-section factor;
- β_0 is the one-dimensional charring rate.

The one-dimensional charring rate is 0,65 mm/min for the MF-type and T-type specimens (softwood, solid timber and glued laminated timber). For the k_s and k_n factors, amply explained in the *Chapters 5.4.1 and 5.4.2*; was taken respectively 1,3 and 1,5. The k_2 factor depends on where the cladding is jointed; in this case was taken the formula for the location where the cladding is unjointed:

$$k_2 = 1{,}05 - 0{,}0073 \cdot h_p \tag{33}$$

where

- h_p is the nominal thickness of the plywood (mm);

For charring rate of the elements protected by plywood is not correct taking the (32) because the (33) for calculating the k_2 factor is valid only for the gypsum plasterboard. Since the plywood is a wood based panel, could be considered the formula for the charring rate after the failure of protection which, included the post-protection factor k_3 instead of the insulation factor k_2. In the post-protection factor was considered the failure of the protection at the same time of the start of charring behind the protection:

$$\beta_n = k_3 \cdot k_s \cdot k_n \cdot \beta_0 \tag{34}$$

where

- k_3 is the post-protection factor;
- k_n is a factor to convert the irregular residual cross section into a notional rectangular cross-section;
- k_s is the cross-section factor;
- β_0 is the one-dimensional charring rate (mm/min).

The one-dimensional charring rate, k_s and k_n are the same for the gypsum plasterboard protected specimens. The post-protection factor k_3 was calculated as:

$$k_3 = 0{,}036 \cdot t_f + 1 \quad (35)$$

where

t_f is the failure time of the protection (min);

Considering $t_f = t_{ch}$.

7.2.3 Design of charring depth

Once that taking account of the start of charring behind the protection and the opportune charring rate, the charring depth was calculated with the (5).

7.3 Analytical analysis according to EC5 part 1-2

Following will be shown the the results of the analytical analysis of the charring depth according to EC5 part 1-2 for each test carried-out, considering as a infinitve wide element (iwe) and a non-infinitive wide element (niwe). First the results will be grouped for the type of fire protection used, therefore will be presented three graphs respectively for the gypsum plaster protected, the plywood protected and the unprotected specimens. Later, a comparison between the performance of the different fire protections used (or not used) will be shown on two different graphs grouped for the type of specimens utilized on the tests.

7.3.1 Analytical charring depth for the gypsum plasterboard protected specimens

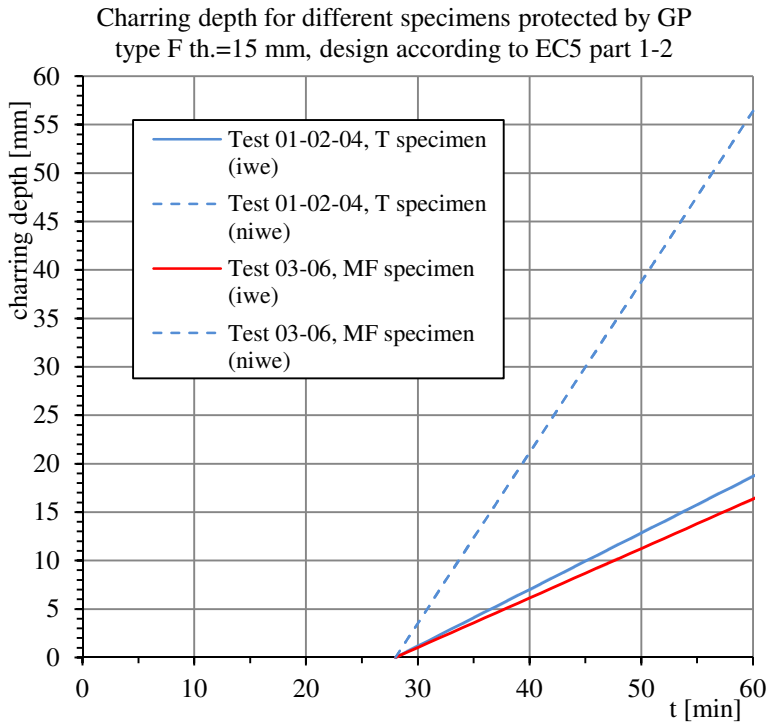

Figure 7-1 Analytical charring depth for the gypsum plasterboard protected specimens

7.3.2 Analytical charring depth for the plywood protected specimens

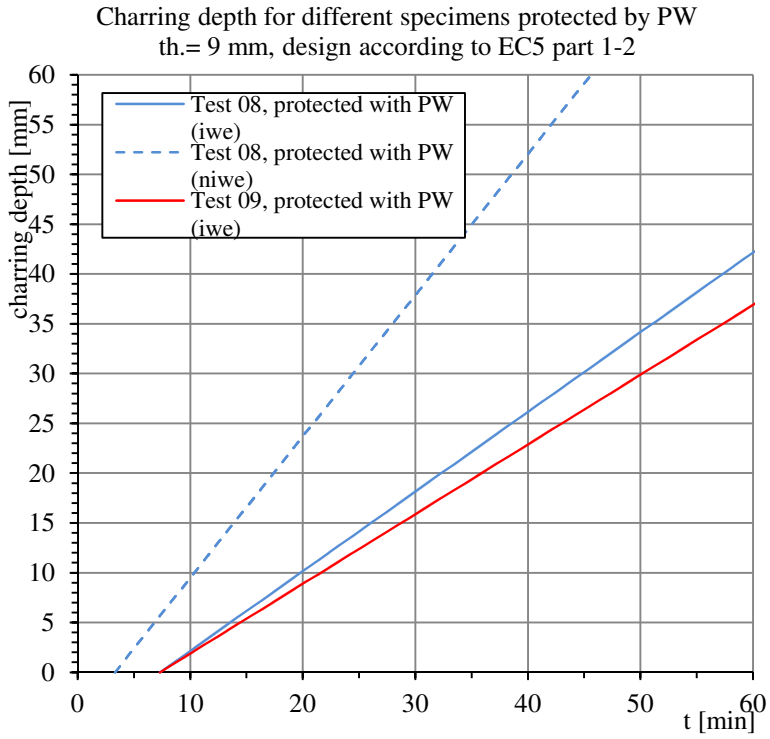

Figure 7-2 Analytical charring depth for the plywood protected specimens

7.3.3 Analytical charring depth for the unprotected specimens

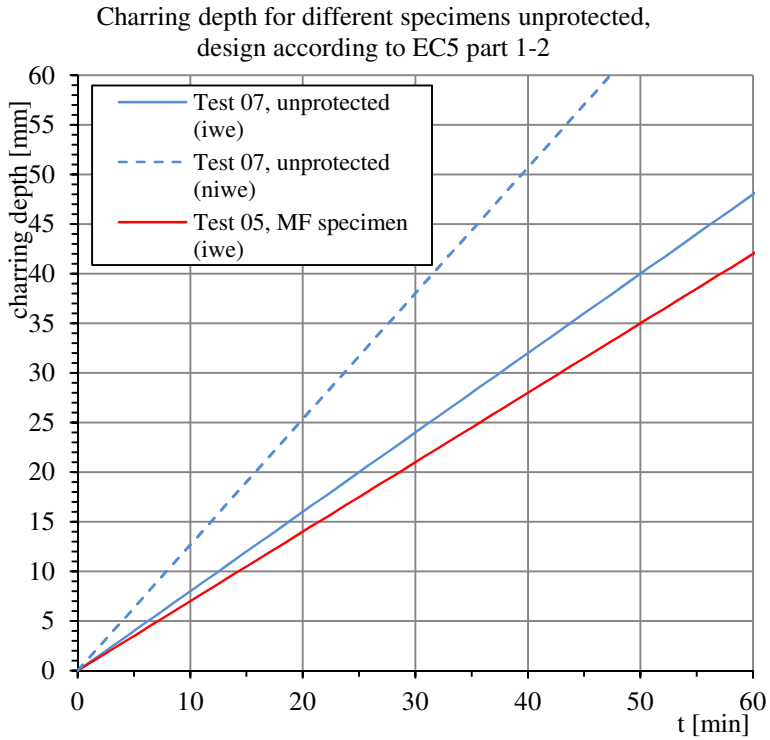

Figure 7-3 Analytical charring depth for the unprotected specimens

7.3.4 Comparison of the analytical charring depth for T-type specimens with different protections

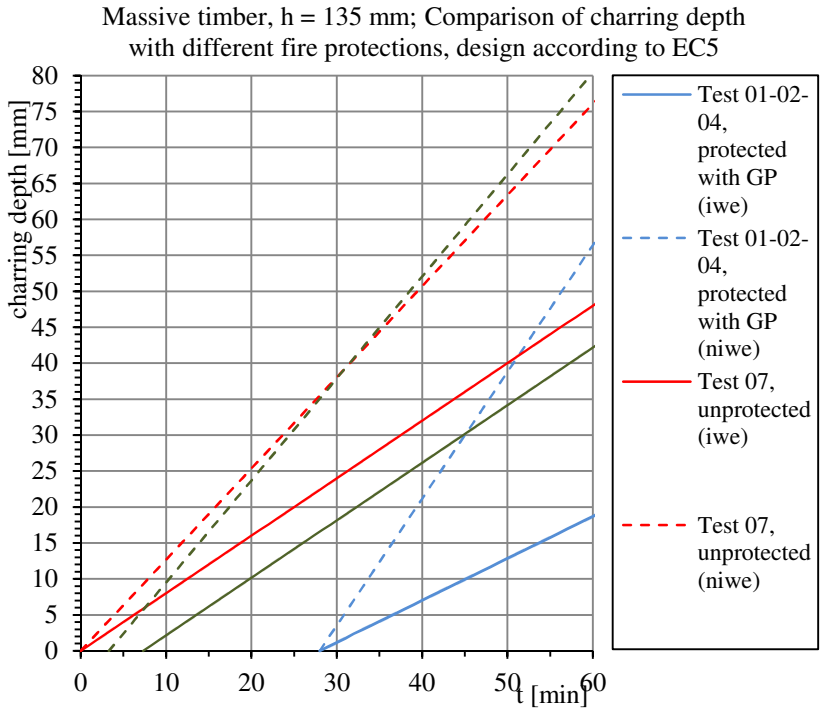

Figure 7-4 Comparison of charring depth according to EC5 part 1-2 for T-type specimens with different fire protections

7.3.5 Comparison of the analytical charring depth for MF-type specimens with different protections

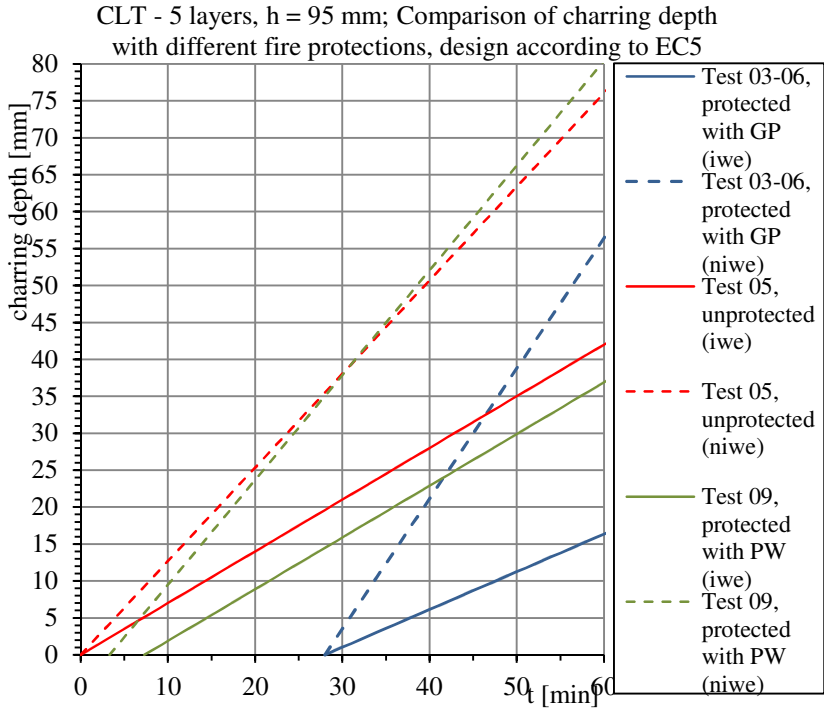

Figure 7-5 Comparison of charring depth according to EC5 part 1-2 for MF-type specimens with different fire protections

8 Discussion

In the previous chapters were described how the charring depth of CLT and massive timber specimens were obtained from experiments, numerical simulations and analytical rules. In this chapter these results will be compared together, keeping separate the results for type of protection or type of specimen.

8.1 Charring depths for CLT protected by gypsum plasterboard

The furnace fire test performed at SP Wood Technology described in the *Chapter 3.1*, as well as the furnace test performed at CNR-IVALSA (*Chapter 3.2*) and some cone calorimeter tests shown in the *Chapter 4* used the same material, which is the 5 layers cross-laminated timber with a height of 95 mm provided by the Swedish company Martinsons.

In these three series of tests there are an amount of eight tests that were performed with a cover of gypsum plasterboard with a thickness of 15 mm as fire protection. In the following graph are shown the experimental results for the tests over mentioned, and the related simulations and analytical results.

8.1.1 Comparison

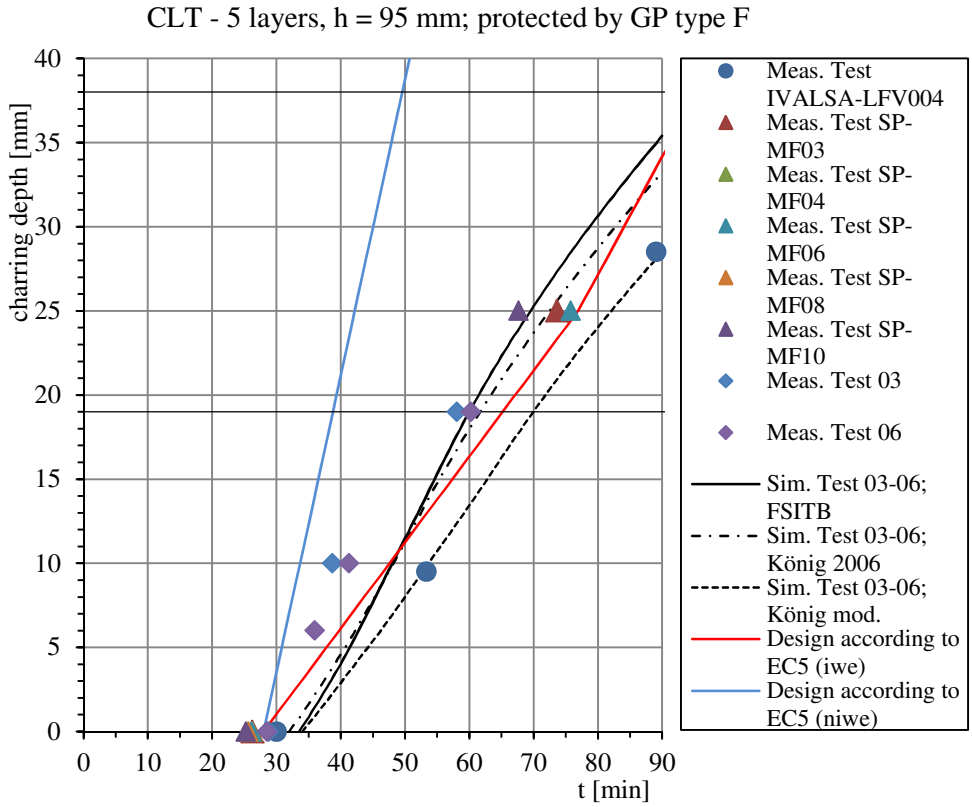

Figure 8-1 Comparison between furnace tests, cone calorimeter tests, simulations and analytical results for CLT protected by gypsum plasterboard

8.1.2 Observations from the comparison

From the *Figure 8-1* it is possible to observe that start of charring behind the gypsum plasterboard it is around 28 min and well agree with the t_{ch} time given by (22), especially for the cone calorimeter tests; instead for the simulations t_{ch} starts a few minutes later. It was expected that the charring depths obtained from the furnace tests well agree with the design according to EC5 for an infinitive wide element, however also the cone tests agree better with the infinitive wide than the non-infinitive wide element, especially around the 60th minute of heat flux exposure.

The charring in the simulations starts later than the experimental tests; the simulations with the gypsum plasterboard properties according to FSITB and "König 2006" until a depth of 10 mm underestimate the design according to EC5, then overestimate but the curve is quite near the line given by Eurocode. For the simulation with the properties called "König modified" the charring depth is underestimate respect the EC5 but well agree with the test performed at CNR-IVALSA.

8.2 Charring depths for CLT unprotected

Eight tests from the furnace and cone calorimeter are available also without the fire protection. It is important remember that also for this comparison the cross-laminated timber has the same height and number of layers, and is provided from the same company. In this case the lower number of tests and simulations allows inserting also the residual cross-section values for the cone calorimeter test that in the previous comparison were neglected.

8.2.1 Comparison

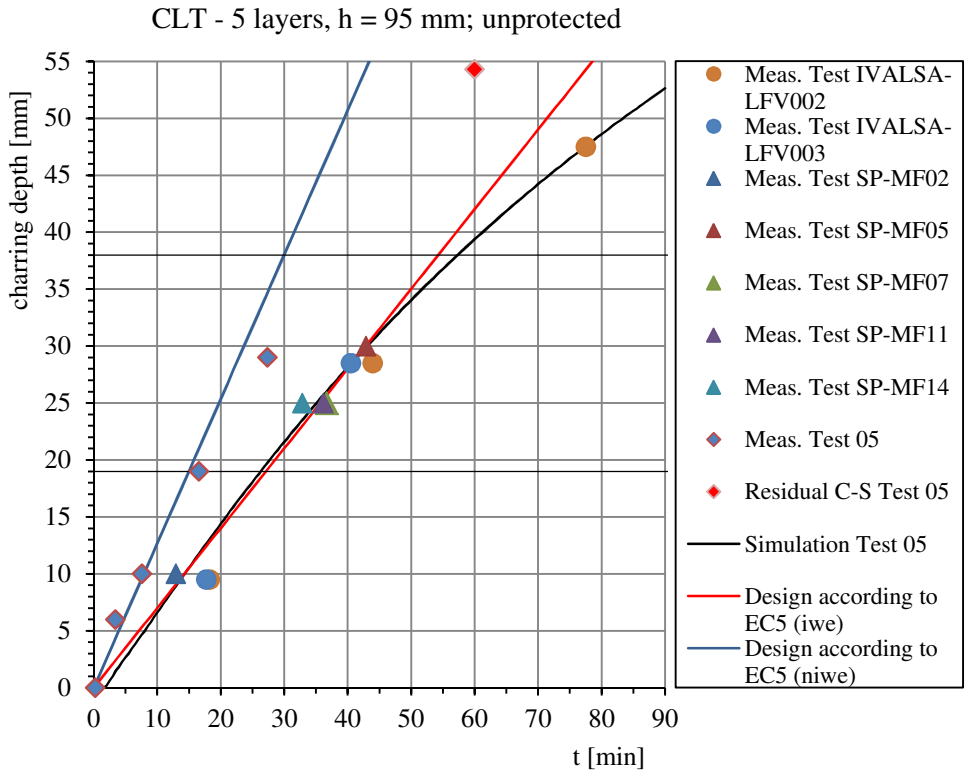

Figure 8-2 Comparison between furnace tests, cone calorimeter tests, simulations and analytical results for CLT unprotected

8.2.2 Observations from the comparison

The first, evident, observation that can be done it is cone calorimeter results that well agree with the charring depths for a non-infinitive wide element given by EC5 for the first 19 mm depth, i.e. the first layer of CLT. Then the rate seems decrease, as can be seen from the point that indicates the residual cross-section. The furnace test results well agree with the design for an infinitive wide element and the simulation. Despite for an unprotected element the ignition is immediate, in the simulation the charring starts some minutes after the zero time.

8.3 Charring depths for the CLT protected by plywood

8.3.1 Comparison

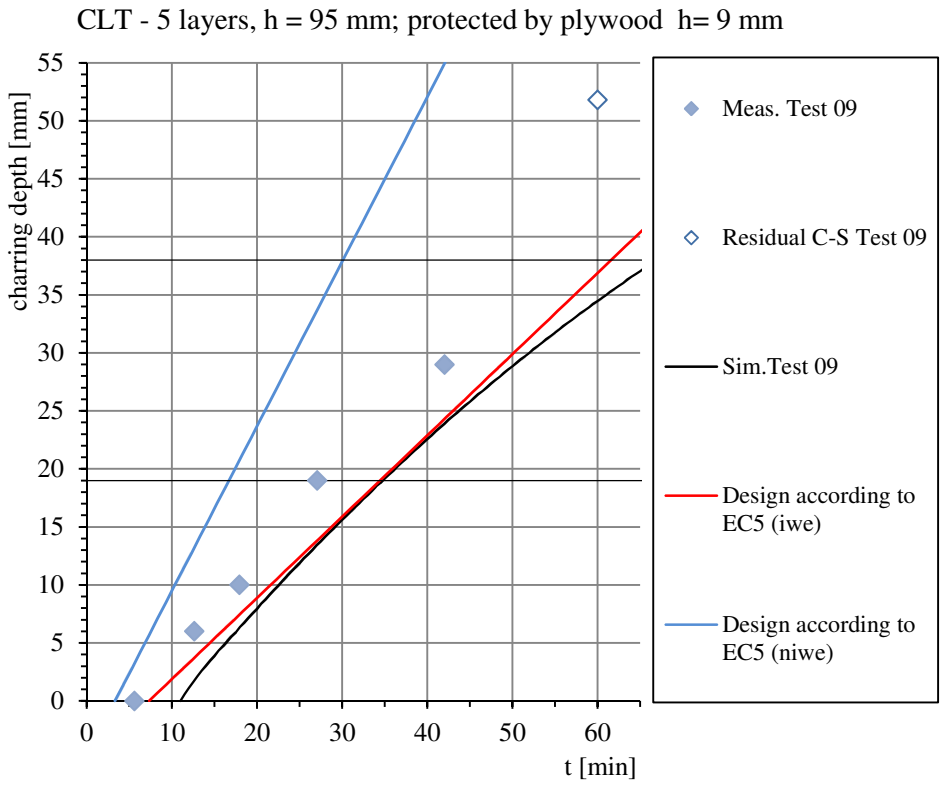

Figure 8-3 Comparison between cone calorimeter tests, simulations and analytical results for CLT protected by plywood

8.3.2 Observationsfrom the comparison

The results for the cone calorimeter test, despite are closer to an iwe, do not agree very well with both the proposals given by EC5. Also in this graph it is evident that the start of charring in the simulation is delayed respect the analytical and numerical results, but it there is not full agree also for the test and the calculated start of charring according to EC5. The simulation and the charring depth for an iwe well agree from the 20th to the 50th minute. The residual cross-section differs from the trend of the measured charring depths for the Test 09 (*cf. Figure 5-13*) but this value could be influenced from the extinguishment of the specimen.

8.4 Charring depths for the massive timber protected by gypsum plasterboard

For this set-up there is the greater number of cone calorimeter tests carried out (for this report) and are compared with three property proposals for the simulations and two ways of analytical for the charring depth calculation.

8.4.1 Comparison

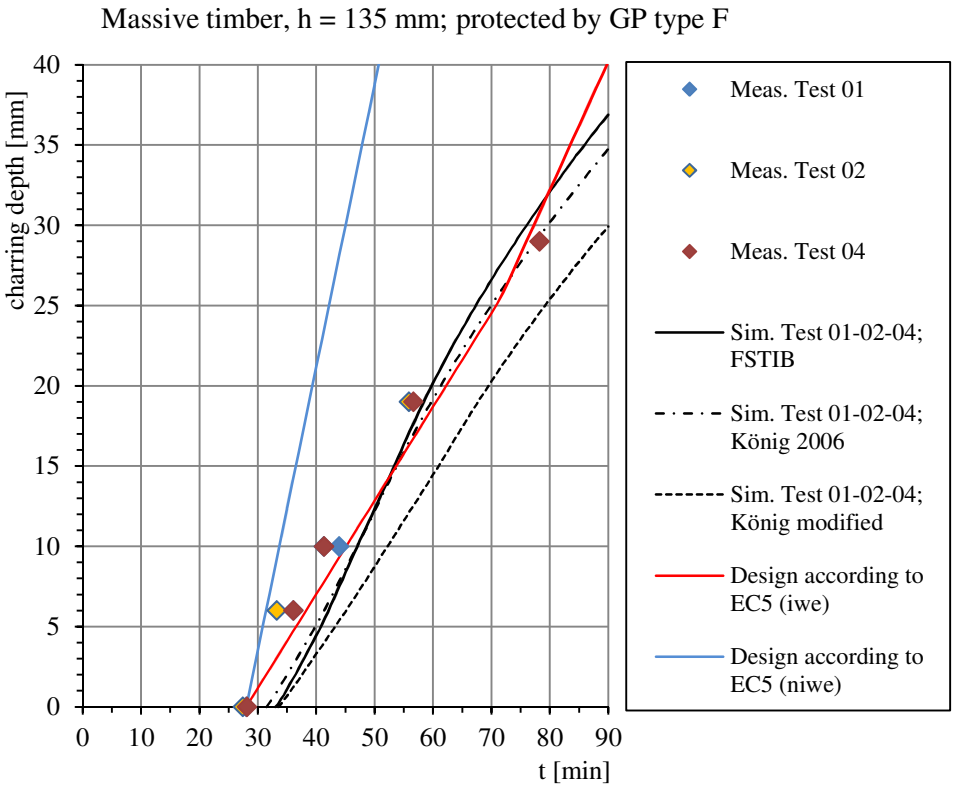

Figure 8-4 Comparison between cone calorimeter tests, simulations and analytical results for massive timber protected by gypsum plasterboard

8.4.2 Observations from the comparison

As the CLT tests protected by gypsum plasterboard, the start of charring time between the tests and the analytical results agree well, instead of the simulations, those start later than the others. It is possible to see a better accordance between the charring depths measured in the tests and the calculated for an infinitive wide element, the same was for the CLT protected by gypsum plasterboard.

Beyond the delayed start of charring, the simulations with the gypsum plasterboard properties according to FSITB and "König 2006" are close to the result of test and the analytical result for an iwe; despite the "König modified" that underestimate too much the results.

It is important remember that this comparison comprise the greater number of cone calorimeter tests with the same set-up. After seeing even the *Figure 5-5*, *Figure 5-6* and *Figure 5-8*; it is possible to see, especially for the first three thermocouples that the time

of reached the 300°C is very near for the three tests, almost superposable. This means that the tests have a good attitude to repeatability.

8.5 Charring depths for massive timber unprotected

This comparison concerns a cone calorimeter test, a simulation and the two proposals that follow the rules given by Eurocode 5 part 1-2. This kind of specimen (as for the protected tests) were selected from a timber studs with width of 45 mm, i.e. a non-infinitive wide element.

8.5.1 Comparison

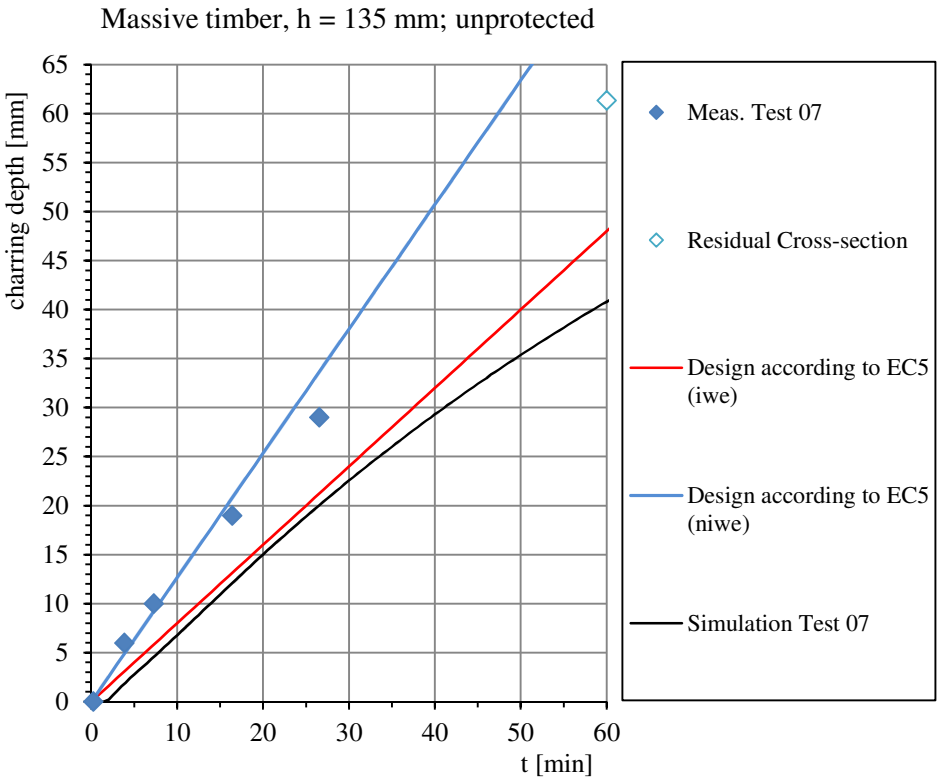

Figure 8-5 Comparison between cone calorimeter tests, simulations and analytical results for massive timber unprotected

8.5.2 Observations from the comparison

As observed for the unprotected CLT, the cone calorimeter results well agree with the charring depths for a non-infinitive wide element given by EC5 for the first 19 mm, after the rate decreases, as can be seen once again, from the point that indicates the residual cross-section.

The simulation agrees well with the design for an infinitive wide element; so it does not agree with the test results. Also in this simulation can be observed that the charring starts some minutes after the zero time, instead that an immediate ignition in an unprotected element, as expected.

8.6 Charring depths for the massive timber protected by plywood

8.6.1 Comparison

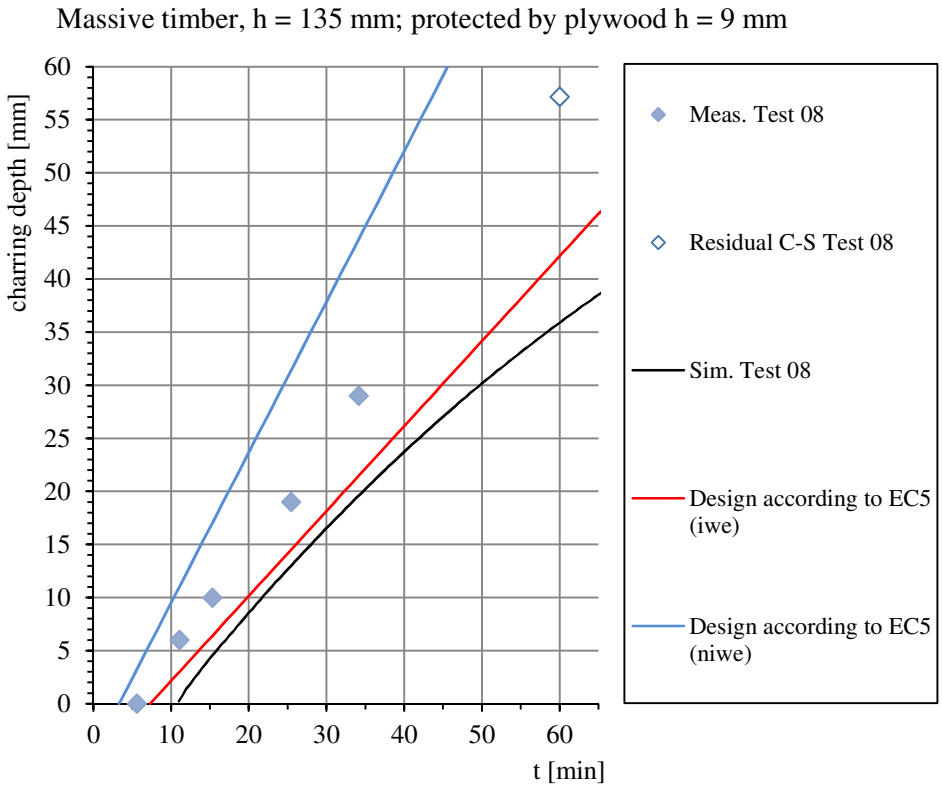

Figure 8-6 Comparison between cone calorimeter tests, simulations and analytical results for massive timber protected by plywood

8.6.2 Observations from the comparison

The observations that can be done for this comparison are not quite different from the observations that were done for the homologous test with the CLT as specimen and the same set-up.

The results for the cone calorimeter test, despite are included between the results of an iwe and a niwe, do not agree very well with both the proposals given by EC5. Once again it is evident that the start of charring in the simulation is delayed respect the analytical and experimental results, but also in this case there is not full agree for the test and the analytical start of charring. The simulation and the charring depth results for an iwe are close from the 20th to the 40th minute.

8.7 Observations regarding the factors k_s and k_n

As explained in the *Chapter 5.4*, the factors k_s and k_n regards the analytical charring depth for a non-infinitive wide element, more particularly the k_s factor takes in account the ratio between the charring rate calculated for a non-infinitive wide element and the charring rate of an infinitive wide element; the k_n factor allow to convert the real geometry of the residual cross-section flange in an equivalent rectangular cross-section

with the original width of the flange and the same modulus of inertia; i.e. this factor considers that in the flange there is not a propagation of the heat parallel at the fire exposed side, but the heat comes also from the insulated side and this phenomena gives a rounded shape of the residual cross-section; for an example see the *Figure 8-7*.

Figure 8-7 Specimen T05 (used in the Test 02) cutted in the middle section where can be seen an evident rounded shape of the residual cross-section

These considerations lead to thinking that if the factors k_s and k_n tend to one, the element can be considered as an infinitive wide element.

Can be useful see the results obtained from the test for these factors; the *Figure 5-14* and the *Table 5-3* show the result obtained for the factor k_s and particularly the mean values gathered for the type of fire protection. The k_s factor for the specimen protected by gypsum plasterboard is closer to the value 1 than the other groups of specimens. For the unprotected specimens k_s is greater than 2 and for the plywood protected the value is included between the first two groups.

In the same way in *Figure 5-15* and in the *Table 5-5* are shown the mean values of factor k_n gathered for the type of fire protection. In this case the mean of factors k_n for the unprotected specimens is closer the value 1 than the other groups. It is interesting to see that the mean values are not so distant each other, but all of them are quite distant to the value suggested by EC5 part 1-2.

8.8 Observations regarding the non-linearity of charring rate

As can be seen from the *Figure 3-5* and the *Figure 3-6* the charring rate for these furnace tests (performed by CNR-IVALSA) seems to be non-linear. Concerning this, it was calculated the charring rates between two thermocouples for each interval for the tests LFV002, LFV003 and LFV004. The table below summarized the results obtained.

Table 8-1 Charring rates evaluated for depth-steps for the furnace tests performed by CNR-IVALSA

Test LFV002		**Test LFV003**		**Test LFV004**	
Intervals (in TC depth)	Charring rates (mm/min)	Intervals (in TC depth)	Charring rates (mm/min)	Intervals (in TC depth)	Charring rates (mm/min)
0 - 9,5	0,52	0 - 9,5	0,54	0 - 9,5	0,41
9,5 - 28,5	0,74	9,5 - 28,5	0,83	9,5 - 28,5	0,53
28,5-47,5	0,57			28,5-47,5	0,75

It is possible observe that in the test LFV004 there is an increase of the charring rate for every depth-step, while an increase for each step does not occur in the test LFV002.

9 Conclusion and followed work

Comparing the results of charring from the cone calorimeter tests and the furnace tests (see *Figure 8-1* and *Figure 8-2*) it is possible to see that the comparison is not immediate. For a gypsum plaster board protected element the charring obtained with a cone calorimeter is close to the charring obtained with the furnace around the 60th minute; i.e. around the 20 mm of depth. For the first 10 mm the charring in the small specimen (cone calorimeter tested) occurs sooner than the furnace tested specimen. In the first place from the comparison between unprotected elements, the charring in cone calorimeter tested and furnace tested elements could not be compared.

Conversely, from the comparisons done from the *Chapter 8.1* to the *Chapter 8.5,* the results suggest that the charring depths for an unprotected specimen tested in a cone calorimeter agree with the charring depths that can be calculated following the rules given by the Annex C of Eurocode 5 part 1-2; i.e. can be considered as non-infinitive wide element. Seeing in the same chapters the comparisons for the gypsum plasterboard protected specimens, it is evident that the charring depths are closer to the analytical charring depth given by EC5 for an infinitive wide element.

The greater difference between the charring on infinitive wide and a non-infinite wide element could be given from the heat that comes from the insulated side; as can be seen from the *Chapter 4*, on the test protected by gypsum plaster board the fire protection does not cover only the specimen, but covers also the insulation member. This could be reduced the heat that comes from the insulated side and in this way create a one-dimensional heat propagation as can be found on an infinitive wide element.

From the observations done on the *Chapter* 8.7 the k_s factor calculated confirm the agreement between the charring depth of an non-infinite wide element with unprotected specimen; and between an infinitive wide element and a protected by gypsum plasterboard specimen tested on the cone calorimeter. On the other hand from the results obtained for the calculated k_n factor cannot give a full confirm of these facts.

Ultimately, it is possible to see that the time of reaching the 300°C behind the gypsum plasterboard protection, i.e. the start of charring behind the protection obtained in the furnace tests, the cone calorimeter tests and the analytical results agree well, as an additional confirm of the results obtained in previous works. After that, the charring in an gypsum plasterboard protected specimen is close to the charring that can be obtained for an infinitive wide element, but it is lightly overestimated around the 30th to the 50th minute and agrees better around the 60th minute, it means that the calibration of the cone calorimeter and particularly the changing to a heat flux of 75 kW/m^2 needs further improvement for this set-up. The charring in an unprotected specimen agrees well with a non-infinitive wide element for the first 20-25 minutes, above it is slightly underestimated.

In the results for the specimens protected by plywood there is not full agreement neither for infinitive wide nor the non-infinitive wide elements. Comparing the results for this set-up with the relative simulation and analytical results it is possible to see disagreement for the start of charring time and also for the charring rate.

Analyzing the simulation results for the gypsum plasterboard protected tests it is possible to see for all the three proposals of thermal properties an underestimated time of start charring behind the protection. The behaviors of charring obtained from the simulations with the “FSTIB” and the “König 2006” proposals of thermal properties are sufficiently close to the tests results, while for the proposal called “König modified” there is full

agreement with the vertical test performed at CNR-IVALSA called LFV004, but it underestimates the other results.

Observing the results of the simulations for the unprotected specimens it is clear how the results agree well with an infinitive wide and not with the non-infinitive wide element; i.e. not with the cone calorimeter test results. It is necessary understand if this difference is due to the not correct discretization of the insulation or is not possible compare a simulation with a ISO curve with this set-up of cone calorimeter test.

For validating the results of these tests further investigations are necessary. Understood that there is a slightly overestimated charring after the changing of the heat flux for gypsum plasterboard protected tests, could be interesting to test with an intermediate step between the 50 and 75 kW/m^2. It is also interesting trying to change the set-up of the insulation in the unprotected specimens, in order to achieve a behavior of charring closer to the infinitive wide element. The simulations with the gypsum plasterboard as fire protection need an improving regarding the start time of charring.

References

[1] EN 1991-1-2:2002, Eurocode 1."Action on Structures – Part 1-2: General actions – Actions on structures exposed to fire" European Standard. European Committee for Standardization, Brussels.

[2] EN 1995-1-2:2004, Eurocode 5. "Design of timber structures – Part 1-2: General – Structural fire design" European Standard. European Committee for Standardization, Brussels.

[3] EN 338:2009, "Structural timber – Strength classes" European Standard. European Committee for Standardization, Brussels.

[4] ISO 834-1:1999, "Fire-resistance test – Elements of building construction – Part 1: General requirements" International Organization for Standardization, Genève.

[5] EN 1363–1:1999, "Fire Resistance Tests–Part 1: General Requirements" European Standard. European Committee for Standardization, Brussels.

[6] EN 520: 2004 "Gypsum plasterboards. Definitions, requirements and test methods" European Standard. European Committee for Standardization, Brussels.

[7] EN 789:2004 "Timber structures – Test methods – Determination of mechanical properties of wood based panels" European Standard. European Committee for Standardization, Brussels.

[8] "Fire safety in timber buildings – Technical guideline for Europe" SP Technical Research Institute of Swedish (2010), Stockholm, Sweden.

[9] Buchanan, A. H. (2001) "Structural design for Fire Safety (Vol. 273)" New York: Wiley.

[10] Fragiacomo, M., Menis, A., Clemente, I., Bochicchio, G., & Ceccotti, A. (2013) "Fire Resistance of Cross-Laminated Timber Panels Loaded Out of Plane" J. Struct. Eng. 2013 139.

[11] Tsantaridis, L. D., Östman, B. A. L., & König, J. (1999) "Fire protection of wood by different gypsum plasterboards" Fire and materials, 23(1), 45-48.

[12] Frangi, A., Fontana, M., Knoblock, M., & Bochicchio, G. (2008) "Fire behaviour of cross-laminated solid timber panels" Fire Safety Science, 1279-1290.

[13] König, J., & Schmid, J. (2007) "Bonded timber deck plates in fire" In Proceedings of 40th CIB-W018 Meeting on Timber Structures, Bled, Slovenia.

[14] Frangi, A., Fontana, M., Hugi, E., & Jübstl, R. (2009). "Experimental analysis of cross-laminated timber panels in fire" Fire Safety Journal, 44(8), 1078-1087.

[15] Klippel, M., Leyde, C., Frangi, A., Fontana, M., Lam, F., & Ceccotti, A. (2014) "Fire Tests on Loaded Cross-Laminated Timber Wall and Floor Elements" 11th Symposium on Fire Safety Science (IAFSS), University of Canterbury, New Zeland.

[16] Tsantaridis, L. D., & Östman, B. A. L. (1998) "Charring of protected wood studs" Fire and materials, 22(2), 55-60.

[17] König, J. (2006) "Effective thermal actions and thermal properties of timber members in natural fires" Fire and materials, 30(1), 51-63.

[18] Tsantaridis, L. D. (2003) "Reaction to fire performance of wood and other building products" PhD thesis, KTH – Royal Institute of Technology, Stockholm, Sweden.

[19] Esping, B. (1992) "Trätorkning. 1a, Grunder i toskning" Trätek.

[20] Wilinder, P. (2010). "Fire resistance in cross-laminated timber" Bachelor thesis, Jönköping University, Jönköping, Sweden.

[21] Goina, M. (2010). "Resistenza al fuoco di pareti compresse in legno lamellare incrociato" Master thesis, Universita` degli Studi di Trieste, Trieste, Italy.

[22] Schimd, J. (2014). “Estimation of the fire protection ability of plaster in a historic building – Stockholm central station” Report 3P09084-2. SP Wood Technology: Technical Research Institute of Swedish, Stockholm, Sweden.

[23] König, J. (1995). “Fire Resistance of Timber Joists and Load Bearing Wall Frames” Report I 9412071. SP Wood Technology: Technical Research Institute of Swedish, Sweden.

[24] CSA Standard 0151-09 (2009) “Canandian softwood plywood” Canadian Standards Association, Mississauga, Ontario.

[25] NIST PS 1-07 (2007) “Structural Plywood” Voluntary Product Standard, National Institute of Standards and Technology, Technology Administration, U.S. Department of Commerce.

[26] König, J. (2006). “Fire exposed simply supported wooden I-joists in floor assemblies” Report 2006:44. SP Wood Technology: Technical Research Institute of Swedish, Sweden.

[27] Franssen, J. M. (2007). “User´s Manual For SAFIR 2007 a Computer Program For Analysis of Structures Subjected to Fire” University of Liege, Belgium.

[28] Schaffer, E. L. (1968). “A simplified test for adhesive behavior in wood sections exposed to fire” Forest Products Laboratory

SP Technical Research Institute of Sweden

Our work is concentrated on innovation and the development of value-adding technology. Using Sweden's most extensive and advanced resources for technical evaluation, measurement technology, research and development, we make an important contribution to the competitiveness and sustainable development of industry. Research is carried out in close conjunction with universities and institutes of technology, to the benefit of a customer base of about 10000 organisations, ranging from start-up companies developing new technologies or new ideas to international groups.

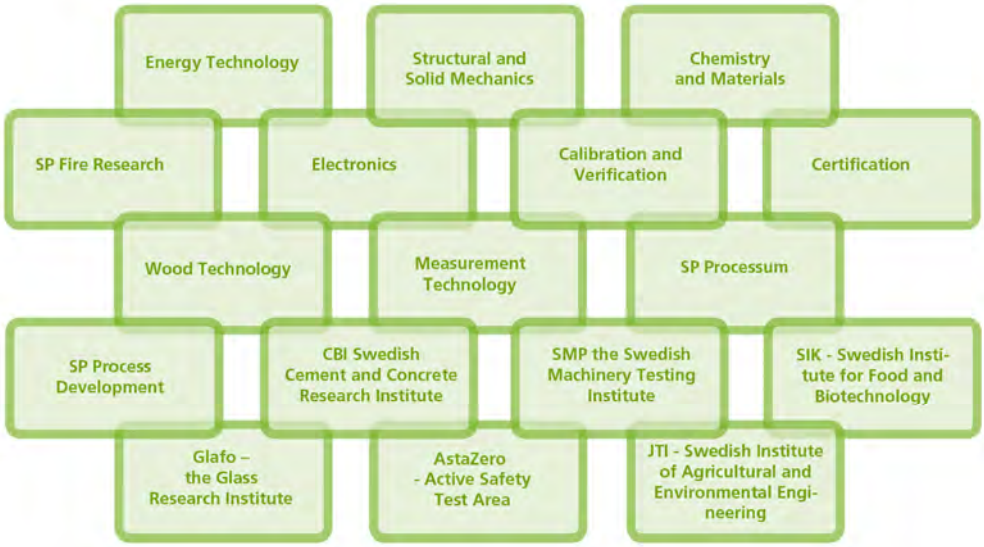

SP Technical Research Institute of Sweden
Box 857, SE-501 15 BORÅS, SWEDEN
Telephone: +46 10 516 50 00, Telefax: +46 33 13 55 02
E-mail: info@sp.se, Internet: www.sp.se
www.sp.se

SP Wood Technology
SP Report 2014:27
ISBN 978-91-88001-12-2
ISSN 0284-5172

More information about publications published by SP: **www.sp.se/publ**